Tools and Methods in Aiding Heat Exchanger Network Retrofit for Better Economic Performance

DOI:10.18136/PE.2019.709

PhD Thesis

Yong Jun Yow

Supervisor

Professor Dr. Jiří Jaromír Klemeš

Co-Supervisor

Dr. Petar Varbanov

Doctoral School of Information Science and Technology

University of Pannonia

Veszprém, Hungary

2018

Tools and Methods in Aiding Heat Exchanger Network Retrofit for Better Economic Performance

Thesis for obtaining a PhD degree in the Doctoral School of Information Science and Technology of the University of Pannonia

in the branch of Information Sciences

Written by Yong Jun Yow

Supervisor(s): Professor Dr. Jiří Jaromír Klemeš and Dr. Petar Varbanov

propose acceptance (yes / no) …….

(supervisor/s)

The PhD-candidate has achieved ..... % in the comprehensive exam,
Veszprém/Keszthely, …….

(Chairman of the Examination Committee)

As reviewer, I propose acceptance of the thesis:

Name of Reviewer: …..... …..... yes / no

…….

(reviewer)

Name of Reviewer: …..... …..... yes / no

…….

(reviewer)

The PhD-candidate has achieved ….....% at the public discussion.

Veszprém/Keszthely, …….

(Chairman of the Committee)

The grade of the PhD Diploma …..... (…….. %)
Veszprém/Keszthely,

…….

(Chairman of UDHC)

Acknowledgement

First and foremost, I would like to offer my highest gratitude to my supervisors, Professor Dr. Jiří Jaromír Klemeš and Dr. Petar Varbanov. I cannot possibly express anymore of my gratitude to them, not only on the guidance they gave during my study as a PhD student but valuable life experiences as well. Being in another county that is far away from home, they constantly make sure that my well-being was taken care off. Even when we are at different parts of the globe sometimes, they never give up on me and keep on guiding me so that I am on track. I would like to thank my family and Keat Liong for being there with me mentally, especially the three years when I was not in Malaysia. They support every decision I made without questioning. They reminds me of home when I am far away.

I would also like to take this opportunity to thank DDr. Lam Hon Loong and DDr. Andreja Nemet. They provides ideas and tremendous help to me during my studies. There will never be enough of thank you and sorry from me for all the trouble I had caused them. I would like to thank the staff from University of Pannonia, especially Mrs Ujvári Orsolya and Mr Dulai Tibor. They assisted me in every possible way and went through all the office works for me to have a good experience in Hungary. I would like to thank my friends, Mr How Bing Shen, Mr Hong Boon Hooi, Mr Goh Wui Seng, Mr Lee Chit Seng and Miss Lim Li Sher. Lastly, I would like to thank all the collaborators and everyone who helped me during my journey as a PhD student.

Jun Yow YONG, 2018

Abstract

This thesis presents novel tools and methods developed specifically to be used during Heat Exchanger Network retrofit for better economic performance. The very first step in starting a retrofit process is collecting and extracting data from measured sets of process data. In the first discovery of this work, a novel method is proposed to ease the process of reconciling data of Heat Exchanger Network for the purpose of Heat Integration analysis. An iterative Method is introduced in the first part of this work differs from conventional data reconciliation method. The method is explained in detail - including its models used and algorithms. Two case studies, an illustrative and an industrial, successfully demonstrate the application of the method. Detailed discussions are given such as the effect of starting parameters to reconcile on the result. A limitation of the Iterative Method was identified and several strategies has been developed to overcome it. In the case studies, the strategies combining the Iterative Method are able to yield satisfying results. This comes at the expense of additional parameters into the models. The scope of data reconciliation is then expended to Total Site. Considering the complexity of Total Site, the model only includes utility systems and equipment, such as heaters, coolers and turbines. Heat exchangers in each individual plant are not considered in the model.

After obtaining the reconciled set of parameters, the next step is to represent them related to the Heat Exchanger Network structure. While the conventional Grid Diagram contains sufficient information for the retrofit process, it does not visualise the data sufficiently well for user interaction and decision making. The second discovery introduces a novel tool to represent all data required for Heat Exchanger Network retrofit in more detail, better supporting the engineer decision during the retrofit process. This tool is the Shifted Retrofit Thermodynamic Diagram. It includes the characteristics of Pinch Analysis. It can be used to easily identify not only the Process Pinch, but also any Network Pinch as well as Utility Pinch occurrences. With better visualisation, several ways are discussed of how to utilise this novel tool for better increase in heat recovery. A case study from the literature is used extensively to demonstrate the use and usefulness of Shifted Retrofit Thermodynamic Diagram.

Although a retrofit action can be thermodynamically feasible, it might not be economically feasible to be implemented. The last chapter is about the discovery of an alternative method to retrofit an existing Heat Exchanger Network, particularly reusing the waste heat. It is demonstrated using a real industrial case study, where it requires a large amount of investment cost to achieve the first retrofit result. In the case study, it is proposed otherwise that the waste heat is reused to heat up some streams. This reduces the utilities consumptions. Although it is similar to the initial proposed retrofit suggestion in terms of utilities saved, performs much better in terms of cost savings and payback.

Összefoglaló

Ez a doktori értekezés új eszközöket és módszereket mutat be, amelyek a specifikusan a hőcserélő hálózat módosítására lettek kifejlesztve. A módosítási (retrofit) folyamat legelső lépése az adatgyűjtés és kivonás a folyamat-adatok mért készleteiből. A munka első felfedezése egy új módszer javaslata, amely megkönnyíti az hőcserélő hálózatokra vonatkozó adatok összeegyeztetését a hő-integrálás elemzésére. Ezen munka elején bemutatott iteratív módszer különbözik a hagyományos összeegyeztetés módszertől. A módszert részletesen ismertetjük – beleértve a felhasznált modelleket és algoritmusokat. Bemutatjuk a részletes értekezést mint pl. az összeegyeztetés kezdő paramétereinek a hatása az eredményekre. Az iteratív módszer hátrányait azonosítottuk és különböző stratégiákat fejlesztettünk ki a hátrányok megoldására. Az esettanulmányokban az iteratív módszerek különböző stratégiáinak az egyesítésével elfogadható eredményeket értünk el. Ez a nagyobb számú paraméterek felhasználásával érhető el. Az adatok összeegyeztetését ezután kiterjesztettük az ún. Total Site szintre. A Total Site bonyolultságát figyelembe véve, a modell magába foglalja a segédközeg-rendszert és felszerelést, mint pl. a fűtők, hűtők és turbinák, viszont a hőcserélők az egyes üzemekben nem szerepelnek a modellben.

Az összeegyeztetett paraméter készletek elérése után, a következő lépés ezek bemutatása volt a hőcserélő hálózat struktúrájával összefüggésben. Míg a hagyományos rácsábrázolás elég információt tartalmaz a retrofit folyamathoz, nem tartalmaz elég adatot a felhasználó interakciójához és döntés hozatalához. A második felfedezés bevezet egy új eszközt a hőcserélő hálózat módosításához a szükséges részletes adatok bemutatására, amely jobban támogatja a mérnökök döntéseit a módosítás folyamatában. Ez az eszköz a módosított retrofit termodinamikai diagram (angolul: Shifted Retrofit Thermodynamic Diagram). Ez tartalmazza a pinch elemzés jellemzőit. Az eszközt fel lehet használni nem csak a folyamat pinch, hanem a hálózati pinch valamint a segédközeg pinch előfordulásának a meghatározására. A jobb vizualizálással, az új eszköz többféle felhasználását tárgyaljuk meg a hő-visszanyerés jobb növekedés érdekében. Irodalmi esettanulmány használtunk fel a módosított retrofit termodinamikai diagram felhasználásának és hasznosságának a bemutatására.

A termodinamikailag megvalósítható retrofit tevékenységek gazdaságilag nem feltétlenül megvalósíthatóak. Az utolsó fejezet a meglévő hőcserélő hálózat alternatív retrofit módszer felfedezést tárgyalja, különösen a hulladék-hő újrafelhasználásával. A módszer reális ipari esettanulmány felhasználásával kerül bemutatásra, amelynek magasak a beruházási költségei az első retrofit javaslatok elérésére. Az esettanulmányban a hulladék-hő újrafelhasználása javasolt némely áramok fűtésére. Ezzel csökkentjük a segédközegek felhasználását. Bár a javasolt megoldást hasonlít az eredeti javasolt módosításhoz a segédközegek felhasználásának a csökkentése szempontjából, sokkal jobban teljesít a költségek megtakarítás és a megtérülés szempontjából.

Table of Contents

1. Introduction

It has been four decades since Heat Integration analysis has been introduced for energy recovery in chemical plants (Klemeš and Kravanja, 2013). An important part of physical-insight methods is Process Integration. One of the first works on this has been that of Linnhoff and Flower (1978). The development up to present level has been summarised elsewhere (Klemeš et al., 2014) and specifically for Heat Integration in (Klemeš and Kravanja, 2013). Bakhtiari and Bedard (2013) modified the Network Pinch Approach to handle more complex networks with stream segmentation and splitting, also using heat exchanger specific values for the minimum allowed temperature difference.

Mathematical Optimisation usually employs algebraic models to solve the retrofit problem. Yee and Grossmann (1990) proposed a MINLP model with a stage-wise superstructure. Due to the numerical difficulty of solving the MINLP model, a number of options and assumptions are considered in a specialised superstructure. Bogataj and Kravanja (2012) proposed another alternative strategy for global optimization of HENs. The global optimal result is obtained on small HEN synthesis and good locally optimal solutions for larger problems. A recent mathematical model has been developed by Sreepathi and Rangaiah (2014) that uses continuously varying heat capacity. They apply single and multiple objective optimisation. As the next logical step from the retrofit of single process, the scope has been extended to cover Total Sites. For example, Liew et al. (2014) analysed all the streams involved in Total Site Heat Integration. They present a retrofit framework to determine the most cost-effective retrofit options and maximise the potential savings.

While it is important to have Heat Integration in chemical plants, retrofitting an existing HEN is also important (Klemeš, 2013). It is observed that the recent focus of Heat Integration has shifted towards retrofitting existing chemical plants. This is due to existing Heat Exchanger Networks (HEN) have become obsolete after years of service. Chemical, petrochemical, power and other industries are keen to improve the energy efficiency of their plants due to the energy cost (BP, 2013) and increasingly strict environmental regulations (European Commission, 2011). With current fluctuating energy prices, increased production and change in process equipment, retrofitting can reduce operating cost with some capital investment. Various methods have been published for solving the retrofit problem. They are generally based on physical insight, mathematical optimisation or combination of both.

During the HEN retrofit process, most of the attention is given to how the network can achieve better heat recovery or throughput. The steps on how to collect and process data from HEN to be used in the analysis are usually given very little attention. From the search in the literature, very few research works are available on heat exchanger data acquisition and processing, let alone on HEN. One of the early works, that could be found, is by Shenoy (1995). In that, the data reconciliation problem is modelled by Nonlinear Programming, based on average measurement values. The model formed the very base tool set that is even used until today. From there, ways of solving the model to obtain the reconciled result are developed.

The model can be solved as it is with the current computer technology and advancement. As shown in part of the current thesis by Yong et al. (2016), the data reconciliation model is solved simultaneously (i.e. solving for all unknowns at the same time). It was performed using a Local solver GAMS/CONOPT with the global optimization algorithm (GOA) reported in Faria and Bagajewicz (2011). The original non-convex nonlinear optimisation problem was converted into a convex one by replacing the bilinear terms with McCormick's envelopes. It might be deemed too difficult for user without advanced mathematical and computational knowledge.

The book by Narasimhan and Jordache (2000) covers provides basic introduction, explanations and ways to solve the data reconciliation problems. Among the methods mention in the book, one of the simpler method to solve the problem is Modified Iterative Measurement Test (MIMT). Details of the method are not discussed here. The method employs the use of matrix and equations involving statistical calculation to find the result. It is possible to be solved manually or implemented into Microsoft Excel. For example, detailed usage and discussion of this method can be found in the master's thesis work of Mayo (2015). It should be noted that the method is only capable of solving one type of parameter. For the case of data reconciliation for the purpose of Heat Integration analysis, which contains two types of parameters, the method is deemed unsuitable. For this reason, a non-simultaneous data reconciliation algorithm on HEN was introduced in the work of Ijaz et al. (2013). It involves using formulae to reconcile one parameter via QR factorisation. The idea of the non-simultaneous method is good but is also not suitable for the purpose of Heat Integration analysis as it includes the overall heat transfer coefficient for each heat exchanger, which is irrelevant to some types of Heat Integration analysis.

The Grid Diagram is the most common way of representing a HEN during Heat Integration analysis. Particularly for an insight-based method such as Pinch Analysis, after targeting minimum utility consumption, the HEN design is done on the Grid Diagram. Streams are represented as horizontal lines with individual heat capacity flowrates. The direction of the line depends on the nature of the streams with the starting and ending temperatures indicated at the ends of the line. With identified Pinch temperature, the HEN is designed according a set of algorithms by connecting the horizontal lines with vertical lines representing heat exchangers. The designed HEN will finally achieve the targeted result. As for designing a HEN using mathematical optimisation, the whole process does not require the visualisation of HEN. It is however that the final result will represented on HEN grid diagram. Beside Grid Diagram, there are other visualisation tools to represent HEN. For example, Retrofit Thermodynamic Diagram (RTD) by Lakshmanan and Bañares-Alcántara (1996), Heat Loads Plot by Piacentino (2011) and Streams Temperature vs. Enthalpy Plot (STEP) by Wan Alwi and Manan (2010). Gadalla (2015) plotted temperatures of hot process streams versus cold process streams. Further discussions of these tools are made in Section 4.1. While these tools are used to design HEN, the usability on HEN retrofit process is not made known by the authors.

Most of HEN retrofit procedures are performed using mathematical optimisation. Due to the mathematical optimisation, it is possible to include more objectives in the model during the

retrofit process. To list a few, in the work of Kang and Liu (2017), a systematic strategy for multi-period HEN is developed with the objective of minimising the total annual cost and total annual carbon dioxide emissions. Ayotte-Sauvé et al. (2017) uses superstructure with new stepwise approach to optimise the HEN retrofit. Using new algorithms and at each iteration, these superstructures are thinned out to reduce calculation times. Other consideration can also be included during the retrofit process, as shown in the work of Rangfak and Siemanond (2017). The proposed model is based on stage-wise superstructure with fouling effect included. Using a crude oil preheat train as case study, the large-scale MINLP problem is solved by applying initialisation and sequential techniques.

There are HEN retrofit procedures based on insight. Tjoe and Linnhoff (1986) are some of the first to use Pinch Technology for HEN retrofit. Following on that, Li and Chang (2010) have eliminated cross-Pinch heat transfer in HENs using Pinch Analysis. In the work of Smith and Akpomiemie (2017), heat transfer enhancement is focused to reduce the number of structural modification and minimize the capital investment. The work presents a new Pinch retrofit method for structural modifications and a combined method that simultaneously considers enhancement alongside structural modification. Bonhivers et al. (2017) claimed that mathematical approaches to HEN retrofit are complex and do not guarantee the global optimum. In the first part of the work, an energy transfer diagram called Energy Transfer Diagram (ETD) is proposed. The graphical approach to identify the heat exchanger configurations is shown to be able to reduce the energy consumption. The authors claimed that the method is practical, visual and user-friendly.

For HEN retrofit an interesting concept has been introduced by Asante and Zhu (1996). Their discovery of the Network Pinch (NP) that occurs due to HEN topology has provided key insights into the HEN retrofit problem. The location of the NP is determined by the HEN topology limitations, so it is usually different from the Process Pinch (PP) Temperature identified using Pinch Analysis. The NP concept has proved beneficial in retrofitting existing HENs.

1.1 References

Asante, N.D.K., Zhu X.X., 1997, An automated and interactive approach for heat exchanger network retrofit, Chemical Engineering Research and Design, 75(part A), 349-360.

Ayotte-Sauvé E., Ashrafi O., Bédard S., Rohani N., 2017, Optimal retrofit of heat exchanger networks: A stepwise approach, Computers & Chemical Engineering, 106, 243-268.

Bakhtiari B., Bedard S., 2013, Retrofitting Heat Exchanger Network using a Modified Network Pinch Approach, Applied Thermal Engineering, 51 (1-2), 973 – 979.

Bogataj M., Kravanja Z., 2012. An alternative strategy for global optimization of heat exchanger network, Applied Thermal Engineering, 43, 75 – 90.

Bonhivers J.-C., Alva-Argaez A., Srinivasan B., Stuart P.R., 2017, New analysis method to reduce the industrial energy requirements by heat-exchanger network retrofit: Part 2 – Stepwise and graphical approach, Applied Thermal Engineering, 119, 670-686.

BP, 2013, BP Statistical Review of World Energy June 2013, <www.bp.com/content/dam/bp/pdf/statistical-review/statistical_review_of_world_energy_2013.pdf> accessed 01.04.2014

European Commission, 2011, Poor Energy Use is Chemical Industry's Top Environmental Issue, Science for Environment Policy, <ec.europa.eu/environment/integration/research/newsalert/pdf/243na2_en.pdf> accessed 09.01.2014

Faria D.C., Bagajewicz M.J., 2011, Novel bound contraction for global optimization of bilinear MINLP problems with applications to water management problems, Computers and Chemical Engineering, 35, 446–455.

Gadalla M.A., 2015, A new graphical method for Pinch Analysis applications: Heat exchanger network retrofit and energy integration, Energy, 81, 159 – 174.

Ijaz H., Ati U. M. K., Mahalec V., 2013, Heat exchanger network simulation, data reconciliation & optimization, Applied Thermal Engineering, 52(2), 328 - 335.

Kang L., Liu Y., 2017, A systematic strategy for multi-period heat exchanger network retrofit under multiple practical restrictions, Chinese Journal of Chemical Engineering, 25(8), 1043-1051.

Klemeš J.J. Kravanja Z., 2013. Forty years of Heat Integration: Pinch Analysis (PA) and Mathematical Programming (MP), Current Opinion in Chemical Engineering, 2(4), 461 – 474.

Klemeš J.J., 2013, Handbook of Process Integration (PI): Minimisation of Energy and Water Use, Waste and Emission, Woodhead Publishing/Elsevier: Cambridge, UK

Klemeš J.J., Varbanov P.S., Wan Alwi S.R., Manan Z.A., 2014, Process Integration and Intensification: Saving Energy, Water and Resources, Walter de Gruyter: Berlin, Germany

Lakshmanan R., Bañares-Alcántara R., 1996, A Novel Visualisation Tool for Heat Exchanger Network Retrofit, Industrial & Engineering Chemistry Research, 35, 4507-4522.

Li B.-H., Chang C.-T., 2010. Retrofitting heat exchanger networks based on simple pinch analysis, Industrial & Engineering Chemistry Research, 49(8), 3967 – 3971.

Liew P.Y., Lim J.S., Wan Alwi S.R., Manan Z.A., Varbanov P.S., Klemeš J.J., 2014, A retrofit framework for Total Site heat recovery systems, Applied Energy, 135, 778 – 790.

Linnhoff B., Flower J.R., 1978. Synthesis of heat exchanger network: I. Systematic generation of energy optimal networks, AIChE Journal, 24, 633 – 642.

Mayo C.M., 2015, Process Stream Data Analysis: Data Reconciliation and Gross Error Detection for Process Integration Studies, Master's Thesis, Chalmers University of Technology.

Narasimhan S., Jordache C., 2000, Data Reconciliation & Gross Error Detection: An Intelligent Use of Process Data, Gulf Publishing Company, Houstan, Texas.

Piacentino A., 2011, Thermal Analysis and New Insights to Support Decision Making in Retrofit and Relaxation of Heat Exchanger Networks, Applied Thermal Engineering, 31(16), 3479 – 3499.

Rangfak S., Siemanond K., 2017, Heat Exchanger Network Retrofit with Fouling Effects, Computer Aided Chemical Engineering, 40, 775-780.

Shenoy U.V., 1995, Heat exchanger network synthesis, Gulf Professional Publishing, Houston, USA.

Smith R., Akepomiemie M.O., 2017, Low Cost Retrofit Methods for Heat Exchanger Networks, Computer Aided Chemical Engineering, 40, 1789-1794.

Sreepathi B.K., Rangaiah G.P., 20154, Retrofitting of Heat Exchanger Networks Involving Streams with Variable Heat Capacity: Application of Single and Multi-Objective Optimisation, Applied Thermal Engineering, 75, 677 – 684.

Tjoe T.N., Linnhoff B., 1986. Using Pinch Technology for process retrofit, Chemical Engineering (New York), 93(8), 47 – 60.

Wan Alwi S.R., Manan Z.A., 2010, STEP – A new graphical tool for simultaneous targeting and design of a heat exchanger network, Chemical Engineering Journal, 162(1), 106 – 121.

Yee T.F., Grossman I.E., 1990, Simultaneous optimization models for heat integration – II. Heat exchanger network synthesis, Computers & Chemical Engineering. 14(10), 1165 – 1184.

Yong J.Y., Nemet A., Bogataj M., Zore Ž., Varbanov P.S., Kravanja Z., Klemeš J.J., 2016, Data Reconciliation for Energy System Flowsheets, Computer Aided Chemical Engineering, 38, 2277-2282.

2. Research Goals

The general process of retrofitting an existing heat exchanger network (HEN) for better heat integration can be divided into several stages. The first stage is to acquire data from the chemical plant. For this purpose, process flow diagram is used to have an overall view of the process and equipment of the plant. It is important that the boundary for heat integration analysis is defined, especially if it involves several plants together. The second stage of the process is data extraction. As the purpose is for heat integration analysis, only streams with changed temperature should be considered in the extraction. This is to avoid unnecessary data being extracted without being used. These streams can be easily identified as they pass through either heat exchanger, cooler or heater. Low grade heat such as in waste heat streams ejected to environment are also to be extracted.

After the relevant streams are being identified, repeated measurements of temperature and mass flowrate taken for a period of time of each stream are extracted. The repeated measurements are then processed to remove any outliers. For more details on data processing prior to data reconciliation, it is provided in the appendix section of this work. The topology of the HEN is also extracted. Data reconciliation is performed on the measurements in order to obtain a representative data that satisfy the system constraints. The third stage is heat integration analysis where retrofit options are explored and proposed. At this stage, the retrofit options are continuously send to industrial partner for feedback. If the retrofit option is found to be expensive in terms of investment or time, other options are explored such as generating side-product for extra revenue. Once the retrofit option is decided and finalised, implementation is performed on the chemical plant. The changes and results are recorded for future reference.

Data reconciliation has a wide implementation in the industry. On the search of the keyword “Data Reconciliation” in scientific journal website, ScienceDirect shows more than thousands of work discussing data reconciliation on various processes and equipment. The current state of the art for data reconciliation is to employ an MINLP model to solve the data reconciliation problem. The model generally consists of an objective function that uses least square method and set of constraints governing the process or equipment. It is important to state the focus and purpose of the data reconciliation before it begins. As the main topic of this work is HEN retrofit, the focus is therefore on the HEN and the purpose is heat integration analysis. Narrowing down the search on data reconciliation on HEN, however to the knowledge of author, does not produce much finding in the literature. Although these works focus on HEN, the purpose for heat integration analysis is even fewer. For example, in the master’s thesis of Mayo (2015), Microsoft Excel is introduced to be used to perform data reconciliation due to its user friendly feature. In the work, it is also assumed that temperatures are the only adjustable variable, while the mass flowrates are kept constant. For heat integration analysis, both of these parameters are equally important and should not be left out in the data reconciliation process. The other works found are discussed in detail in chapter 3 in this thesis. Furthermore, on further investigation, certain

constraints used for data reconciliation poses additional complexity to the model. Of all the constraints used, energy balance constraint causes the non-linearity in the model.

The first main research goal is to develop a less computational effort requiring method during data reconciliation process with two types of parameters. The goal is then further extended to only include energy systems in data reconciliation process in Total Site. A new method is introduced to solve this non-linearity in section 3.2 that iterates between two linear sub-models. Through case studies iterative method is shown to be able to provide satisfying result with less computational time. In section 3.3, limitation encountered when using iterative method is discussed. To overcome this limitation, three different strategies are developed. Section 3.4 presents a new way to solve data reconciliation problem on Total Site. Model to solve data reconciliation on utility system is presented with demonstration from both illustrative case study and industrial case study.

The topology data of HEN is crucial to heat integration analysis. While stream data can be stored in the form of table, the topology data of HEN cannot be stored easily in table form. Although process flow diagram is able to show the whole HEN, it contains other equipment that is not relevant to heat integration analysis. The most conventional way of representing HEN is by using Grid Diagram. In the diagram, streams are involved in heat exchange is represented in horizontal lines. Heat exchangers are then shown in Grid Diagram connecting hot streams and cold streams vertically. Grid Diagram is used intensively in designing HEN especially after performing Pinch Analysis. Coupling with heuristic from Pinch Analysis, the found pinch divide HEN Grid Diagram into two parts where no heat transfer is allowed across the pinch. It should be noted that while Grid Diagram provides visualisation of the HEN, it is still lacking visual information of some other important parameters. Various studies are found in the literature to have added extra feature to improve the conventional Grid Diagram. For example, in the work of Gadalla (2015), HEN is represented in graph with cold process stream temperature in the x-axis and hot process stream temperature in the y-axis. From the graph it can be seen that improvement is made on visualising heat exchanger using arrow. The coordinates at the start and end of the arrow indicates the temperatures of both hot and cold streams. For other works it is discussed in chapter 4. However, according to the knowledge of author, there is still a need for a HEN representation that includes other important parameters to be considered during HEN retrofitting analysis. This includes location of pinches and mass capacity flowrates.

The second research goal is to develop HEN representations from conventional Grid Diagram to include more parameters for better visualisation and decision making. Referring to the second part of these research works, section 4 introduced an extended Grid Diagram – the Shifted Retrofit Thermodynamic Grid Diagram (SRTGD). SRTGD has unique feature set, helping to identify favourable retrofit options. It shows heat capacity flowrates (CP), temperatures and the network in the same view. It allows the users to simultaneously account for the thermodynamics, stream capacities and the topology as factors during heat recovery. The goal is further extended to develop a representation in the form of table without drawings. Later in the section the

suggestion to represent HEN numerically in a matrix form is proposed. HEN Stream Matrix (HENSM) is able to improve the discussed limitations faced by graphical representations.

While retrofitting HEN, the boundary is conventionally set only within the plant itself. Doing so may result in economically unfavourable option and missing other opportunity to utilise low grade heat. When retrofit for utilities usage reduction is deemed economically unfavourable for a HEN, the next level in hierarchy is to analyse heat utilisation options to produce value-added products. The last research goal is to identify other retrofit solutions when a thermodynamic driven retrofit solution is deemed economically infeasible. This is shown in the last part of these research works in section 5.

3. Iterative Method for Data Reconciliation on Energy System

3.1 Introduction

Data extraction is the very first and crucial step performed before any Heat Integration study can commence (Klemeš, 2013). Particularly for existing plants for retrofitting, data reconciliation is a step that must be performed in data extraction to obtain representative data (Klemeš and Varbanov, 2010). It is a procedure that extracts an accurate and reliable set of data from repeated raw measurements that satisfies the system constraints. Shenoy (1995) published a nonlinear programming model for Heat Exchanger Network (HEN) data reconciliation, based on average measurement values. Vocciante et al. (2014) developed a reconciliation strategy that assesses the convenience of using enthalpy balances in the reconciliation of flowrates. The resulting algorithm based on interval analysis provides a general framework on selection of equation to be used in reconciliation process. In the work of Kongchuay and Siemanond (2014), gross detection error technique is in data reconciliation to improve the data measurement of a simulated hot-oil heat exchanger using non-linear programming.

The main Heat Integration analysis method – Pinch Analysis, requires heat capacity flowrates (*CP*) and temperatures (*T*) of process streams. While there are already some publications on reconciliation of measured HEN data (Nemet et al., 2015), works presenting data reconciliation for Pinch Analysis are scarce. The models proposed in the literature reconcile *CP* and *T* simultaneously. A non-simultaneous data reconciliation algorithm on HEN was introduced in the work of Ijaz et al. (2013). It involves using formulae to reconcile one parameter via QR factorisation. Although the algorithm is non-simultaneous, it is non-iterative as well. It reconciles one parameter at a time and stops after reconciling the last parameter. The algorithm first reconciles mass flowrates using only mass balance equations and then proceeds to reconciling measured temperatures using energy balance equations where the already calculated mass flowrate values are supplied as fixed parameters. As only mass balance equations are used in the first step of the algorithm, the mass flowrate values have influence on the result when temperatures are reconciled. It is noted that the temperature values have no influence on the result when mass flowrates are reconciled.

There is a need for a method to solve data reconciliation suited to Heat Integration for retrofit. The method should be easily understandable to the users who wish to perform data reconciliation without much knowledge in solving complex models and should require less computational effort. The method described in this work is only consists of linear constraints equations and linear least square method is used on objective function. User is then only required to have skills and knowledge in linear programming and coding using mathematical optimisation software. This chapter is composed of 3 main sections. First, in section 3.2, the new method, called iterative method is introduced. It allows overcoming the non-linear complexity in the data reconciliation model. Section 3.3 discusses the limitation encountered when using iterative method. A few strategies are developed to overcome this limitation. The last section being section 3.4 explores the use of iterative method on utility system found in Total Site Heat Integration.

3.2 Iterative Method for HEN in a Single Site

In data reconciliation on HEN, the only two types of parameters to be reconciled are heat capacity flowrates (*CP*) and temperatures (*T*) of process streams.

3.2.1 Problem Statement

Consider a single HEN, where it has heat exchangers and utility consuming equipment, i.e. heaters and coolers. All this equipment are considered for data reconciliation. All heaters and coolers are modelled in exactly the same way as heat exchangers. It is because the only difference between these utility consuming equipment and heat exchanger is one of the streams is containing utility. These utility carrying streams can also be modelled as normal stream in the network. All equipment is labelled as i ∈ I. On every heat exchanger, there are two inlets (I) and two outlets (O) for hot (H) and cold (C) streams. These generate a set of streams, s ∈{HI, HO, CI, CO}. Two types of parameters are only considered in the data reconciliation, which are temperature (T) and heat capacity flowrate (*CP*). Given a repeated set of measurements of all heat exchangers in a set period of time for n times, the aim is to find the corresponding reconciled parameters, $RT_{i,s}$ and $RCP_{i,s}$ for all heat exchangers.

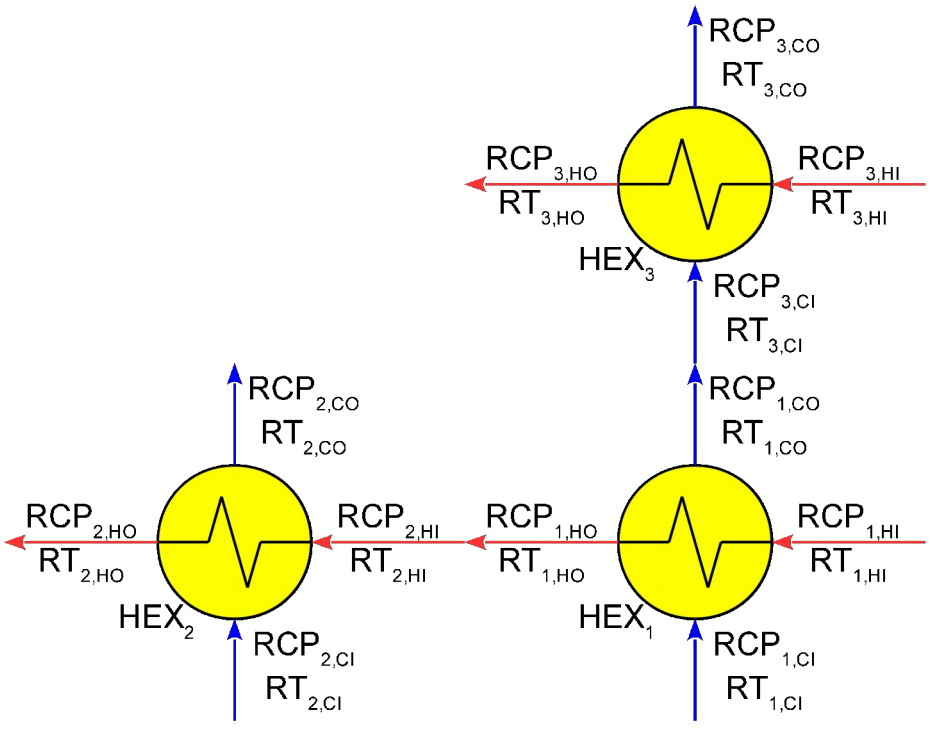

Figure 3.1: Example of a HEN

Simultaneous Solving Method

$$Min \sum_{i}^{I} \sum_{s}^{S} \sum_{n}^{N} \left(\left(RCP_{i,s} - CP_{i,s,n} \right)^2 + \left(RT_{i,s} - T_{i,s,n} \right)^2 \right) \quad (3.1)$$

subject to:
Mass balance constraints around each heat exchanger, for all heat exchanger
For example, HEX_1 in Figure 3.1

$$RCP_{1,HI} = RCP_{1,HO} \quad (3.2)$$

$$RCP_{1,CI} = RCP_{1,CO} \quad (3.3)$$

Energy balance constraints around each heat exchanger, for all heat exchanger
For example, HEX_1 in Figure 3.1

$$RCP_{1,HI} \left(RT_{1,HI} - RT_{1,HO} \right) = RCP_{1,CI} \left(RT_{1,CO} - RT_{1,CI} \right) \quad (3.4)$$

Constraints from network arising from the connections between heat exchangers
For example, according to Figure 3.1

$$RCP_{1,HO} = RCP_{2,HI} \quad (3.5)$$

$$RCP_{1,CO} = RCP_{3,CI} \quad (3.6)$$

$$RT_{1,HO} = RT_{2,HI} \quad (3.7)$$

$$RT_{1,CO} = RT_{3,CI} \quad (3.8)$$

Figure 3.2: Data reconciliation model for solving two parameters simultaneously

Figure 3.2 shows the model is conventionally solved when two types of parameters are reconciled simultaneously. In this context this is a simultaneous method. Linear least square method Eq(3.1) is used in the objective function to find reconciled values of all parameters using statistically given data. Least absolute method can be used in objective function and doing so eliminates the non-linearity in the objective function. It is however that least square method provides better accuracy as larger sums are penalised more. Least absolute method also may cause discontinuous function in the model that needs extra coding. It should be noted that heat capacity, CP is expressed in Eq(3.9):

$$CP = cp \times \dot{m} \quad (3.9)$$

where *cp* is the specific heat capacity of the stream and $\dot{m}$ is the mass flowrate. *cp* is a function of *T*. Depending on the *cp* function found in literature, it has at least power of three of *T*. Including this non-linear function into the model will cause it to be complex. Solving such highly non-linear model requires very high computational effort and time. The high non-linearity of the model also means no guarantees of finding the global optimum or – in extreme cases- even for numerical convergence. To reduce the degree of non-linearity, it is assumed that in this work *cp* is independent of *T*. Another factor which will increase the complexity of the model is the number of heat exchangers, which in turn affect the number of parameters to be reconciled.

There are three types of constraint equations used in the model. Mass balance constraint equations around a heat exchanger for all heat exchanger are shown in Eq(3.2) and Eq(3.3). The equations are straight forward since the equations only involve *RCP*. There are also constraint equations from network, shown in Eq(3.5) and Eq(3.6). These equations are used when the outlet of a heat exchanger is connected to an inlet of another heat exchanger. Energy balance constraint equations are however complicating the model as shown in Eq(3.4) when solved simultaneously. This is due to the equations containing the product of *RCP* and *RT*. The products of these two parameters, if solved simultaneously, increase the difficulty to solve the model. Doing so requires more computational effort and time. To reduce the degree of non-linearity in the model, iterative method is introduced in this work.

3.2.2 Iterative method and models

The iterative method is an alternative to the simultaneous method. The method partitions the model used in the simultaneous method into two sub-models. Iterating between the two sub-models, the method keeps one type of parameters constant (e.g. *T*) while reconciling the parameters of the other type (e.g. *CP*), until satisfactory convergence is achieved. Two types of parameters are reconciled separately while still maintaining the importance of other parameters in the models. Although the iterative method features some inaccuracy, compared to the simultaneous method, it is significantly less computationally intensive and simple to implement. Figure 3.3 shows the models used in iterative method. Compared to model shown in Figure 2.1, the constraint equations used are same except for the objective functions. Two models are used iteratively namely CP model and T model. CP model has only *CP* to be reconciled as shown in Eq(3.9) while keeping *RT* constant in Eq(3.4) and without Eq(3.7) and Eq(3.8). It is vice versa for T model. Each model shown is only required to reconcile one type of parameters. For CP model, it has both mass balance constraint and energy balance constraint equations. In the respective objective function in the models, the dimension of the parameters is the same, as this is not the case with simultaneous method.

CP Model	T Model
$Min \sum_{i}^{I} \sum_{s}^{S} \sum_{n}^{N} \left(RCP_{i,s} - CP_{i,s,n} \right)^2$ (3.9)	$Min \sum_{i}^{I} \sum_{s}^{S} \sum_{n}^{N} \left(RT_{i,s} - T_{i,s,n} \right)^2$ (3.10)
subject to: Mass balance constraints	subject to:
$RCP_{i,HI} = RCP_{i,HO}$ (3.2)	
$RCP_{i,CI} = RCP_{i,CO}$ (3.3)	
Energy balance constraints $RCP_{i,HI}\left(RT_{i,HI} - RT_{i,HO} \right) = RCP_{i,CI}\left(RT \right.$ (3.4)	Energy balance constraints $RCP_{i,HI}\left(RT_{i,HI} - RT_{i,HO} \right) = RCP_{i,CI}\left(R \right.$ (3.4)
where RT is set to be constant	where RCP is set to be constant
Constraints from network for example $RCP_{i1,HO} = RCP_{i2,HI}$ (3.5)	Constraints from network for example $RT_{i1,HO} = RT_{i2,HI}$ (3.7)

$$RCP_{i1,CO} = RCP_{i2,CI} \quad (3.6)$$

$$RT_{i1,CO} = RT_{i2,CI} \quad (3.8)$$

Figure 3.3: Equations used in CP model and T model

Figure 3.5 shows the algorithm to deploy these models. The algorithm starts with step 1 being collecting the necessary information for the data reconciliation problem. Step 2 is finding out the mean values of all parameters, which is important and will be used as the initial guess in either model. As for step 3, user has to choose either to reconcile *CP* or *T* first. For example, if *CP* is to be chosen to be reconciled first, the algorithm leads to step 3(a). Using the mean value of *T* found in step 2, substitute it into *RT* and solve using CP model to obtain *RCP*. Step 4(a) ensures that only one type of parameter is reconciled at a time. To obtain values for *RT*, the found value of *RCP* in step 4(a) is kept constant and substitute into T model in step 5(a). To find if the results are acceptable and consistence, in step 6, the percentage difference of the constant parameter in previous 2 steps and obtained parameter in previous step is calculated. That is, until this step, the percentage difference is calculated between constant *RT* values used in step 4(a) and reconciled *RT* values in step 5(a). If the percentage difference falls below satisfactory level, then proceed to and end at step 7. Else if it is not, then it should be iterated until it achieves the set satisfactory level. It should be noted that before step 6, reconciled *RT* values obtained in step 5(a) can be used in step 5(b). Then at step 6, the percentage difference is calculated between constant *RCP* values used in step 5(a) and reconciled *RCP* values in step 5(b). It is vice versa if *T* is to be reconciled first. The number of iterations is determined by the number of step 6 encountered. Overall if it does not stop at first iteration, the steps when choosing *CP* to be reconciled first would be:

1 → 2 → 3(a) → 4(a) → 5(a) → 6 → 5(b) → 6 → 5(a) → 6 → 5(b) →…→ 7

3.2.3 Illustrative Case Study

An illustrative case study is used to demonstrate the use of the algorithms. The HEN is shown in Figure 3.4. Over the years, the chemical plants underwent several modifications and twitching. This resulted in changes in the heat exchangers as well. It is desired to retrofit the current HEN to achieve minimal utility consumption with limited investment cost. It is included in the data reconciliation problem. It is assumed that measurements are taken at every inlets and outlets of every heat exchangers, heaters and coolers. After sets of measurements are taken repeatedly for a fixed period of time, the outliers are discarded using statistics. Out of these sets of measurements, 10 are chosen to be used as the input data.

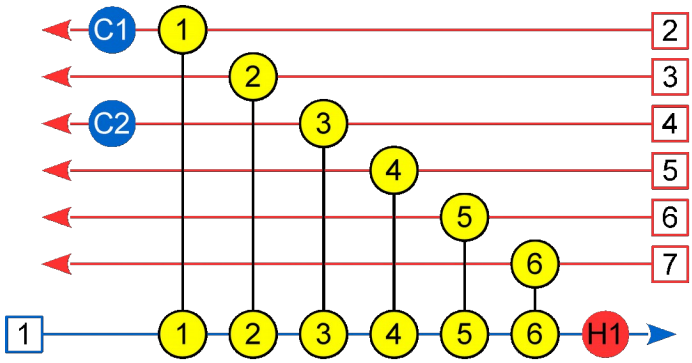

Figure 3.4: HEN for illustrative case study

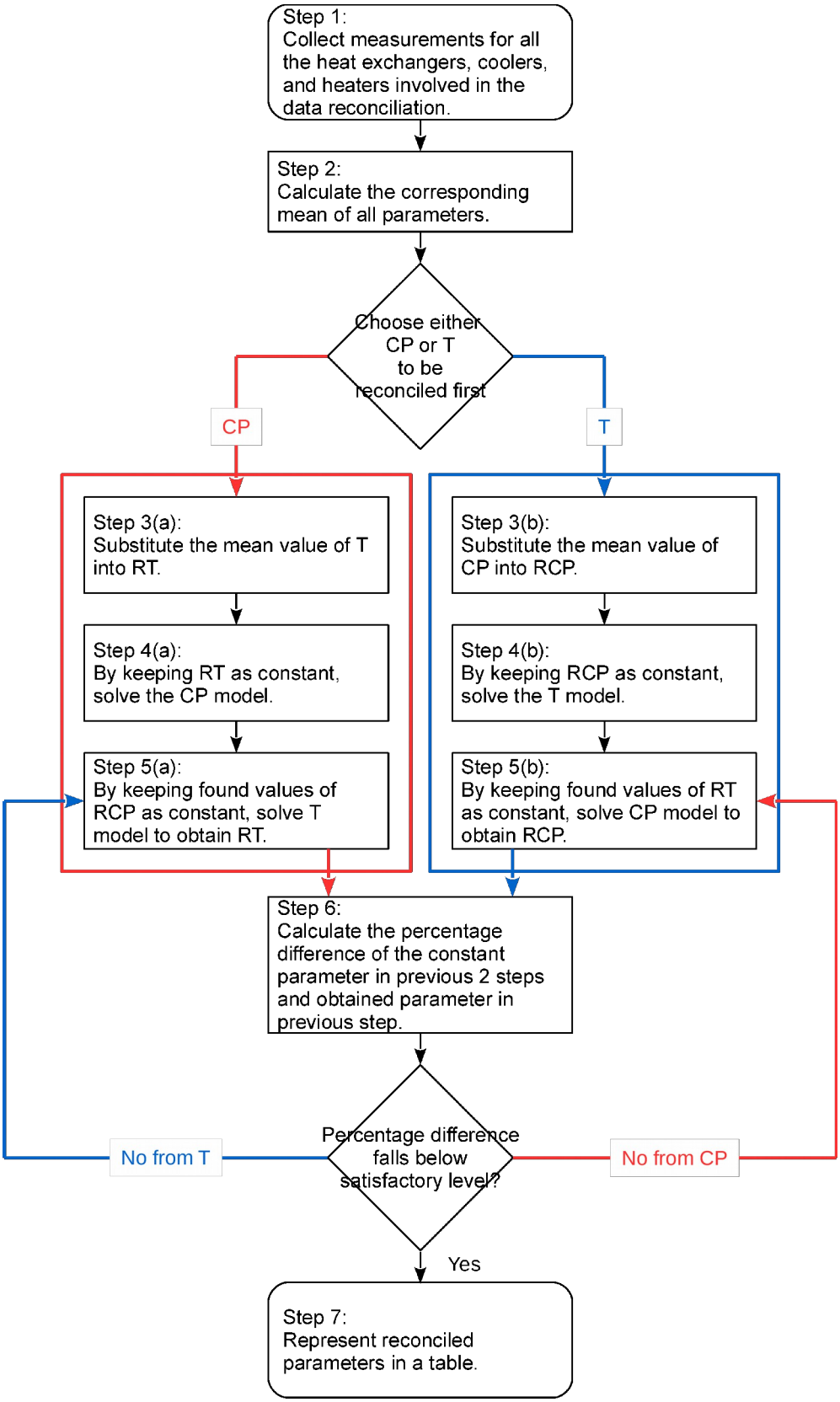

Figure 3.5: Algorithms of proposed iterative method

The next step is to calculate the mean values for all parameters. It is shown in Table 3.1.

Table 3.1: Mean values for all the parameters in the illustrative case study.

i	$T_{i,HI}$ (°C)	$T_{i,HO}$ (°C)	$CP_{i,HI}$ (kW/°C)	$CP_{i,HO}$ (kW/°C)	$T_{i,CI}$ (°C)	$T_{i,CO}$ (°C)	$CP_{i,CI}$ (kW/°C)	$CP_{i,CO}$ (kW/°C)
1	184.9	62.0	400.9	399.9	28.6	129.6	498.0	498.3
2	249.6	170.5	501.5	500.9	129.7	210.6	500.1	500.1
3	569.3	369.6	301.1	301.2	210.0	330.1	499.7	500.3
4	410.3	339.3	200.1	200.2	330.9	358.4	501.4	500.5
5	467.9	367.7	299.3	300.1	358.6	418.3	499.5	500.6
6	560.2	524.6	1,000.8	1,000.6	417.8	487.2	500.0	501.1
H1	800.2	700.1	299.5	299.9	488.9	548.3	499.5	499.7
C1	60.3	19.0	299.3	400.1	4.6	9.9	3,197.6	3,199.0
C2	370.9	319.5	302.8	301.2	5.0	9.9	3,000.6	3,000.6

Every heat exchanger has its own individual mass and energy constraint equations, for example for HEX-01:

$$RCP_{1,HI} = RCP_{1,HO} \tag{3.11}$$

$$RCP_{1,CI} = RCP_{1,CO} \tag{3.12}$$

$$RCP_{1,HI}\left(RT_{1,HI} - RT_{1,HO}\right) = RCP_{1,CI}\left(RT_{1,CO} - RT\right. \tag{3.13}$$

As for the constraints raised from network

$$RCP_{1,HO} = RCP_{C1,HI} \tag{3.14}$$

$$RCP_{3,HO} = RCP_{C2,HI} \tag{3.15}$$

$$RCP_{1,CO} = RCP_{2,CI} \tag{3.16}$$

$$RCP_{2,CO} = RCP_{3,CI} \tag{3.17}$$

$$RCP_{3,CO} = RCP_{4,CI} \tag{3.18}$$

$$RCP_{4,CO} = RCP_{5,CI} \tag{3.19}$$

$$RCP_{5,CO} = RCP_{6,CI} \tag{3.20}$$

$$RCP_{6,CO} = RCP_{H1,CI} \tag{3.21}$$

$$RT_{1,HO} = RT_{C1,HI} \tag{3.22}$$

$$RT_{3,HO} = RT_{C2,HI} \tag{3.23}$$

$$RT_{1,CO} = RT_{2,CI} \tag{3.24}$$

$$RT_{2,CO} = RT_{3,CI} \tag{3.25}$$

$$RT_{3,CO} = RT_{4,CI} \tag{3.26}$$

$$RT_{4,CO} = RT_{5,CI} \tag{3.27}$$

$$RT_{5,CO} = RT_{6,CI} \tag{3.28}$$

$$RT_{6,CO} = RT_{H1,CI} \tag{3.29}$$

In this case study, both CP and T solution routes will be investigated. In the following section has CP path is to be chosen first. It is decided that step 3(a) and 4(a) are to be followed next. The mean value of *T* parameters are substituted and kept constant while solving the CP model. The result after Step 4(a) is shown in Table 3.2.

Using the result in Table 3.2, in Step 5(a), *RCP* obtained is kept constant and *RT* is solved in T model. The result is shown in Table 3.3.

Table 3.2: Result for the illustrative case study after Step 4(a) in first iteration following CP path

i	$T_{i,HI}$ (°C)	$T_{i,HO}$ (°C)	$CP_{i,HI}$ (kW/°C)	$CP_{i,HO}$ (kW/°C)	$T_{i,CI}$ (°C)	$T_{i,CO}$ (°C)	$CP_{i,CI}$ (kW/°C)	$CP_{i,CO}$ (kW/°C)
1	184.9	62.0	402.6	402.6	28.6	129.6	490.0	490.0
2	249.6	170.5	501.1	501.1	129.7	210.6	490.0	490.0
3	569.3	369.6	294.7	294.7	210.0	330.1	490.0	490.0
4	410.3	339.3	189.8	189.8	330.9	358.4	490.0	490.0
5	467.9	367.7	291.9	291.9	358.6	418.3	490.0	490.0
6	560.2	524.6	955.1	955.1	417.8	487.2	490.0	490.0
H1	800.2	700.1	290.7	290.7	488.9	548.3	490.0	490.0
C1	60.3	19.0	402.6	402.6	4.6	9.9	3,137.6	3,137.6
C2	370.9	319.5	294.7	294.7	5.0	9.9	3,090.9	3,090.9

Table 3.3: Result for the illustrative case study after Step 5(a) in first iteration following CP path

i	$T_{i,HI}$ (°C)	$T_{i,HO}$ (°C)	$CP_{i,HI}$ (kW/°C)	$CP_{i,HO}$ (kW/°C)	$T_{i,CI}$ (°C)	$T_{i,CO}$ (°C)	$CP_{i,CI}$ (kW/°C)	$CP_{i,CO}$ (kW/°C)
1	184.7	61.3	402.6	402.6	28.3	129.8	490.0	490.0
2	249.6	170.5	501.1	501.1	129.8	210.6	490.0	490.0
3	569.6	370.1	294.7	294.7	210.6	330.6	490.0	490.0
4	410.5	339.1	189.8	189.8	330.6	358.3	490.0	490.0
5	468.0	367.6	291.9	291.9	358.3	418.0	490.0	490.0
6	560.4	524.4	955.1	955.1	418.0	488.2	490.0	490.0
H1	800.4	699.9	290.7	290.7	488.2	547.9	490.0	490.0
C1	61.3	19.0	402.6	402.6	4.5	10.0	3,137.6	3,137.6
C2	370.1	319.5	294.7	294.7	5.0	9.9	3,090.9	3,090.9

According to Step 6, the difference of the constant parameter in Step 4(a) (i.e. *RT* in Table 3.2) and obtained parameter in Step 5(a) (i.e. *RT* in Table 3.3) is calculated.

Table 3.4: Percentage difference of *RT* in first iteration for illustrative case study following CP path

i	$T_{i,HI}$ (%)	$T_{i,HO}$ (%)	$CP_{i,HI}$ (%)	$CP_{i,HO}$ (%)	$T_{i,CI}$ (%)	$T_{i,CO}$ (%)	$CP_{i,CI}$ (%)	$CP_{i,CO}$ (%)
1	-0.11	-1.21	-	-	-0.90	0.12	-	-
2	-0.02	0.02	-	-	0.05	-0.01	-	-
3	0.05	0.14	-	-	0.27	0.14	-	-
4	0.06	-0.07	-	-	-0.10	-0.04	-	-
5	0.02	-0.02	-	-	-0.10	-0.06	-	-
6	0.04	-0.04	-	-	0.06	0.21	-	-
H1	0.03	-0.04	-	-	-0.14	-0.08	-	-
C1	1.58	0.04	-	-	-1.30	0.61	-	-
C2	-0.22	0.00	-	-	0.76	-0.38	-	-

From Table 3.4, it is shown that the differences are well below 2 %. Since in this case study the required satisfactory level is below 5 %, the results are accepted. For primary analysis, one round of iteration is sufficient to achieve the result and solve the data reconciliation problem. It can be further iterated to achieve stricter satisfactory level. To do so, according to Figure 3.5,

the next step is Step 5(b), where the obtained *RT* is kept constant and CP model is solved to obtain *RCP*.

Table 3.5: Result for the illustrative case study after Step 5(b) in second iteration following CP path

i	$T_{i,HI}$ (°C)	$T_{i,HO}$ (°C)	$CP_{i,HI}$ (kW/°C)	$CP_{i,HO}$ (kW/°C)	$T_{i,CI}$ (°C)	$T_{i,CO}$ (°C)	$CP_{i,CI}$ (kW/°C)	$CP_{i,CO}$ (kW/°C)
1	184.7	61.3	407.8	407.8	28.3	129.8	495.7	495.7
2	249.6	170.5	506.4	506.4	129.8	210.6	495.7	495.7
3	569.6	370.1	298.2	298.2	210.6	330.6	495.7	495.7
4	410.5	339.1	192.3	192.3	330.6	358.3	495.7	495.7
5	468.0	367.6	294.8	294.8	358.3	418.0	495.7	495.7
6	560.4	524.4	966.7	966.7	418.0	488.2	495.7	495.7
H1	800.4	699.9	294.5	294.5	488.2	547.9	495.7	495.7
C1	61.3	19.0	407.8	407.8	4.5	10.0	3,136.1	3,136.1
C2	370.1	319.5	298.2	298.2	5.0	9.9	3,079.3	3,079.3

After step 5(b), step 6 is visited again. The obtain *RCP* results in Table 3.5 are used to compare with the *RCP* results in Table 3.3. The differences are shown in Table 3.6. The calculated differences are around 1 %, which are lower than pervious iteration.

Table 3.6: Percentage difference of *RCP* in second iteration for illustrative case study following CP path

i	$T_{i,HI}$ (%)	$T_{i,HO}$ (%)	$CP_{i,HI}$ (%)	$CP_{i,HO}$ (%)	$T_{i,CI}$ (%)	$T_{i,CO}$ (%)	$CP_{i,CI}$ (%)	$CP_{i,CO}$ (%)
1	-	-	1.27	1.27	-	-	1.18	1.18
2	-	-	1.06	1.06	-	-	1.18	1.18
3	-	-	1.20	1.20	-	-	1.18	1.18
4	-	-	1.35	1.35	-	-	1.18	1.18
5	-	-	1.00	1.00	-	-	1.18	1.18
6	-	-	1.21	1.21	-	-	1.18	1.18
H1	-	-	1.29	1.29	-	-	1.18	1.18
C1	-	-	1.27	1.27	-	-	-0.05	-0.05
C2	-	-	1.20	1.20	-	-	-0.38	-0.38

To see how well the iterative method performs using CP path, the final result from Table 3.6 is compared with respective mean values in . Most of the reconciled parameters do not defer more than 2 % from mean values, with the highest being less than 4 %.

T path is to be demonstrated next to show the effect of choosing different part. After step 2, step 3(b) and 4(b) are to be followed next. While solving the T model, the mean values of *CP* parameters are substituted and kept constant. Table 3.8 shows the result after step 4(b).

Table 3.7: Percentage difference of the results obtained after second iteration for illustrative case study following CP path with respective mean values

i	$T_{i,HI}$ (%)	$T_{i,HO}$ (%)	$CP_{i,HI}$ (%)	$CP_{i,HO}$ (%)	$T_{i,CI}$ (%)	$T_{i,CO}$ (%)	$CP_{i,CI}$ (%)	$CP_{i,CO}$ (%)
1	-0.11	-1.21	1.71	1.98	-0.90	0.12	-0.45	-0.51
2	-0.02	0.02	0.98	1.11	0.05	-0.01	-0.87	-0.87
3	0.05	0.14	-0.97	-1.00	0.27	0.14	-0.79	-0.90
4	0.06	-0.07	-3.89	-3.93	-0.10	-0.04	-1.13	-0.94
5	0.02	-0.02	-1.51	-1.76	-0.10	-0.06	-0.75	-0.97
6	0.04	-0.04	-3.41	-3.38	0.06	0.21	-0.85	-1.06
H1	0.03	-0.04	-1.67	-1.81	-0.14	-0.08	-0.75	-0.78
C1	1.58	0.04	2.12	1.91	-1.30	0.61	-1.92	-1.97
C2	-0.22	0.00	-1.52	-1.00	0.76	-0.38	2.62	2.62

Table 3.8: Result for the illustrative case study after step 4(b) in first iteration following T path

i	$T_{i,HI}$ (°C)	$T_{i,HO}$ (°C)	$CP_{i,HI}$ (kW/°C)	$CP_{i,HO}$ (kW/°C)	$T_{i,CI}$ (°C)	$T_{i,CO}$ (°C)	$CP_{i,CI}$ (kW/°C)	$CP_{i,CO}$ (kW/°C)
1	185.5	60.9	400.9	399.9	29.3	129.6	498.0	498.3
2	250.2	169.9	501.5	500.9	129.6	210.1	500.1	500.1
3	569.5	370.2	301.1	301.2	210.1	330.2	499.7	500.3
4	410.2	339.4	200.1	200.2	330.2	358.4	501.4	500.5
5	467.6	368.0	299.3	300.1	358.4	418.2	499.5	500.6
6	559.9	524.9	1,000.8	1,000.6	418.2	488.2	500.0	501.1
H1	800.2	700.1	299.5	299.9	488.2	548.2	499.5	499.7
C1	60.9	19.0	399.3	400.1	4.6	9.9	3,197.6	3,199.0
C2	370.2	319.5	302.8	301.2	4.9	10.0	3,000.6	3,000.6

In step 5(b), using the result in Table 3.8, *RT* is kept constant and *RCP* is solved in CP model. Table 3.9 shows the result after step 5(b).

Table 3.9: Result for the illustrative case study after step 5(b) in first iteration following T path

i	$T_{i,HI}$ (°C)	$T_{i,HO}$ (°C)	$CP_{i,HI}$ (kW/°C)	$CP_{i,HO}$ (kW/°C)	$T_{i,CI}$ (°C)	$T_{i,CO}$ (°C)	$CP_{i,CI}$ (kW/°C)	$CP_{i,CO}$ (kW/°C)
1	185.5	60.9	403.7	403.7	29.3	129.6	501.5	501.5
2	250.2	169.9	502.8	502.8	129.6	210.1	501.5	501.5
3	569.5	370.2	302.2	302.2	210.1	330.2	501.5	501.5
4	410.2	339.4	199.8	199.8	330.2	358.4	501.5	501.5
5	467.6	368.0	301.1	301.1	358.4	418.2	501.5	501.5
6	559.9	524.9	1,003.0	1,003.0	418.2	488.2	501.5	501.5
H1	800.2	700.1	300.6	300.6	488.2	548.2	501.5	501.5
C1	60.9	19.0	403.7	403.7	4.6	9.9	3,191.5	3,191.5
C2	370.2	319.5	302.2	302.2	4.9	10.0	3,004.3	3,004.3

According to Step 6, the difference of the constant parameter in Step 4(b) (i.e. *RCP* in Table 3.8) and obtained parameter in Step 5(b) (i.e. *RCP* in Table 3.9) is calculated. The results are shown in Table 3.10.

Table 3.10: Percentage difference of *RCP* in the first iteration for illustrative case study following T path

i	$T_{i,HI}$ (%)	$T_{i,HO}$ (%)	$CP_{i,HI}$ (%)	$CP_{i,HO}$ (%)	$T_{i,CI}$ (%)	$T_{i,CO}$ (%)	$CP_{i,CI}$ (%)	$CP_{i,CO}$ (%)
1	-	-	0.70	0.96	-	-	0.70	0.64

2	-	-	0.25	0.38	-	-	0.28	0.28
3	-	-	0.37	0.34	-	-	0.36	0.25
4	-	-	-0.17	-0.22	-	-	0.02	0.21
5	-	-	0.60	0.35	-	-	0.40	0.18
6	-	-	0.22	0.25	-	-	0.30	0.09
H1	-	-	0.37	0.23	-	-	0.40	0.37
C1	-	-	1.10	0.90	-	-	-0.19	-0.23
C2	-	-	-0.19	0.34	-	-	0.12	0.13

From Table 3.10, the differences are mostly well below 1 %. As the differences are lower than the satisfactory level of 5 %, it shows that for this case study, T path is more suitable in this reconciliation problem. A round of iteration is sufficient to achieve the satisfactory result. Further iteration is carried out to check the performance of T path in this case study. According to Figure 3.5, the next step is Step 5(a), where the obtained *RCP* is kept constant and T model is solved to obtain *RT*.

Table 3.11: Result for the illustrative case study after Step 5(a) in second iteration following T path

i	$T_{i,HI}$ (°C)	$T_{i,HO}$ (°C)	$CP_{i,HI}$ (kW/°C)	$CP_{i,HO}$ (kW/°C)	$T_{i,CI}$ (°C)	$T_{i,CO}$ (°C)	$CP_{i,CI}$ (kW/°C)	$CP_{i,CO}$ (kW/°C)
1	185.5	60.9	403.7	403.7	29.3	129.6	501.5	501.5
2	250.2	169.9	502.8	502.8	129.6	210.1	501.5	501.5
3	569.5	370.2	302.2	302.2	210.1	330.2	501.5	501.5
4	410.2	339.4	199.8	199.8	330.2	358.4	501.5	501.5
5	467.6	368.0	301.1	301.1	358.4	418.2	501.5	501.5
6	559.9	524.9	1,003.0	1,003.0	418.2	488.2	501.5	501.5
H1	800.2	700.1	300.6	300.6	488.2	548.2	501.5	501.5
C1	60.9	19.0	403.7	403.7	4.6	9.9	3,191.5	3,191.5
C2	370.2	319.5	302.2	302.2	4.9	10.0	3,004.3	3,004.3

Following Step 6, the obtained *RT* results in Table 3.11 are used to compare with the kept constant *RT* results in Table 3.9. The calculated differences are shown in Table 3.12. All calculated differences are near to 0 %, with the highest value not exceeding 1 %. Further iteration is not required as it will produce similar result.

Table 3.12: Percentage difference of RT in second iteration for illustrative case study following T path

i	$T_{i,HI}$ (%)	$T_{i,HO}$ (%)	$CP_{i,HI}$ (%)	$CP_{i,HO}$ (%)	$T_{i,CI}$ (%)	$T_{i,CO}$ (%)	$CP_{i,CI}$ (%)	$CP_{i,CO}$ (%)
1	0.00	-0.01	-	-	0.01	0.00	-	-
2	0.00	0.00	-	-	0.00	0.00	-	-
3	0.00	0.00	-	-	0.00	0.00	-	-
4	0.00	-0.00	-	-	0.00	-0.01	-	-
5	-0.01	0.01	-	-	-0.01	0.01	-	-
6	0.00	0.00	-	-	0.01	0.00	-	-

H1	0.00	0.00	-	-	0.00	-0.00	-	-
C1	-0.01	0.02	-	-	-0.71	0.33	-	-
C2	0.00	0.00	-	-	0.16	-0.08	-	-

To see how well the iterative method performs using CP path, the final result in Table 3.12 is compared with respective mean values. Table 3.13 shows the calculated difference with respective mean values. Most of the difference values are not more than 2 %, with only one value not exceeding 2.5 %. This shows that T path is more suitable to be used in this case study, as reconciled parameters do not deviate from mean values compared to CP path. Overall, it shows that iterative method, whether CP path or T path, is suitable to be used to obtain reconciled parameters in this case study. The possible difference between the CP path and T path is the initial parameters to be reconciled, as CP model involves lower number of parameters than T model. When compared to respective mean values, the differences have low values in an iteration. As for computational effort, since this case study is smaller scale in comparison, the results are obtained in less than 1 s.

Table 3.13: Percentage difference of the results obtained after second iteration for illustrative case study following T path with respective mean values

i	$T_{i,HI}$ (%)	$T_{i,HO}$ (%)	$CP_{i,HI}$ (%)	$CP_{i,HO}$ (%)	$T_{i,CI}$ (%)	$T_{i,CO}$ (%)	$CP_{i,CI}$ (%)	$CP_{i,CO}$ (%)
1	0.31	-1.83	0.70	0.96	2.45	0.00	0.70	0.64
2	0.24	-0.36	0.25	0.38	-0.08	-0.22	0.28	0.28
3	0.03	0.15	0.37	0.34	0.06	0.04	0.36	0.25
4	-0.03	0.04	-0.17	-0.22	-0.21	0.00	0.02	0.21
5	-0.06	0.08	0.60	0.35	-0.05	-0.02	0.40	0.18
6	-0.06	0.06	0.22	0.25	0.10	0.20	0.30	0.09
H1	0.01	-0.01	0.37	0.23	-0.15	-0.01	0.40	0.37
C1	0.94	0.00	1.10	0.90	0.04	-0.02	-0.19	-0.23
C2	-0.20	0.00	-0.19	0.34	-1.96	1.00	0.12	0.13

3.2.4 Industrial Case Study

The following case study is taken from a small petroleum refinery located in Central Europe. (Nemet et al., 2015). The data reconciliation problem is discussed in the work of Yong et al. (2016). In the HEN shown in Figure 3.7, there are 13 heat exchangers, 5 heaters and 16 coolers. Note that in the HEN utility streams are included, including arbitrary heater and cooling stream. It does not accurately represent the actual refinery to protect the sensitive information. There are some utility streams exchanging heat with multiple process streams in a pass. In actual refinery, the heating or cooling requirement might be provided individually.

The HEN is required to be reconciled for Heat Integration analysis purpose. For iterative method, it is decided to follow CP path to have lower number of parameters during initial stage. For comparison purpose, normal method (simultaneous reconciliation) is also employed to solve the data reconciliation problem.

Table 3.14 shows the normalized sum of the squares of errors (objective function) at different stages of iteration. The objective function after step 4(a) is the lowest, it is due to the constraint regarding outlet and inlet temperature equality of stream was not active yet. After the first iteration, it is found that the obtained result is less than satisfactory level. Second iteration is carried out and has result confirmed to satisfactory level although the objective value only decreased marginally.

Table 3.14: Objective values at different stages of iteration

	After step 4(a)	First iteration	Second iteration
Objective value	3,378.1	4,366.0	4,365.5

As for simultaneous reconciliation, the final objective function obtained is 3,961.5, decreased by 404 (9.25 %). Frequency analysis of the normalized errors is performed in order to compare the results obtained by the iterative and the simultaneous methods. It is shown in Figure 3.6. Note that the normalization is performed by standard deviations in order to merge errors of different variables on the same graph. As expected, the dispersion is wider when the iterative method is used, especially as it can be observed in the areas marked with boxes.

According to the work of Yong et al. (2016), it is reported that while using simultaneous method, obtaining global optimum was not a straightforward task either. Using described model for simultaneous method, the relative gap of less than 1 % in 8 major iterations is reached after 1,485 CPU s (Intel Core i7; 3.4 GHz). As for iterative method, the results are reached in less than 100 CPU s. The accuracy achieved by the iteration method in this case study is less than 10 % higher. This shows that iterative method has significantly lower computational effort at some expense of accuracy.

From the two case studies, the second iteration showed decreased in objective function values. This indirectly indicates that this algorithm converges. Similar work (Beck, 2015) has shown that such algorithm converges.

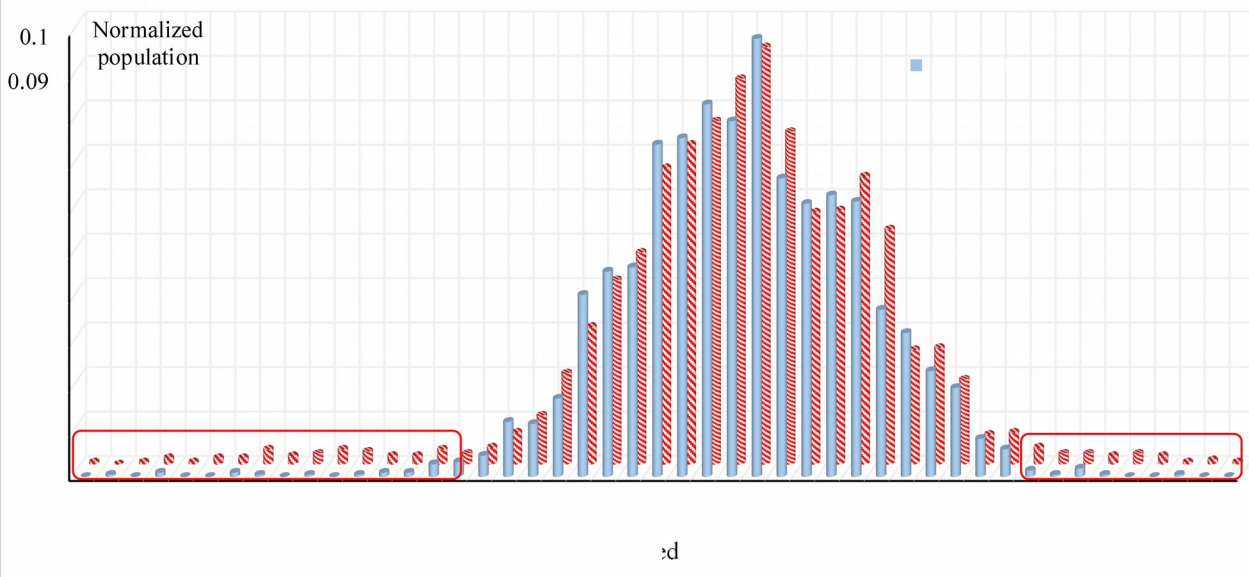

Figure 3.6: Frequency analysis of the iterative and simultaneous approaches for normalized differences between measured and reconciled values

Limitations are encountered in this industrial case study when using the iterative method. It occurs when more than one consecutive heat exchanger is located between the same hot and cold streams. For example, in this case study, it can be seen from heat exchanger number 1, 2 and 3. After CP model is solved in step 4(a), these heat exchangers have the same values of cold and hot streams *CP*. This becomes too constrained and infeasible when solving T model at step 5(a). For now, the infeasibility has been overcome by assuming these heat exchangers as one and the in-between data was recalculated after the optimization. The next section discusses these limitations and strategies to overcome them.

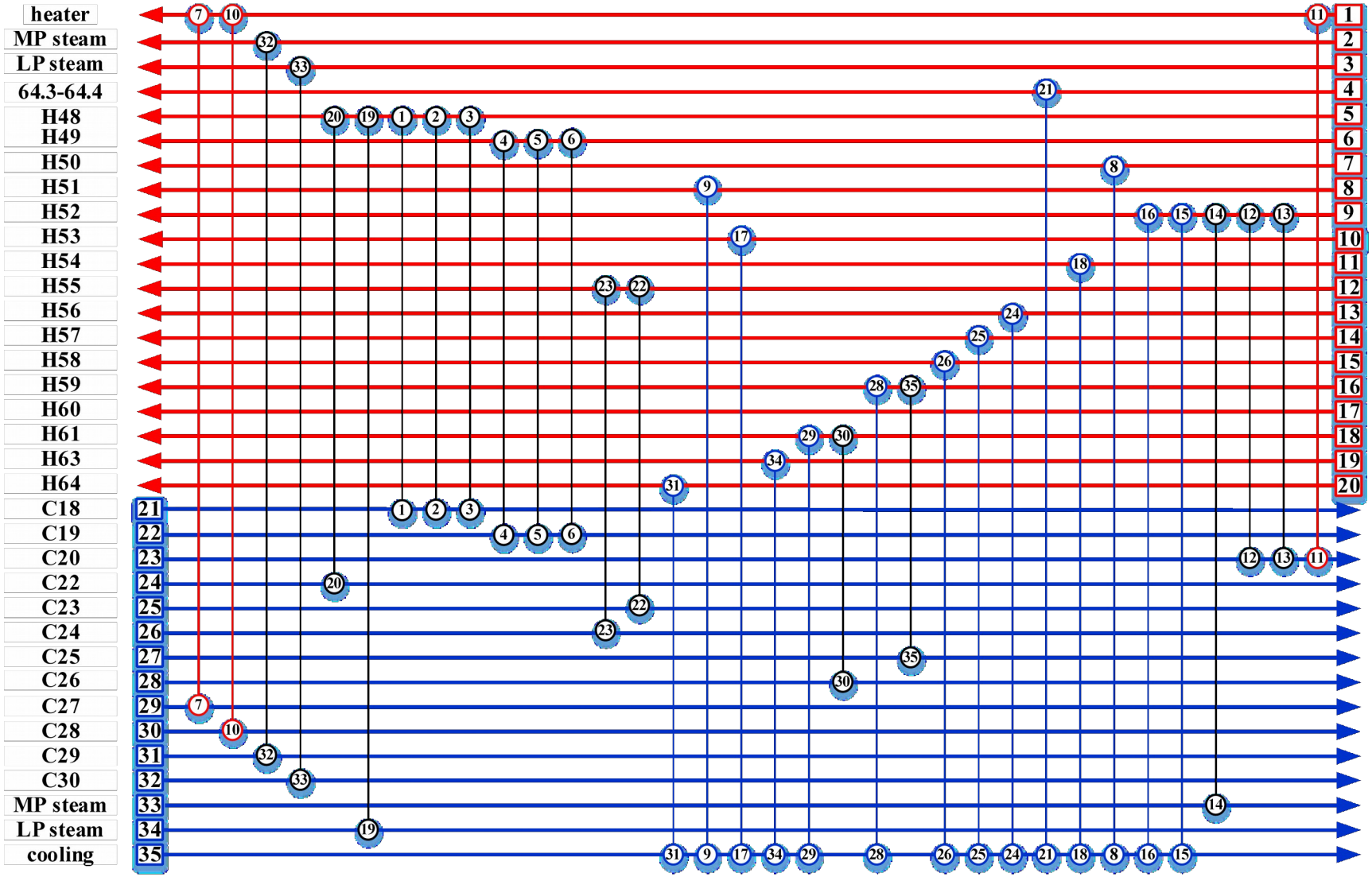

Figure 3.7: HEN of a petroleum refinery in Central Europe

3.3 Limitation and Strategies for Application of the Iterative Method

As discussed in industrial case study in the section 3.2, the iterative method has a limitation. Applied directly it is unable to reconcile HEN that has one or more heat loops. The simplest heat loop consists of two consecutive heat exchangers that connect the same hot and cold streams (Figure 3.8). This is a common industrial practice when heat load is too large to be performed by a single heat exchanger. The arrangement usually includes two or more smaller heat exchangers. Heat loops may also occur spanning across different streams, as shown in Figure 3.9.

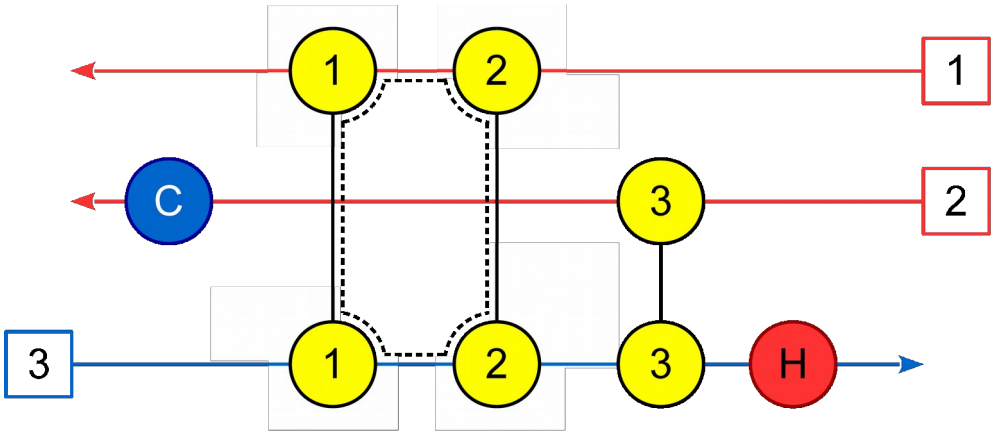

Figure 3.8: HEN having consecutive heat exchangers

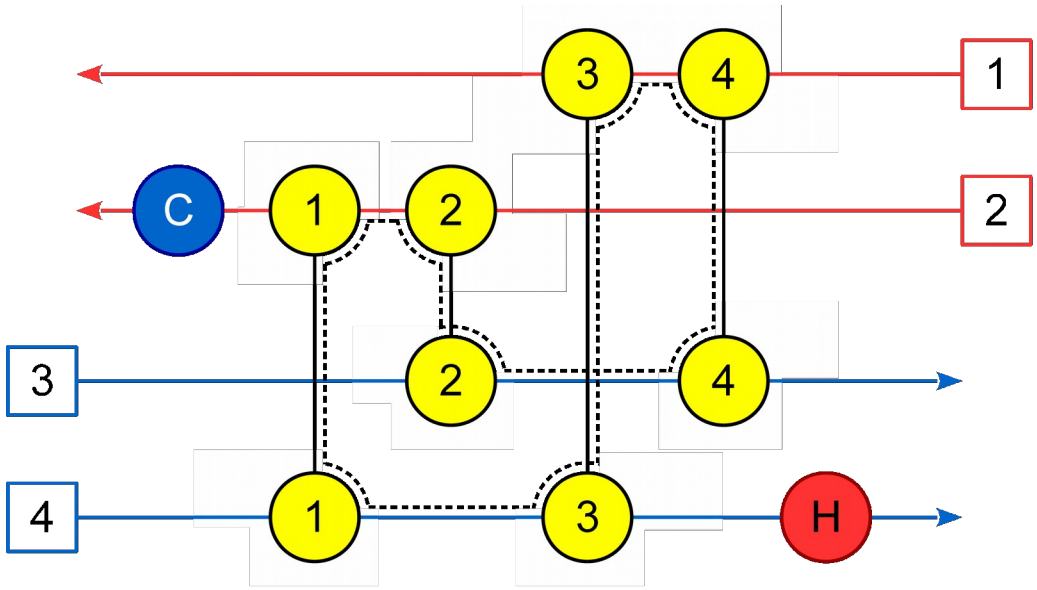

Figure 3.9: HEN with heat loop involving different streams

As the iterative method operates by assuming either one of the parameter types (*T* or *CP*) to be constant, the problem becomes too constrained and infeasible. For example in Figure 2.7, when *RT* in CP model is kept constant, focusing on only HEX-01 and HEX-02

Mass balance around HEX-01 for both hot and cold streams

$$RCP_{1,HI} = RCP_{1,HO} \tag{3.30}$$

$$RCP_{1,CI} = RCP_{1,CO} \tag{3.31}$$

Mass balance around HEX-02 for both hot and cold streams

$$RCP_{2,HI} = RCP_{2,HO} \tag{3.32}$$

$$RCP_{2,CI} = RCP_{2,CO} \tag{3.33}$$

Energy balance around HEX-01

$$RCP_{1,HI}\left(RT_{1,HI} - RT_{1,HO}\right) = RCP_{1,CI}\left(RT_{1,CO} - RT_{1,CI}\right) \tag{3.34}$$

where *RT* is set to be constant

Energy balance around HEX-02

$$RCP_{2,HI}\left(RT_{2,HI} - RT_{2,HO}\right) = RCP_{2,CI}\left(RT_{2,CO} - RT_{2,CI}\right) \tag{3.35}$$

where *RT* is set to be constant

From the connections of HEX-01 and HEX-02

$$RCP_{1,HO} = RCP_{2,HI} \tag{3.36}$$

$$RCP_{2,CO} = RCP_{1,CI} \tag{3.37}$$

From Eq(2.30), Eq(2.31) and Eq(2.36), trivially

$$RCP_{1,HI} = RCP_{1,HO} = RCP_{2,HI} = RCP_{2,HO} \tag{2.38}$$

And from Eq(2.32), Eq(2.33) and Eq(2.37), trivially

$$RCP_{1,CI} = RCP_{1,CO} = RCP_{2,CI} = RCP_{2,CO} \tag{2.39}$$

This results in Eq(2.34) and Eq(2.35) becoming

$$RCP_{1,HI}\left(RT_{1,HI} - RT_{1,HO}\right) = RCP_{1,CI}\left(RT_{1,CO} - RT_{1,CI}\right) \tag{2.40}$$

$$RCP_{1,HI}\left(RT_{2,HI} - RT_{2,HO}\right) = RCP_{1,CI}\left(RT_{2,CO} - RT_{2,CI}\right) \tag{2.41}$$

In most cases, as this is due to *RT* has to be set to be constant according to the procedure

$$RT_{1,HI} - RT_{1,HO} \neq RT_{2,HI} - RT_{2,HO} \tag{2.42}$$

$$RT_{1,CO} - RT_{1,CI} \neq RT_{2,CO} - RT_{2,CI} \tag{2.43}$$

Thus in this scenario it is too constrained resulting in only having one answer

$$RCP_{1,HI} = RCP_{1,HO} = RCP_{2,HI} = RCP_{2,HO} = 0 \quad (2.44)$$

$$RCP_{1,CI} = RCP_{1,CO} = RCP_{2,CI} = RCP_{2,CO} = 0 \quad (3.45)$$

The following section discusses a few strategies are attempted to solve this limitation.

3.3.1 Strategies Employed to Solve the Limitation

3.3.1.1 Merging consecutive heat exchangers (Strategy 1)

The consecutive heat exchangers with their loads are modelled as a lump. The intermediate temperatures are estimated separately after the reconciliation. The number of parameters to be reconciled decreases due to certain parameters eliminated from the model. This is the simplest strategy but only applicable to consecutive heat exchangers as shown in Figure 3.8. This strategy cannot be applied to HENs with heat loops involving other heat exchanger or other stream.

3.3.1.2 Assume heat exchangers in heat loop with different CPs (Strategy 2)

This strategy assumes heat exchangers in the heat loop to have different *CP*s. This direct strategy disables the connecting *CP* constraints of involving heat exchangers in CP model. The number of parameters to be reconciled remains the same. It is noted that using this strategy would cause difficulties in Heat Integration analysis – particularly in Pinch Analysis. The multiple reconciled CP values of a stream may differ too much, in a discontinuous manner. The reconciled *CP* value may suddenly increase or decrease when a certain temperature is reached. This may cause Heat Integration analysis to have streams represented in two segments and hinder better Heat Integration.

3.3.1.3 Assume heat exchangers in heat loop with small different heat load (Strategy 3)

Heat exchangers are allowed to have differences in heat load instead in the models. The energy balance equation (Eq(3.4)) is added with a variable - *α* as shown in Eq(3.46). The variable, α relax Eq(3.36) and Eq(3.37) as it allows different values of *CP* of the same heat exchanger to exist. The constraint will have value between 0 and 1. To minimise these differences, the objective functions of both models also include *α* to be minimised, as shown in Eq(2.47) and Eq(3.48). This strategy adds more variables to the models, depending on the number of heat exchangers involved in the heat loop. Generally, using the iterative method with this strategy still has lower number of variables per model, compared to the simultaneous method.

$$RCP_{i,HI}\left(\quad (3.46)$$

CP Model

$$Min \sum_{i}^{I} \sum_{s}^{S} \sum_{n}^{N} \left(\left(RCP_{i,s} - CP_{i,s,n} \right)^2 + \alpha_i \right) \quad (3.47)$$

T Model

$$Min \sum_{i}^{I} \sum_{s}^{S} \sum_{n}^{N} \left(\left(RT_{i,s} - T_{i,s,n} \right)^2 + \alpha_i \right) \quad (3.48)$$

3.3.2 Illustrative Case Study – HEN Loops

The illustrative case study is derived partially from Liew et al. (2012). In the case study, chemical plant A is chosen out of the two plants. Figure 3.10 shows the HEN of chemical plant A. Eight parameters are considered in every heat exchanger, namely inlet and outlet temperatures for hot and cold streams ($T_{i,HI}$, $T_{i,HO}$, $T_{i,CI}$, $T_{i,CO}$) and heat capacities for hot and cold streams ($CP_{i,HI}$, $CP_{i,HO}$, $CP_{i,CI}$, $CP_{i,CO}$). Measurements are taken repeatedly over a period of time for every heat exchanger in steady state. Outliers are removed statistically and 10 sets of measurements are chosen to be included in the reconciliation. Table 3.15 shows the respective mean values for all the parameters. All T measured are in °C and CP in kW/°C.

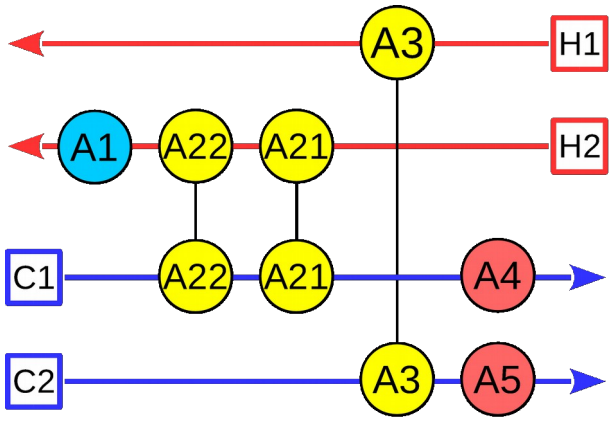

Figure 3.10: Illustrative case study with consecutive heat exchangers

Table 3.15: Mean values for all parameters in the illustrative case study with consecutive heat exchangers

i	$T_{i,HI}$ (°C)	$T_{i,HO}$ (°C)	$CP_{i,HI}$ (kW/°C)	$CP_{i,HO}$ (kW/°C)	$T_{i,CI}$ (°C)	$T_{i,CO}$ (°C)	$CP_{i,CI}$ (kW/°C)	$CP_{i,CO}$ (kW/°C)
A1	70.05	60.06	40.07	39.87	14.92	19.87	79.93	79.94
A22	150.21	110.02	39.89	40.77	72.87	95.60	70.05	70.07
A21	110.16	70.03	40.01	39.91	50.10	72.90	70.01	69.95
A3	199.79	99.99	19.98	19.42	49.96	183.60	14.85	14.96
A4	133.60	132.60	1,702.30	1,699.50	95.76	120.19	70.03	70.01
A5	270.00	269.00	549.80	550.60	183.30	219.96	15.24	14.96

3.3.2.1 Strategy 1

The values of reconciled parameters after step 5(b) are shown in Table 3.16.

Two iterations are gone through to achieve the satisfactory result as the differences are near 0 %. It should be noted that the intermediate temperatures (marked with *) are calculated manually after the results are obtained. The comparisons with respective mean values are shown in Table 3.17.

Table 3.16: Reconciled values for all parameters in the illustrative case study with consecutive heat exchangers using strategy 1

i	$T_{i,HI}$ (°C)	$T_{i,HO}$ (°C)	$CP_{i,HI}$ (kW/°C)	$CP_{i,HO}$ (kW/°C)	$T_{i,CI}$ (°C)	$T_{i,CO}$ (°C)	$CP_{i,CI}$ (kW/°C)	$CP_{i,CO}$ (kW/°C)
A1	70.05	60.07	39.90	39.90	14.90	19.90	79.60	79.60
A22	150.18	110.12*	39.90	39.90	50.05	72.88*	70.03	70.03
A21	110.12*	70.05	39.90	39.90	72.88*	95.71	70.03	70.03
A3	199.58	100.20	20.52	20.52	49.81	183.53	15.25	15.25
A4	133.60	132.60	1,701.02	1,701.02	95.71	120.19	70.03	70.03
A5	270.01	269.00	550.17	550.17	183.53	219.96	15.25	15.25

Table 3.17: Percentage difference of the results with respective mean values using Strategy 1

i	$T_{i,HI}$ (%)	$T_{i,HO}$ (%)	$CP_{i,HI}$ (%)	$CP_{i,HO}$ (%)	$T_{i,CI}$ (%)	$T_{i,CO}$ (%)	$CP_{i,CI}$ (%)	$CP_{i,CO}$ (%)
A1	0.00	0.02	-0.42	-0.15	-0.17	0.13	-0.41	-0.42
A22	-0.02	0.09*	0.03	-0.17	0.01	0.11*	-0.03	-0.06
A21	-0.04*	0.03	-0.27	-0.24	-0.10*	-0.03	0.03	0.11
A3	-0.10	0.21	2.71	2.15	-0.31	-0.04	2.71	1.95
A4	0.00	0.00	-0.08	0.09	-0.06	0.00	0.00	0.03
A5	0.00	0.00	0.07	-0.08	0.12	0.00	0.08	1.95

3.3.2.2 Strategy 2

The values of reconciled parameters after step 5(b) are shown in Table 3.18.

Table 3.18: Reconciled values for all parameters in the illustrative case study with consecutive heat exchangers using strategy 2

i	$T_{i,HI}$ (°C)	$T_{i,HO}$ (°C)	$CP_{i,HI}$ (kW/°C)	$CP_{i,HO}$ (kW/°C)	$T_{i,CI}$ (°C)	$T_{i,CO}$ (°C)	$CP_{i,CI}$ (kW/°C)	$CP_{i,CO}$ (kW/°C)
A1	70.06	60.07	39.82	39.82	14.89	19.90	79.43	79.43
A22	150.17	110.09	39.82	39.82	72.89	95.72	69.92	69.92
A21	110.09	70.06	39.82	39.82	50.02	72.89	69.67	69.67
A3	199.58	100.20	20.52	20.52	49.81	183.53	15.25	15.25
A4	133.60	132.60	1,701.06	1,701.06	95.72	120.19	69.92	69.92
A5	270.01	269.00	550.17	550.17	183.53	219.96	15.25	15.25

Two iterations are gone through to achieve the satisfactory result as the differences are near 0 %. It should be noted that in the process, it is assumed that heat exchangers A21 and A22 have different heat capacity of the same cold stream. In this illustrative case study, the difference between these two values is small, at 0.36 %. The results obtained are compared with respective mean value, shown in Table 3.19.

Table 3.19: Percentage difference of the results with respective mean values using Strategy 2

i	$T_{i,HI}$ (%)	$T_{i,HO}$ (%)	$CP_{i,HI}$ (%)	$CP_{i,HO}$ (%)	$T_{i,CI}$ (%)	$T_{i,CO}$ (%)	$CP_{i,CI}$ (%)	$CP_{i,CO}$ (%)
A1	0.01	0.02	-0.63	-0.36	-0.18	0.14	-0.62	-0.63
A22	-0.03	0.06	-0.19	-0.39	0.03	0.12	-0.18	-0.21

A21	-0.07	0.04	-0.48	-0.46	-0.17	-0.01	-0.48	-0.40
A3	-0.10	0.21	2.71	2.15	-0.31	-0.04	2.71	1.95
A4	0.00	0.00	-0.07	0.09	-0.05	0.00	-0.15	-0.13
A5	0.00	0.00	0.07	-0.08	0.12	0.00	0.08	1.95

3.3.2.3 Strategy 3

The values of reconciled parameters after step 5(b) are shown in Table 3.20.

Table 3.20: Reconciled values for all parameters in the illustrative case study with consecutive heat exchangers using strategy 3

i	$T_{i,HI}$ (°C)	$T_{i,HO}$ (°C)	$CP_{i,HI}$ (kW/°C)	$CP_{i,HO}$ (kW/°C)	$T_{i,CI}$ (°C)	$T_{i,CO}$ (°C)	$CP_{i,CI}$ (kW/°C)	$CP_{i,CO}$ (kW/°C)
A1	70.06	60.07	39.96	39.96	14.89	19.90	79.72	79.72
A22	150.13	110.10	39.96	39.96	72.87	95.75	69.92	69.92
A21	110.10	70.06	39.96	39.96	49.99	72.87	69.92	69.92
A3	199.58	100.20	20.52	20.52	49.81	183.53	15.25	15.25
A4	133.60	132.60	1,701.02	1,701.02	95.75	120.19	69.92	69.92
A5	270.01	269.00	550.17	550.17	183.53	219.96	15.25	15.25

Two iterations are gone through to achieve the satisfactory result as the differences are near 0 %. Table 3.21 also shows that the α for all heat exchangers are very close to unity. This indicates that heat differences between hot streams and cold streams only deviate by a small margin. Comparisons are done with respective mean values, shown in Hiba: A hivatkozás forrása nem található.

Table 3.21: Heat capacity of heat exchangers at each side with respective α.

i	$Q_{i,H}$ (kW)	$Q_{i,H}$ (kW)	α_i
A1	399.20	399.20	1.00000
A22	1,599.65	1,599.65	1.00006
A21	1,599.69	1,599.69	1.00000
A3	2,039.49	2,039.49	1.00000
A4	1,708.97	1,708.97	1.00000
A5	555.68	555.68	1.00000

Table 3.22: Percentage difference of the results with respective mean values using Strategy 3

i	$T_{i,HI}$ (%)	$T_{i,HO}$ (%)	$CP_{i,HI}$ (%)	$CP_{i,HO}$ (%)	$T_{i,CI}$ (%)	$T_{i,CO}$ (%)	$CP_{i,CI}$ (%)	$CP_{i,CO}$ (%)
A1	0.02	0.02	-0.28	-0.01	-0.19	0.15	-0.27	-0.28
A22	-0.05	0.07	0.17	-0.03	0.00	0.16	-0.19	-0.21
A21	-0.06	0.05	-0.13	-0.11	-0.22	-0.04	-0.13	-0.04
A3	-0.10	0.21	2.71	2.15	-0.31	-0.04	2.71	1.95
A4	0.00	0.00	-0.08	0.09	-0.01	0.00	-0.16	-0.13

A5	0.00	0.00	0.07	-0.08	0.12	0.00	0.08	1.95

3.3.2.4 Comparison between strategies

Using respective mean values as the benchmarks, comparisons can be done between the strategies. The differences of all 48 parameters in Hiba: A hivatkozás forrása nem található (in absolute values) are represented in Figure 3.11. They are listed first from $T_{i,HI}$ of A1, followed by of A22, and then column by column. In Figure 3.11, all three strategies have high differences at *CP* parameters, between 13th and 24th parameters, and between 37th and 48th parameters. The strategies have the same highest peaks as well. In this case study, all three strategies perform similarly. Summing up all the differences, strategy 1 has 15.81 %, and strategies 2 and 3 have 18.88 % and 15.79 %. It can be concluded that, in this case study, strategy 3 performs the best, followed by strategy 3 and strategy 2.

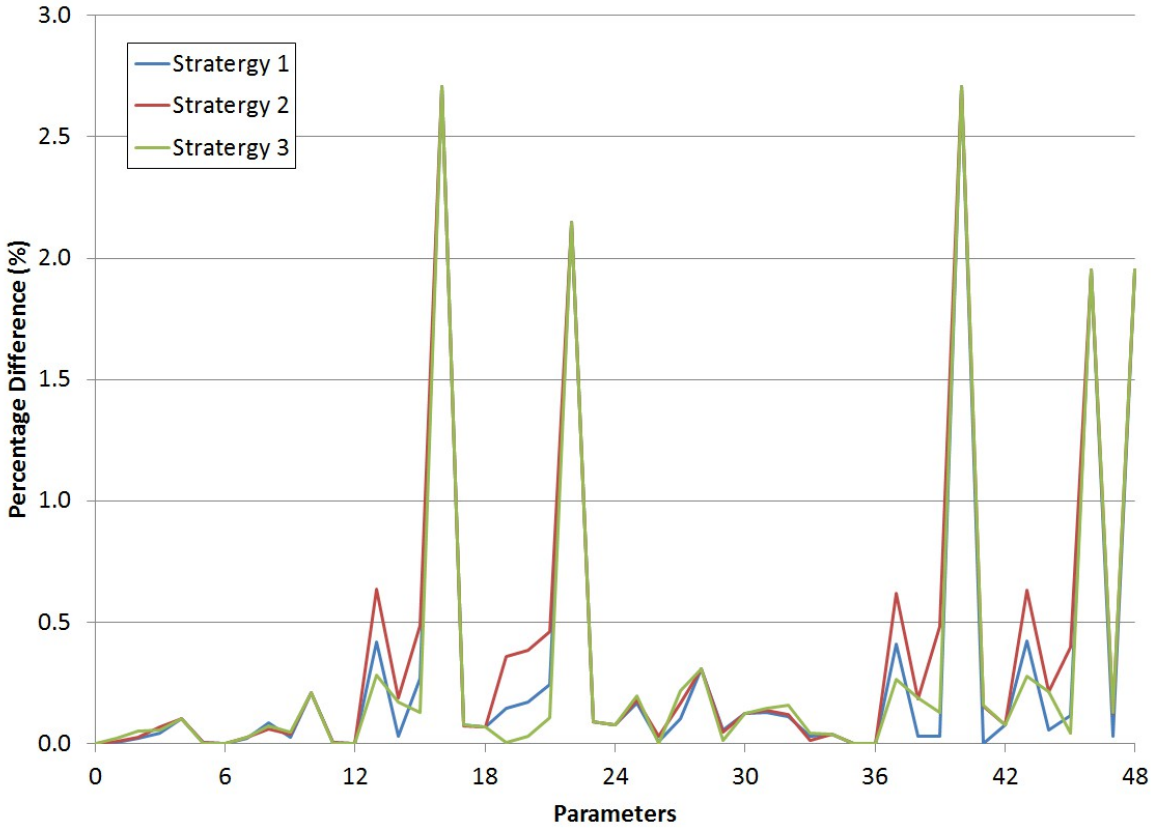

Figure 3.11: Comparisons of different strategies with mean values

3.4 Data Reconciliation on Utility System of a Total Site

Although the non-linearity in the energy constraint is dealt with in sections 3.2 and 3.3, the data reconciliation problem is further made complex when the number of heat exchangers increases. This is especially encountered when the scope of data reconciliation is expanded to the Total Site level. In this section, the direction of how a data reconciliation problem solved in Total Site is relooked.

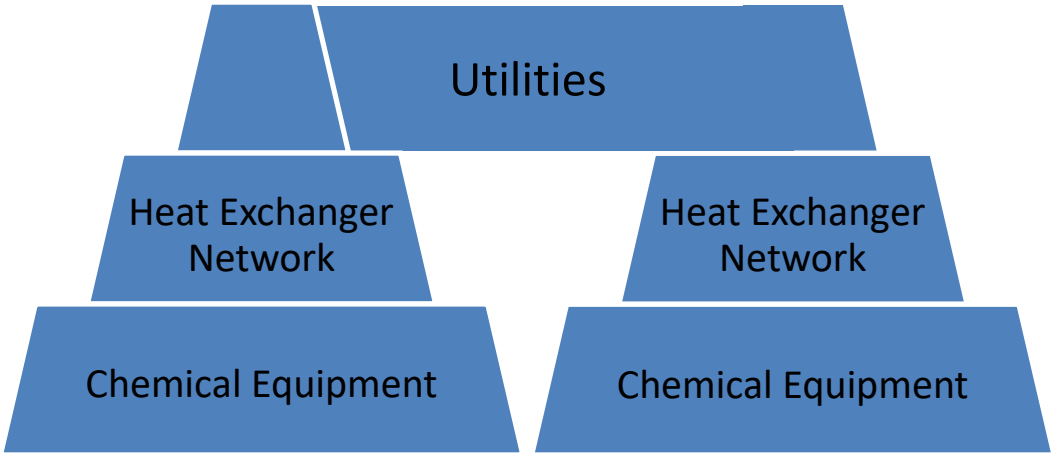

Figure 3.12: Total Site showing sharing of utilities among different chemical plants

Within a Total Site there are large amount of heat exchangers, heaters and coolers. Each chemical plant has its own individual sets of chemical equipment and HENs. One common and only characteristic among these chemical plants is they are connected to the same utilities systems, as shown in Figure 3.12. Instead of including all heat exchangers in every plant in the data reconciliation problem, utility system can be reconciled first. After obtaining the reconciled result for utility system, each HEN from each plant can be reconciled using the method introduced in previous sections.

In this section, parameters of inlets and outlets of utility systems such as heaters, coolers, furnace and cooling tower in Total Site are only involved in the data reconciliation problem solving process. All parameters belongs to heat exchangers in respective plants are not involved in the data reconciliation problem solving process. This will reduce the amount of parameters as variables to be reconciled in the model significantly.

3.4.1 Problem Statement

An existing utility system is considered in the analysis. The utilities used are either isothermal (e.g. steam) or non-isothermal (e.g. cooling water and hot oil). Nevertheless, all utilities are

modelled as steam headers. Let $UI_P \in p$ be the isothermal utility, $UN_P \in p$ be the non-isothermal utility, $F_{f,P} \in f$ be the furnace, $CT_{ct,P} \in ct$ for the cooling tower, $H_{h,P} \in h$ be the heater, $C_{c,P} \in c$ be the cooler, $T_{t,P1,\ P2} \in t$ be the turbine, $COM_{com,P1,\ P2} \in com$ be the compressor, and $V_{v,P1,\ P2} \in v$ be the valve. The aim of this work is to obtain a representative set of data for analysis using data reconciliation process without heavy burden on computational effort.

3.4.2 Assumptions and Equations Used

All utilities used in the Total Site do not mix. Each type of utilities used (e.g. steam, hot oil, cooling water) has its own sets of steam headers. All steam headers, coolers and heaters are modelled as black boxes. In Heat Integration analysis, flows in steam header diagram are usually expressed in terms of energy flowrate, such as kW. It should be noted that energy flowrate cannot be measured directly. In data reconciliation process, all flows are measured and expressed in terms of mass flowrate instead. Especially for heaters or coolers using non-isothermal utilities, the supply and return streams are measured in terms of mass flowrates.

3.4.2.1 Isothermal Utility

For streams containing steam used as isothermal utility, the streams are grouped according to pressure and assumed to be in saturated stage. Steam headers are used as black boxes for each steam pressure level. There should be no connection between two steam headers, except the usage of turbine, compressor or valve. Figure 3.13 shows steam used as the utility. The steam pressure levels are highest at *P-1* in the order of *P-1* > *P* > *P+1*. Only turbines, compressors and valves are connecting between two steam headers. Any outstanding steam are generated and provided in the furnace.

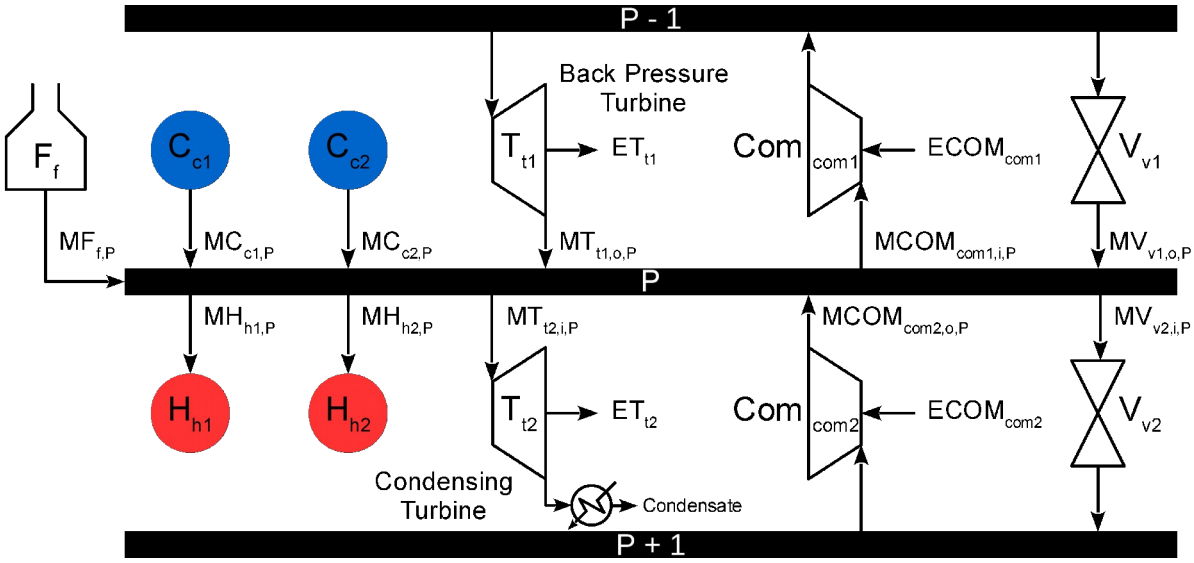

Figure 3.13: Different headers for isothermal utility in Total Site

Cooler and Heater

The steam is generated in coolers (if the temperature is sufficiently high) and consumed in heaters. The inlets for coolers and outlets for heaters are not considered in the study. This is due to the qualities of the steam is different, although the streams are at the same pressure. As steam header is assumed to have only saturated steam, only latent heats are involved in these coolers and heaters. It is also assumed that there is no pressure drop in both coolers and heaters. Only mass flowrates are considered, as steams with known pressure are fed directly from/to steam header. Furnace is modelled as a cooler.

Steam Turbine

Steam turbine takes higher pressure steam to produce electricity and rejects lower pressure steam. Back pressure turbine and condensing turbine are commonly used. In Total Site, back pressure turbine is more common as lower pressure steam can be used for further heating. Back pressure turbine connects between two steam headers. If lower pressure steam is not required, condensing turbine can be used. Since the outlet of condensing turbine is not included into any steam header, condensing turbine has only inlet is being reconciled.

For back pressure turbine, T_t which connects from UI_{P1} to UI_{P2}, the mass balance around the turbine is shown in Eq(3.49). As for condensing turbine, Eq(3.49) is not used as there is no outlet.

$$RMT_{t,i,P1} = RMT_{t,o,P2} \tag{3.49}$$

As for the energy balance around the turbine, it is simplified to have power generated per unit mass steam fed in, h_t. The efficiency, ηT_t is considered a constant.

$$RMT_{t,i,P1} \times h_t \times \eta T_t = RET_t \quad (3.50)$$

Compressor

Although compressor is uncommon in Total Site, it is used sometimes to upgrade lower grade isothermal utilities to higher grade. The compressor must connect two headers (from UI_{P2} to UI_{P1}).

For compressor, COM_{com} which connects from UI_{P2} to UI_{P1}, the mass balance around the compressor is shown in Eq(3.51).

$$RMCOM_{com,i,P2} = RMCOM_{com,o,P1} \quad (3.51)$$

As for the energy balance around the compressor, it is simplified to have power required per unit mass steam fed in, h_{com}. The efficiency, ηCOM_{com} is considered a constant.

$$RMCOM_{COM,i,P1} \times h_{com} \times \eta COM_{com} = RECOM_{com} \quad (3.52)$$

Valve

For isothermal utility, temperature is assumed to be constant. Only mass flowrate is being reconciled for valve.

For valve, V_v which connects from UI_{P1} to UI_{P2}, the mass balance around the valve are given in Eq(3.53).

$$RMV_{v,i,P1} = RMV_{v,o,P2} \quad (3.53)$$

Overall Mass Balance

The mass balance around one steam header for isothermal utility, UI_P is given in Eq(3.54).

$$\sum_{\square}^{f} RMF_{f,P} + \sum_{\square}^{c} RMC_{c,P} + \sum_{\square}^{t} RM\,T_{t,o,P} + \sum_{\square}^{com} RMCOM_{com,o,P} + \sum_{\square}^{v} RMV_{v,o,P} = \sum_{\square}^{h} RMH_{h,P} + \quad (3.54)$$

3.4.2.2 Non-isothermal utility

As for non-isothermal utilities, they are modelled using pseudo steam headers as well. Unlike isothermal utility, non-isothermal utility has two temperatures which are supply temperature and return temperature. To simplify the analysis, all incoming streams to steam header are assumed to be collected and mixed before being distributed. It should be noted that in real case, it might not be in this configuration. Some stream is sent directly for heating or cooling without mixing with other streams.

For non-isothermal utility, UN_P for the purpose of cooling (i.e. cooling water) is shown in Figure 3.14. In the figure, solid arrows represent higher temperature streams and dashed arrows represent lower temperature streams. Cooling water is distributed from the header to coolers, represented in C_i, and returned to the header in higher temperature. The cooling towers, CT_i receives the heated cooling water from the header, cools it down before returning it to the header. If the process stream temperatures in the heaters, H_i are sufficiently low to produce low temperature cooling water, heated cooling water is directed from header into the heaters.

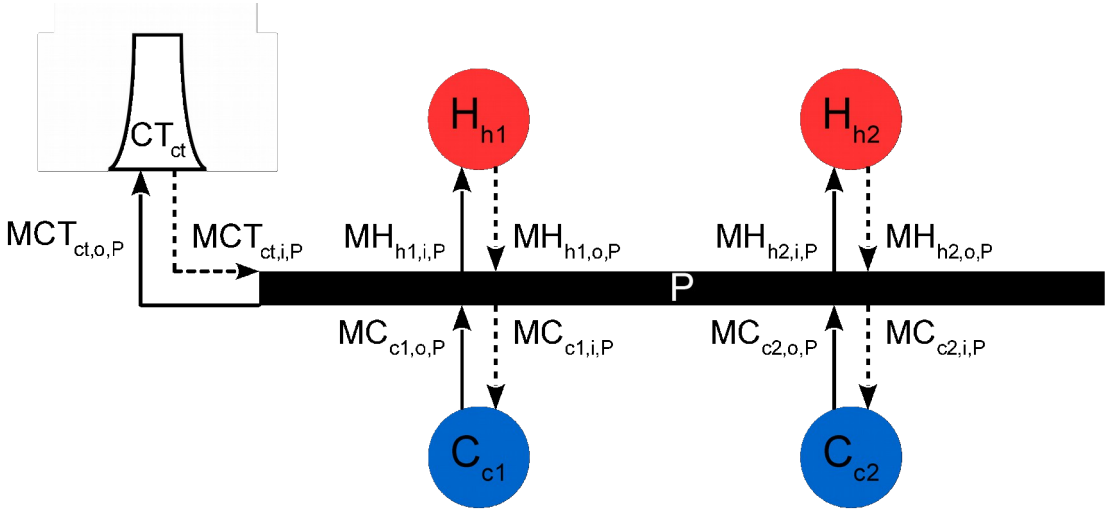

Figure 3.14: Non-isothermal cooling utility in Total Site

For non-isothermal utility, UN_P for the purpose of heating (i.e. hot oil) is shown in Figure 3.15. In the figure, solid arrows represent higher temperature streams and dashed arrows represent lower temperature streams. Hot oil is distributed from the header to heaters, represented in H_i and returned to the header in lower temperature. The furnace, F_i receives the cooled hot oil from the header, heats it up before returning it to the header. If the process stream temperatures in the coolers, C_i are sufficiently high to produce high temperature hot oil, cooled hot oil is directed from header into the coolers.

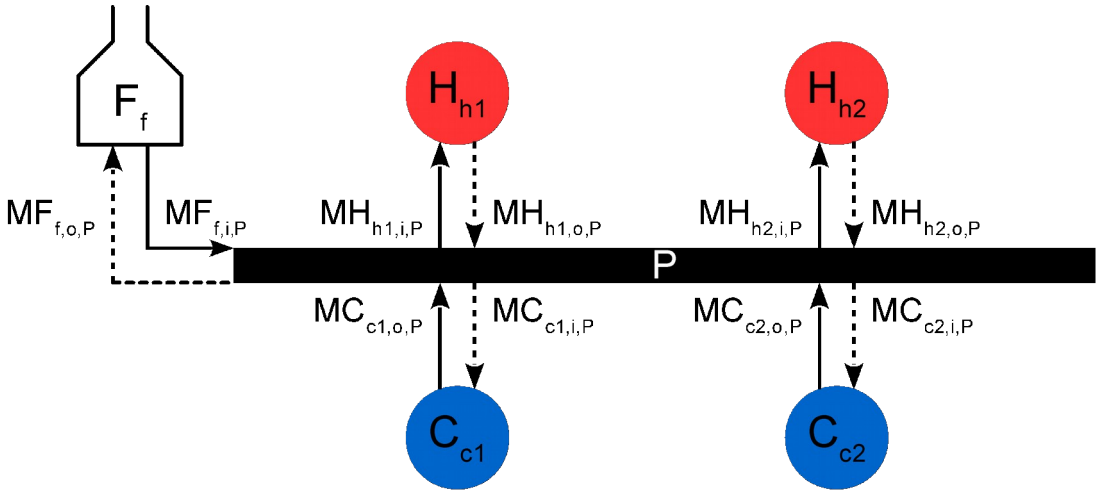

Figure 3.15: Non-isothermal heating utility in Total Site

Cooler and Heater

As for heater or cooler using non-isothermal utility, both inlet and outlet are considered if the data is available. The mass balance equation around a heater, H_h or cooler, C_c is shown in Eq(3.55) and Eq(3.56).

$$RMC_{c,o,P} = RMC_{c,i,P} \tag{3.55}$$

$$RMH_{h,o,P} = RMH_{h,i,P} \tag{3.56}$$

Cooling tower

Cooling tower is modelled as heater. The mass balance around cooling tower, CT_{ct} is shown in Eq(3.57).

$$RMCT_{ct,o,P} = RMCT_{ct,i,P} \tag{3.57}$$

Furnace

Furnace is modelled as a cooler. The mass balance around furnace, F_f is shown in Eq(3.58).

$$RMF_{f,o,P} = RMF_{f,i,P} \tag{3.58}$$

Overall Mass Balance

The mass balance around one steam header for non-isothermal utility, UI_P is given in Eq(3.59) and Eq(3.60). For cooling utilities,

$$\sum_{\square}^{ct} RMCT_{ct,i,P} + \sum_{\square}^{h} RMH_{h,i,P} = \sum_{\square}^{c} RMC_{c,o,P} \tag{3.59}$$

For heating utilities,

$$\sum_{\square}^{f} RMF_{f,i,P} + \sum_{\square}^{c} RMC_{c,o,P} = \sum_{\square}^{h} RMH_{h,i,P} \tag{3.60}$$

Given a repeated set of measurements of heaters, coolers, turbines, compressors, valves, cooling towers and furnaces in a set period of time for n times, the aim is to find the corresponding reconciled parameters, appeared from Eq(3.49) to Eq(3.60). All the constraints equations are linear and linear least square method is used on the objective functions. For example, one of the parameters is mass flowrate of heater *h* at header *p*, $MH_{h,p}$. Measurements are taken and repeated for *n* times, with each assigned to be $MH_{h,P,n}$. It is desired to find the reconciled value for this parameter, given in $RMH_{h,p}$. The difference between these two parameters can be found using subtraction, ($MH_{h,P,n}$ – $RMH_{h,p}$). It is then squared to avoid negative value difference upsetting the positive value, if any. The differences are sum first according to all *n* in the operation $\sum^{n}$, then according to all h in the operation $\sum^{h}$ and lastly according to all p in the operation $\sum^{p}$. All other parameters goes through the same process. All these are shown in Eq(3.61) to Eq(3.64). For all Isothermal Utilities, UI_P, to account for all the parameters involved in the isothermal utility appeared from Eq(3.49) to Eq(3.54).

$$OBJ_I = \sum_{\square}^{P}\sum_{\square}^{h}\sum_{\square}^{n}\left(MH_{h,P,n} - RMH_{h,P}\right)^2 + \sum_{\square}^{P}\sum_{\square}^{c}\sum_{\square}^{n}\left(MC_{c,P,n} - RMC_{c,P}\right)^2 + \sum_{\square}^{P}\sum_{\square}^{f}\sum_{\square}^{n}\left(MF_{f,P}\right. \\ \sum_{\square}^{com}\sum_{\square}^{n}\left(MCO \\ \sum_{\square}^{com}\sum_{\square}^{n}\left(ECOM_{com,n} - \\ \sum_{\square}^{com}\sum_{\square}^{n}\left(MCOM_{com,o,P,n} - RMCOM_{com,o,P}\right)^2 \tag{3.61}$$

For all non-isothermal Utilities, UN_P to account for all the parameters involved in the non-isothermal utility appeared from Eq(3.55) to Eq(3.60).

$$OBJ_N = \sum_{\square}^{P}\sum_{\square}^{c}\sum_{\square}^{n}\left(MC_{c,P,o,n} - RMC_{c,P,o}\right)^2 + \sum_{\square}^{P}\sum_{\square}^{h}\sum_{\square}^{n}\left(MH_{h,P,i,n} - RMH_{h,P,i}\right)^2 + \sum_{\square}^{P}\sum_{\square}^{f}\sum_{\square}^{n}\left(M\right. \tag{3.62}$$

And if there is data about inlets of coolers and outlets of heaters

$$OBJ_N = \sum_{\square}^{P}\sum_{\square}^{c}\sum_{\square}^{n}\left(MC_{c,P,o,n} - RMC_{c,P,o}\right)^2 + \sum_{\square}^{P}\sum_{\square}^{h}\sum_{\square}^{n}\left(MH_{h,P,i,n} - RMH_{h,P,i}\right)^2 + \sum_{\square}^{P}\sum_{\square}^{c}\sum_{\square}^{n}\left(M\right. \tag{3.63}$$

Overall the objective is to

$$\sum_{\square}^{com}\sum_{\square}^{n}\left(MCOM_{com,o,P,n}-RMCOM_{com,o,P}\right)^2+\sum_{\square}^{com}\sum_{\square}^{n}\left(ECOM_{com,n}-R\,ECOM_{com}\right)^2+¿\sum_{\square}^{P}\sum_{\square}^{v}\sum_{\square}^{n}$$

(3.64)

subjects to constraints from Eq(3.49) to Eq(3.60)

3.4.3 Illustrative Case Study

The following case study is adapted from Liew et al. (2012). As shown in Figure 3.16, the isothermal utility used is steam with three different pressures. The pressures are at 55 bar (P_1 = HPS), 10 bar (P_2 = MPS) and 3 bar (P_3 = LPS). The specifications for the utilities are further listed in Table 3.23. For HPS, there are only heaters without any coolers, furnace (F_1) producing HPS is installed to satisfy the demand. There is excess of MPS, which is fed to turbine (T_1) to produce LPS and electricity. Even so, it is still insufficient to satisfy the demand of LPS even with some LPS generation from coolers. Another furnace (F_2) is installed for this purpose. As for non-isothermal utility, only cooling water (P_4) is used as shown in Figure 3.17. There are only coolers, therefore cooling water is installed to keep the water in circulation. As for the turbine, the efficiency is assumed to be 75 % and 163.5 kJ/kg.

In this case study, it is assumed that all streams are recorded, including the outlets of coolers and inlet to cooling tower. All streams parameters are measured repeatedly in a period of time. Using statistical method, outliers are identified and consequently discarded. Ten sets of measurements are selected for data reconciliation. Table 3.24 below shows mean measured values.

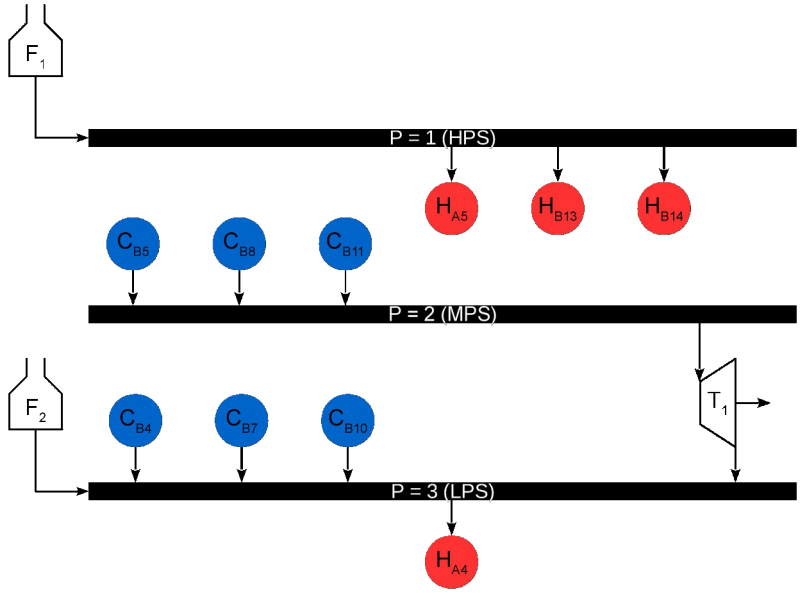

Figure 3.16: Different steam headers as the isothermal utility for the illustrative case study.

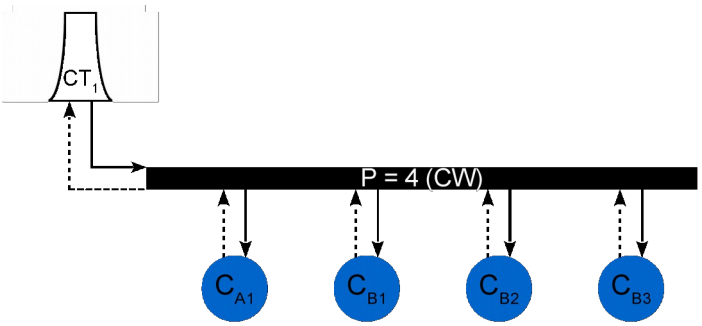

Figure 3.17: Cooling water as the only non-isothermal utility for the illustrative case study.

Table 3.23: Properties for the steam headers used in the illustrative case study.

Header	Utility Used	Pressure (bar)	Temperature (°C)	Energy Content
P1	High Pressure Steam (HPS)	55	270	L_{P1} = 1,604.6 kJ/kg
P2	Medium Pressure Steam (MPS)	10	180	L_{P2} = 2,014.6 kJ/kg
P3	Low Pressure Steam (LPS)	3	133.5	L_{P3} = 2,163.5 kJ/kg
P4	Cooling Water (CW)	1	15 - 35	cp_{P4} = 4.2 kJ/kg K

Table 3.24: Mean values for all the parameters for the illustrative case study.

Parameters	Mean value	Unit
For P = 1		
$MH_{A5,1}$	1,233.5	kg/h
$MH_{B13,1}$	89.7	kg/h
$MH_{B14,1}$	134.4	kg/h
$MF_{1,1}$	1,459.0	kg/h
For P = 2		
$MC_{B5,2}$	17.8	kg/h
$MC_{B8,2}$	26.7	kg/h
$MC_{B11,2}$	338.8	kg/h
$MT_{1,i,2}$	385.2	kg/h
For P = 3		
$MC_{B4,3}$	77.3	kg/h
$MC_{B7,3}$	116.1	kg/h
$MC_{B10,3}$	1,467.3	kg/h
$MT_{1,o,3}$	384.3	kg/h
$MF_{2,3}$	783.4	kg/h
$MH_{A4,3}$	2,832.6	kg/h
ET_1	47,127.3	kJ/h
For P = 4		
$MCT_{1,i,4}$	31,284.3	kg/h
$MCT_{1,o,4}$	31,349.6	kg/h
$MC_{A1,i,4}$	17,127.9	kg/h
$MC_{A1,o,4}$	17,130.0	kg/h
$MC_{B1,i,4}$	4,860.0	kg/h
$MC_{B1,o,4}$	4,870.7	kg/h
$MC_{B2,i,4}$	2,798.6	kg/h
$MC_{B2,o,4}$	2,794.3	kg/h
$MC_{B3,i,4}$	6,501.4	kg/h
$MC_{B3,o,4}$	6,475.7	kg/h

Table 3.25 shows the reconciled values. All the parameters satisfy all the constraints imposed. When compared with respective mean values, the differences are no more than 2 %. It is however noticeable that low value parameters tend to have higher differences, particularly those having values below 100 kg/h. To solve this issue, weightage can be given to low value parameters such that they carry the same importance as high value parameter. This will have more evenly distributed difference. It is noted that introducing weightage will complicate the model. It is not being implemented in this case study. When this method is compared with iterative method, in this illustrative case the differences are mostly less than 1 %, with at most 2.5 %. As with simultaneous method, in this illustrative case study the differences are all below 2.5 %. It can be concluded that this method of just considering the utility systems is performing well as close as iterative method and simultaneous method. Some parameters have better results when Iterative Method is used. It is believed that it is due to the parameters having lower value, which Iterative Method performs better with lower value. The computational effort when using this method is significantly lower than the other two methods. The parameters are reduced from 168 to 25. In terms of computational speed, in this case study although it just merely cut the time from 2 s to 1 s, it will have significant differences when a larger total site study is used.

Table 3.25: Reconciled values for all the parameters in the illustrative case study, along with comparisons.

Parameters	Reconciled value	Unit	Percentage difference (%)		
			Mean	Iterative Method	Simultaneous Method
For P = 1					
$RMH_{A5,1}$	1,233.9	kg/h	0.03	-0.37	-1.17
$RMH_{B13,1}$	90.0	kg/h	0.33	-1.25	-1.54
$RMH_{B14,1}$	134.8	kg/h	0.30	-1.26	-0.06
$RMF_{1,1}$	1,458.7	kg/h	-0.02		
For P = 2					
$RMC_{B5,2}$	18.1	kg/h	1.69	-0.15	-1.98
$RMC_{B8,2}$	27.0	kg/h	1.12	-1.00	-2.20
$RMC_{B11,2}$	339.1	kg/h	0.09	-0.37	-0.30
$RMT_{1,i,2}$	384.2	kg/h	-0.26		
For P = 3					
$RMC_{B4,3}$	78.1	kg/h	1.04	0.54	-1.26
$RMC_{B7,3}$	117.0	kg/h	0.78	-0.24	-0.94
$RMC_{B10,3}$	1,468.2	kg/h	0.06	0.60	0.50
$RMT_{1,o,3}$	384.2	kg/h	-0.03		
$RMF_{2,3}$	784.2	kg/h	0.10		
$RMH_{A4,3}$	2,831.8	kg/h	-0.03	0.75	0.55
RET_{1}	47,127.3	kJ/h	0.00		
For P = 4					
$RMCT_{1,i,4}$	31,309.4	kg/h	0.08		
$RMCT_{1,o,4}$	31,309.4	kg/h	-0.13		
$RMC_{A1,i,4}$	17,136.5	kg/h	0.05	-0.80	0.12
$RMC_{A1,o,4}$	17,136.5	kg/h	0.04	-0.80	0.12
$RMC_{B1,i,4}$	4,872.9	kg/h	0.27	0.56	-0.28
$RMC_{B1,o,4}$	4,872.9	kg/h	0.05	0.56	-0.28
$RMC_{B2,i,4}$	2,804.0	kg/h	0.19	0.05	-0.48

Parameters	Reconciled value	Unit	Percentage difference (%)		
			Mean	Iterative Method	Simultaneous Method
$RMC_{B2,o,4}$	2,804.0	kg/h	0.35	0.05	-0.48
$RMC_{B3,i,4}$	6,496.1	kg/h	-0.08	2.52	1.83
$RMC_{B3,o,4}$	6,496.1	kg/h	0.32	2.52	1.83

3.4.4 Industrial Case Study

The following case study is modified from a small petrochemical refinery in Europe. It has small scale total site across few parts of the refinery. In this case study, only steam with three different pressures is considered as the isothermal utility. The cooling water and hot oil circuit, which are the non-isothermal utilities, are not considered in the study. This is shown in Figure 3.18. The pressures for the steam are at 40 bar (P_1 = HPS), 10 bar (P_2 = MPS) and 3 bar (P_3 = LPS). The properties of the steams are summarised in Table 3.26. As there are only 3 coolers (*C1* to *C3*) at *P1*, the steams are collected and fed to steam turbine *T1* to produce electricity and MPS at *P2*. There are 11 coolers (*C4* to *C14*), 12 heaters (*H1* to *H12*) and a furnace (*F1*) at *P2*. While some of the MPS is used in the heaters, the rest of the steam is sent to let-down valve (*V1*) and steam turbines (*T2* and *T3*). At *P3*, there are 6 coolers (*C15* to *C20*), 14 heaters (*H13* to *H26*) and 6 deaerators (*DA1* to *DA6*) which are modelled as heaters as well. Note that the power output for all turbines are not provided, Eq(8) is not included in the model. The refinery also has leaks from the pipes, and some due to insensitivity from the measuring instruments. There are some levels of uncertainty in the measurements. Nevertheless, all these losses cannot be considered using a separated stream. The losses are distributed to the existing streams. From this case study, it can be seen that although it is said to be a small scale total site, it has more than 30 heaters and 20 coolers. If this problem is to be treated as a whole, i.e. including all the heat exchangers in the network, then it will be too large for data reconciliation. In this case study, all stream parameters are measured repeatedly over a period of time. The mean values for all the parameters are listed in Table 3.27.

Using statistical method, outliers are identified and consequently discarded. Ten sets of measurements are selected for data reconciliation. The Table 3.27 shows the average measured values, reconciled values and the differences.

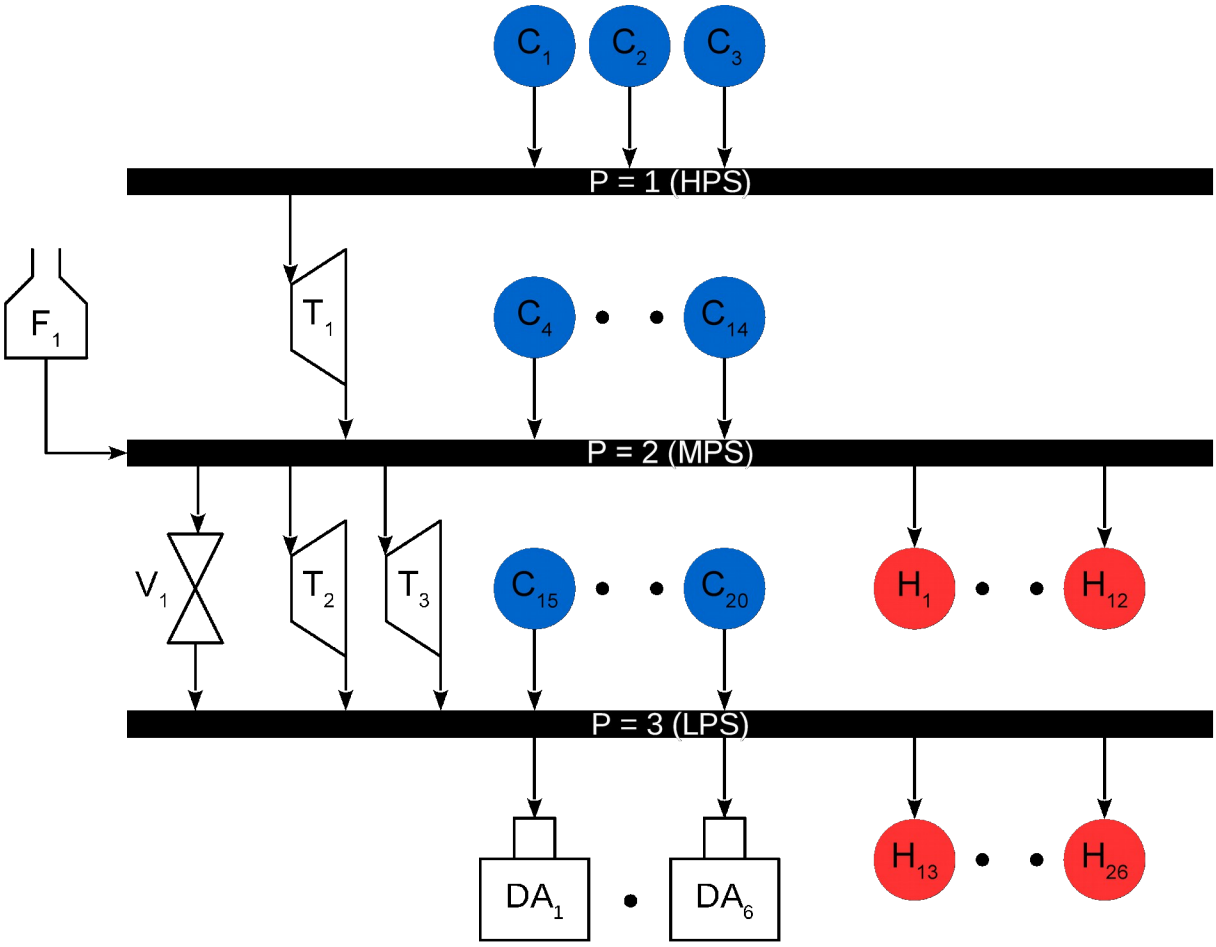

Figure 3.18: Steam as the only utility for the industrial case study.

Table 3.26: Properties for the steam headers used in the industrial case study.

Header	Utility Used	Pressure (bar)	Temperature (°C)	Energy Content
P1	High Pressure Steam (HPS)	40	250	L_{P1} = 1,713.3 kJ/kg
P2	Medium Pressure Steam (MPS)	10	180	L_{P2} = 2,014.6 kJ/kg
P3	Low Pressure Steam (LPS)	3	133.5	L_{P3} = 2,163.5 kJ/kg

Table 3.27: Mean and reconciled values for all parameters in industrial case study.

Parameters	Mean value (kg/h)	Reconciled (kg/h)	Percentage Difference
For P = 1			
$MC_{C1,1}$	1.67	1.68	0.48
$MC_{C2,1}$	7.18	7.18	0.11
$MC_{C3,1}$	22.00	22.01	0.04
$MT_{T1,i,1}$	30.90	30.87	-0.08
P = 2			
$MC_{C4,2}$	2.62	2.54	-3.17
$MC_{C5,2}$	3.29	3.21	-2.52
$MC_{C6,2}$	3.41	3.32	-2.44
$MC_{C7,2}$	3.56	3.48	-2.33
$MC_{C8,2}$	6.30	6.22	-1.32
$MC_{C9,2}$	11.64	11.56	-0.71
$MC_{C10,2}$	13.70	13.61	-0.61
$MC_{C11,2}$	16.31	16.22	-0.51
$MC_{C12,2}$	18.22	18.14	-0.46
$MC_{C13,2}$	34.51	34.43	-0.24
$MC_{C14,2}$	36.15	36.07	-0.23
$MT_{T1,o,2}$	30.92	30.87	-0.15
$MF_{F1,2}$	46.08	45.99	-0.18
$MH_{H1,2}$	1.70	1.78	4.88
$MH_{H2,2}$	2.83	2.91	2.93
$MH_{H3,2}$	3.15	3.23	2.64
$MH_{H4,2}$	4.79	4.88	1.73
$MH_{H5,2}$	7.13	7.22	1.16
$MH_{H6,2}$	7.82	7.90	1.06
$MH_{H7,2}$	9.31	9.39	0.89
$MH_{H8,2}$	9.51	9.59	0.87
$MH_{H9,2}$	9.50	9.58	0.87
$MH_{H10,2}$	10.26	10.35	0.81
$MH_{H11,2}$	17.66	17.74	0.47
$MH_{H12,2}$	27.53	27.61	0.30
$MV_{V1,i,2}$	83.61	83.64	0.03
$MT_{T2,i,2}$	17.43	17.46	0.19
$MT_{T3,i,2}$	12.32	12.37	0.39
P = 3			
$MC_{C15,3}$	1.11	1.14	2.71
$MC_{C16,3}$	1.30	1.33	2.31
$MC_{C17,3}$	1.98	2.01	1.52
$MC_{C18,3}$	2.71	2.74	1.11
$MC_{C19,3}$	7.42	7.45	0.40
$MC_{C20,3}$	10.23	10.26	0.29
$MV_{V1,o,3}$	83.56	83.64	0.10
$MT_{T2,o,3}$	17.38	17.46	0.45
$MT_{T3,o,3}$	12.30	12.37	0.52
$MH_{H13,3}$	1.00	0.97	-2.99
$MH_{H14,3}$	1.02	0.99	-2.94
$MH_{H15,3}$	1.06	1.03	-2.84
$MH_{H16,3}$	1.25	1.22	-2.41
$MH_{H17,3}$	1.40	1.37	-2.14
$MH_{H18,3}$	2.07	2.04	-1.45
$MH_{H19,3}$	2.72	2.69	-1.10

Parameters	Mean value (kg/h)	Reconciled (kg/h)	Percentage Difference
$MH_{H20,3}$	2.94	2.91	-1.02
$MH_{H21,3}$	4.53	4.50	-0.66
$MH_{H22,3}$	5.85	5.82	-0.51
$MH_{H23,3}$	6.20	6.17	-0.48
$MH_{H24,3}$	6.92	6.89	-0.43
$MH_{H25,3}$	8.04	8.01	-0.37
$MH_{H26,3}$	71.92	71.89	-0.04
$MH_{DA1,3}$	3.09	3.06	-0.97
$MH_{DA2,3}$	3.16	3.13	-0.95
$MH_{DA3,3}$	3.35	3.32	-0.90
$MH_{DA4,3}$	3.62	3.59	-0.83
$MH_{DA5,3}$	4.13	4.10	-0.73
$MH_{DA6,3}$	4.75	4.72	-0.64

Table 3.27 shows the reconciled values. All the parameters satisfy all the constraints imposed. When compared with respective mean values, the differences of most parameters are below 2 %. There are some parameters having differences as high as close to 5 %. Again, these are low value parameters, they tend to have higher differences although the magnitude changes were around the level of 0.1 kg/h. To solve this issue, weightage can be given to low value parameters such that they carry the same importance as high value parameter. This will have more evenly distributed difference. It should be noted that introducing weightage will complicate the model. It is therefore not being implemented in this case study as well. Another deduction is that those lost measurement from leaking pipes and insensitive measuring instruments are added up those these parameters.

3.5 Summary

Data reconciliation is an important step in the process of extracting data for retrofitting heat exchanger. Of all the constraints used, energy balance constraint causes the non-linearity in the model. A new method is introduced to solve this non-linearity in section 3.2 that iterates between two linear sub-models. Through case studies iterative method is shown to be able to provide satisfying result with less computational time. The result returns with less than 3 % difference when compared to respective mean values. In section 3.3, limitation encountered when using iterative method is discussed. To overcome this limitation, three different strategies are developed. Through an illustrative case study, it is found that results applying all three strategies have less than less than 3 % difference when compared to respective mean values. Among the strategies, in the case study, strategy 3 performs the best, followed by strategy 3 and strategy 2. Section 3.4 presents a new way to solve data reconciliation problem on Total Site. Model to solve data reconciliation on utility system is presented with demonstration from both illustrative case study and industrial case study. In illustrative case study, the difference compared to respective mean values has no more than 2 %. Compared to iterative method and simultaneous method at no more than 2.5 %, it is found to perform better by not including all heat exchangers in the data reconciliation problem. As for industrial case study that has insensitivity from measuring instruments as well as leakage, the differences are no more than 5 %. Overall, iterative method is shown to have less computational effort in the expense of lower accuracy, when compared to simultaneous method. It is suitable to be used in Heat Integration study particularly retrofitting heat exchange network, which does not need high level of accurate data.

3.6 Nomenclatures

3.6.1 Alphabets

…E…	Energy input	LPS	Low pressure steam
…M…	Mass flowrate	$\dot{m}$	Mass flowrate
C	Cooler	MPS	Medium pressure steam
COM	Compressor	P	Pressure level
CP	Heat capacity flowrate	R…	Reconciled
cp	Specific heat capacity	T	Temperature
CT	Cooling tower	T	Turbine
CW	Cooling water	UI	Isothermal utility
DA	Deaerator	UN	Non-isothermal utility
F	Furnace	V	Let-down valve
H	Heater	α	Relaxation constant
h	Steam enthalpy	η	Efficiency of turbine or compressor
HPS	High pressure steam		

3.6.2 Subscripts

c	of cooler c	i	of equipment *i*
CI	Cold stream inlet	i	of inlet *i*
CO	Cold stream outlet	n	of measurement *n*
com	of compressor *com*	o	of outlet *o*
ct	of cooler tower *ct*	P	of pressure level *p*
f	of furnace *f*	s	of stream *s*
h	of heater *h*	t	of turbine *t*
HI	Hot stream inlet	v	of valve *v*
HO	Hot stream outlet		

3.7 References

Beck A., 2015, On the Convergence of Alternating Minimization for Convex Programming with Applications to Iteratively Reweighted Least Squares and Decomposition Schemes, DOI: 10.1137/13094829X

Ijaz H., Ati U. M. K., Mahalec V., 2013, Heat exchanger network simulation, data reconciliation & optimization, Applied Thermal Engineering, 52(2), 328 - 335.

Klemeš J., Varbanov P., 2010, Process Integration – Successful Implementation and Possible Pitfalls, Chemical Engineering Transactions, 21, 1369-1374.

Klemeš J.J. (ed), 2013, Handbook of Process Integration (PI): Minimisation of Energy and Water Use, Waste and Emissions, Woodhead/Elsevier, Cambridge, UK, 1184 ps. ISBN – 987-0-85709-0.

Klemeš J.J., Kravanja Z., 2013, Forty Years of Heat Integration: Pinch Analysis (PA) and Mathematical Programming (MP). Current Opinion in Chemical Engineering, 2, 4, 461-474.

Kongchuay P., Siemanond K., 2014, Data Reconciliation with Gross Error Detection using NLP for a Hot-Oil Heat Exchanger, Chemical Engineering Transactions, 39, 1087 - 1092.

Liew P.Y., Wan Alwi S.R., Varbanov P.S., Abdul Manan Z., Klemeš J.J., 2012, A numerical technique for Total Site sensitivity analysis, Applied Thermal Engineering, 40, 397.408.

Nemet A., Klemeš J.J., Varbanov P.S., Mantelli W., 2015, Heat Integration retrofit analysis—an oil refinery case study by Retrofit Tracing Grid Diagram, Frontiers of Chemical Science Eng. 2015, 9(2), 163–182.

Shenoy U.V., 1995, Heat exchanger network synthesis, Gulf Professional Publishing, Houston, USA.

Vocciante M., Mantelli V., Aloi N., Reverberi A.P., Dovì V.G., 2014, Application of Interval Analysis to the Reconciliation of Process Data when Models Subject to Uncertainties are Used, Chemical Engineering Transactions, 39, 1675 - 1680.

Yong J. Y., Nemet A., Varbanov P. S., Kravanja Z., Klemeš J. J., 2016, Data Reconciliation for Total Site Integration, Chemical Engineering Transactions, 52, 1045 - 1050.

4. Advanced Visualisation for Retrofitting Heat Exchanger Network in Heat Integration

4.1 Introduction

Heat exchanger network (HEN) retrofit has been an important task in process design as most present designs are retrofits. Many approaches have been presented. However, this important activity can still benefit from an enhanced visualisation and decision-making tool. Therefore the novelty of this work is having a new extended type of Grid Diagram. This type of Grid Diagram properly visualises the HEN arrangements and key parameters such as heat capacity flowrates (CPs), temperatures and temperature differences. Using this novel tool is able to help user to account for thermodynamics and loads simultaneously when performing retrofit on a HEN. It provides a way of screening feasible from infeasible retrofit options and identify the possible trends. This novel Grid Diagram also shows the limits to heat recovery increase after a new HEN path is specified. A case study has been used to demonstrate the retrofit procedure enhancement.

There are different possible retrofit actions modifying an existing HEN – including topology, for improving the heat recovery. These can be generally classified into heat exchanger re-sequencing, re-piping, enhance heat transfer coefficient, stream splitting and addition of new heat exchanger. Such modifications can be combined, resulting in a retrofit plan. The retrofit procedure starts with identifying a heat path. An example is shown in Figure 4.19, where a path starts from a cooler and ends at a heater, while passing through streams and a recovery heat exchanger. Having such a path allows redistributing (shifting) the loads to minimise the utility duties and maximising the recovery heat exchanger duties. Once all the heat paths in the HEN are exhausted, the network would be pushed to form Network Pinch (NP) points. To enable further heat recovery, if the streams allow it, new heat paths can be specified by adding new heat exchangers or performing some of the other possible modifications.

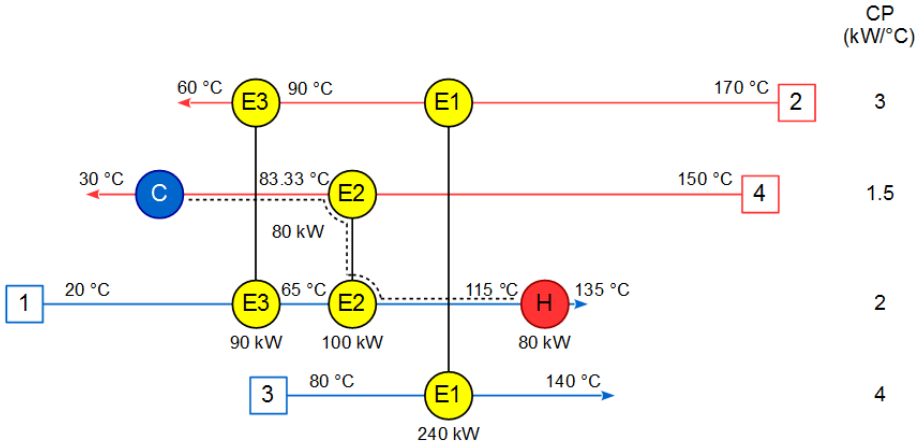

Figure 4.19: HEN showing a heat path (dotted line) connecting a cooler to a heater via a recovery heat exchanger E2

However, there are some cases when NP cannot be found. It is due to the HEN does not having any heat path to enable the retrofit initialisation. Varbanov and Klemeš (2000) introduced an algorithm based on heuristics for developing heat paths, initialising the NP procedure. They used the traditional Grid Diagram (Figure 4.19), which in most cases is not scaled on the temperature dimension and leaves the opportunity to miss beneficial options for placing new recovery heat exchangers.

Beside Grid Diagram, another visualisation tool to represent HEN, called Retrofit Thermodynamic Diagram (RTD) has been developed by Lakshmanan and Bañares-Alcántara (1996) and further extended later Lakshmanan and Bañares-Alcántara (1998). It is one of the first visual tools to represent HENs by considering the temperature span and CPs of process streams simultaneously. The heat content and heat exchanged between streams are shown explicitly. However, RTD does not show thermodynamic feasibility clearly, such that cold stream should have lower temperature than hot stream at both ends of a heat exchanger. RTD does not incorporate minimum allowed temperature difference (ΔT_{min}) as well.

Piacentino (2011) performs a similar thermal analysis and provides new insights in retrofitting and relaxing a HEN by using a so-called Heat Loads Plot. As with RTD showing temperature span and CPs of the process streams, in this work the HEN is represented by overlapping of hot and cold streams.

Two works have been published representing HENs in different graphical ways to cope with the problem of not showing Pinches. In the diagram, the heat content of streams and heat exchanged between streams are clearly shown. Wan Alwi and Manan (2010) developed a graphical tool called Streams Temperature vs. Enthalpy Plot (STEP) for simultaneous targeting and design of HEN. The extension of this tool to become numerical called Segregated Problem Table Algorithm (SePTA) was developed by Wan Alwi et al. (2013). The result of the work is represented on authors' newly developed representation called SePTA Network Diagram (SND). Gadalla (2015) plotted temperatures of hot process streams versus cold process streams. Each existing heat exchanger is represented by a straight arrow with slope proportional to the ratio of heat capacities and flows.

There is still a need for a suitable visualisation and decision-making tool that would be capable of identifying, using and overcoming HEN bottlenecks, enabling more heat recovery. Such a tool is important as it can help users to make decisions and can also efficiently support formulation of mathematical optimisation models. Conventional Grid Diagram (Linnhoff et al., 1994) – for more recent description see (Klemeš, 2013) - is not fully showing this important feature.

4.2 Shifted Retrofit Thermodynamic Diagram

Shifted Retrofit Thermodynamic Grid Diagram (SRTGD) is first proposed in Yong et al. (2014) and further extended in Yong et al. (2015). The hot streams are shifted by subtracting ΔT_{min} from their actual temperatures, and thus the x-axis is expressed as T*. It supports the design and retrofit activities, by illustrating and explaining the effects of various topology changes. SRTGD

can help users to visualise and consider various scenarios especially when developing a heat path. The detailed steps on how to specify SRTGD can be found elsewhere (Yong et al., 2014). Figure 4.20 shows a HEN being represented in SRTGD, based on the example in Klemeš et al. (2014).

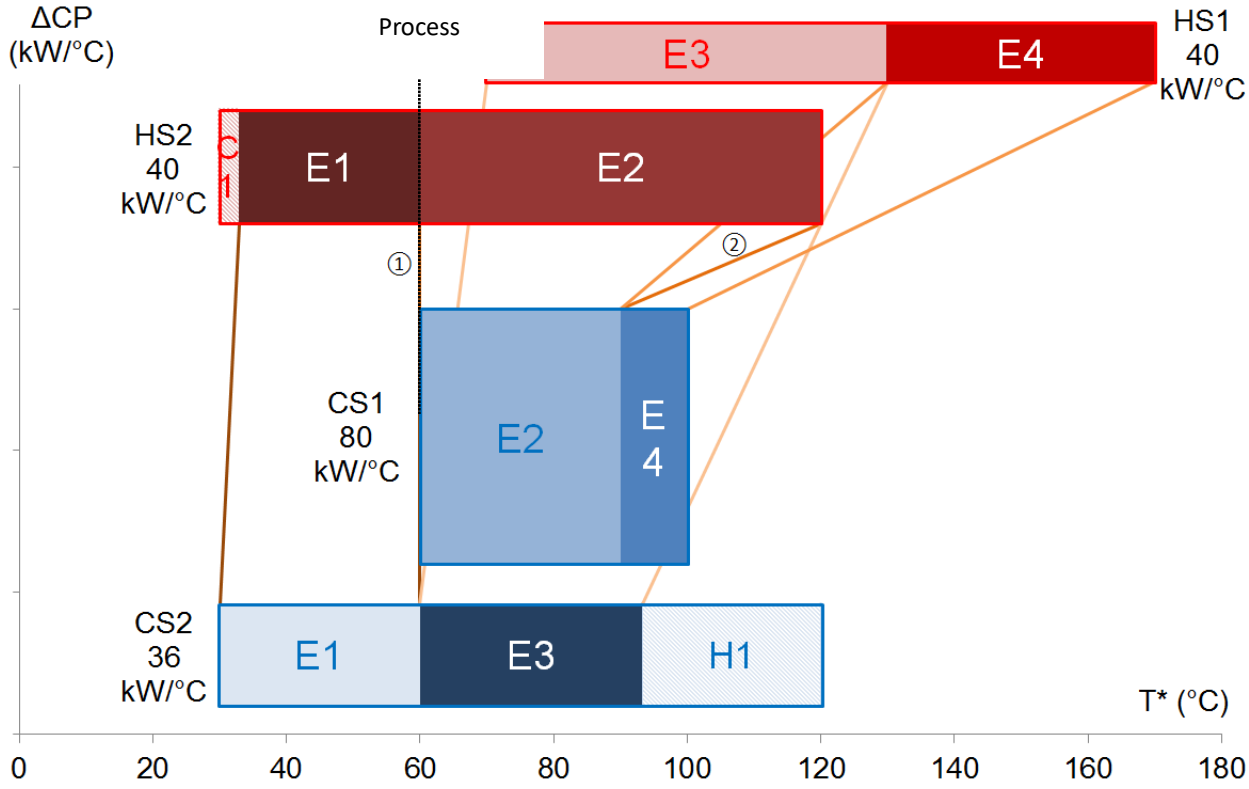

Figure 4.20: An example of a HEN represented using SRTGD (after Klemeš et al. (2014))

The characteristics of SRTGD are as follows. The horizontal axis tracks the temperature scale, while the vertical axis represents the CP scale. All the streams are represented by rectangles. The width of a rectangle is drawn according to the temperature span of the stream while the height is drawn according to the CP. The area of the bar represents the amount of heat available for exchange. The stream may be divided into segments where each segment represents the stream involvement in a heat exchanger. As shown in Figure 4.20, there are two segments of two streams numbered as 2. These are hot and cold parts of heat exchanger E2 and they belong to streams HS2 and CS1. In heat exchanger E2, the lines labelled ① and ② are called cold end link and hot end link for that heat exchanger.

There are two links at the ends of every recovery heat exchanger, while heaters and coolers are denoted only as segments on the stream rectangles. The links are important because they indicate the thermodynamic feasibility of heat transfer. As the hot stream temperatures are shifted by subtracting ΔT_{min} from their actual temperatures, a vertical link (with zero temperature span) indicates a Pinch Point, be it either Process Pinch (PP) or NP. For feasible heat transfer the heat exchanger links should have positive slope, as this is equivalent to hot streams having higher temperatures than the matched cold streams.

Let us consider the conventional Grid Diagram representation of part of a HEN in Figure 4.21. It is assumed that heat exchangers E1 and E2 are connected to other cold and hot streams. There are cooler C1 and heater H1.

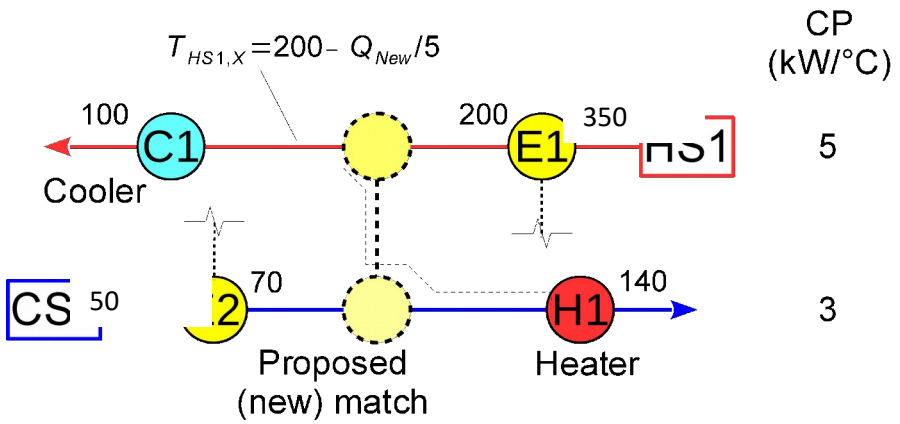

Figure 4.21: Conventional Grid Diagram representation showing part of a HEN

A heat path can be specified between the hot stream HS1 and cold stream CS1 to increase the heat recovery. An option for placing the new heat exchanger would be as shown in Figure 4.21. This positioning means that the new heat exchanger takes the temperature of HS1 after E1 (200 °C) as a development and any duty increase of the new match would produce a lower temperature of HS1 at the inlet of C1, reducing the duty of the cold utility used in C1. The result on the cold stream (CS1) is similar – on the hot end of the new match the temperature should be higher than 70 °C, reducing the hot utility duty.

This is only one of the options for placing a new match – the obvious one. The full set of topological combinations, however, includes also placing the new match after the cooler on stream HS1 and after the heater on stream CS1. These possible positions produce in four options. Which ends of hot and cold stream segments representing heater H1 and cooler C1 should be used during heat path development? For the example in Figure 4.21, should the new match start by fixing on hot stream HS1 the temperature at 200 °C – corresponding to the outlet of exchanger E1? Or should the placement start from the target temperature of hot stream HS1 (100 °C), working back to the stream's supply temperature? The latter would be expressed by a different topology arrangement. For each such option a new conventional Grid Diagram is needed to assess it. Other questions also need answering when placing the new matches. What is the maximum recoverable heat for the new match, and would its load be limited by a (Network) Pinch or by the capacity of the streams?

Conventional Grid Diagram cannot address all these issues – especially to show all options for new match placement in one view. The new SRTGD tool can be used for providing insights clearly indicating the Pinch locations (Process and Network) and gather different arrangement options in one representation during heat path development. The SRTGD can provide visual illustration of the effects of placing a new match on the maximum amount of heat recovered for all options.

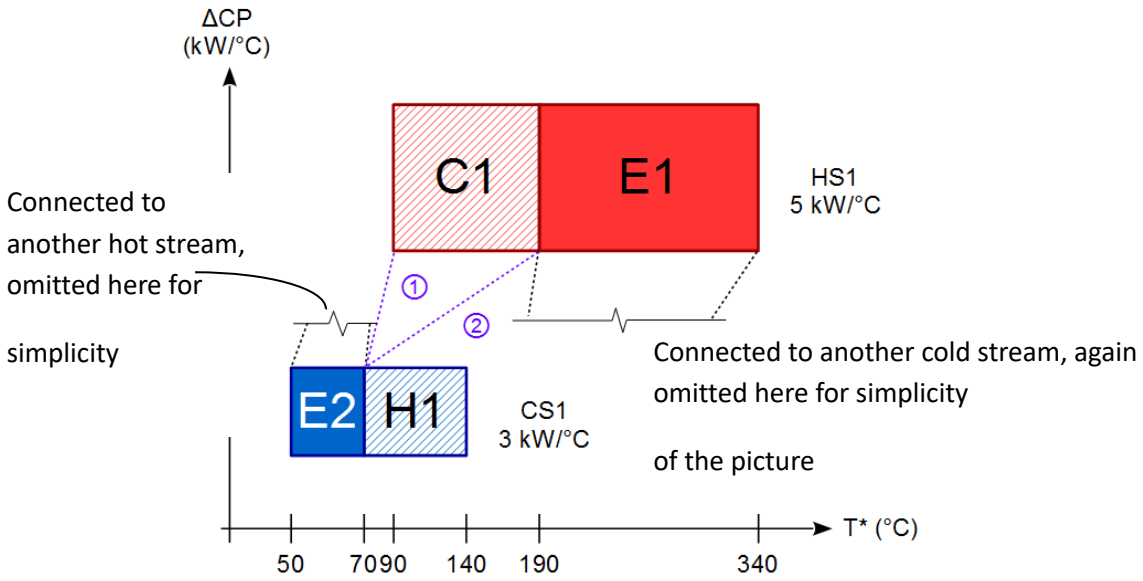

Figure 4.22: SRTGD representation of the mentioned part of the HEN

The example from Figure 4.21 is re-drawn in Figure 4.22 using SRTGD representation. Let just consider two ways of developing the heat path. One option is to start placing the new heat exchanger after cooler C1 on hot stream HS1, then between heat exchanger E2 and heater H1 on cold stream CS1. This placement is indicated with dotted line ① in Figure 4.22. It connects the outlet of the hot stream segment representing cooler C1 to the inlet of hot stream segment representing heater H1. This type of placement is called hot-outlet-to-cold-inlet (HOCI) placement.

A second option involves placing the new heat exchanger between heat exchanger E1 and cooler C1 on the hot stream and between heat exchanger E2 and heater H1 on the cold stream On the SRTGD in Figure 4.22, this option is indicated by dotted line ②. This placement matches the inlet of the hot stream segment representing cooler C1 and inlet of cold stream segment representing heater H1. This type of placement is called hot-inlet-to-cold-inlet (HICI) in this context.

In this specific example, the CP of the hot stream is greater than that of the cold stream. If the heat path development uses the HOCI way, as the load of the new match increases, the temperature of the cold stream outlet would increase faster than the temperature of the hot stream inlet. As a result, the NP position at 120 °C, it is indicated with a vertical line in Figure 4.23. This results in recovering only maximum 150 kW of hot end link indicating a NP at 130/120 °C.

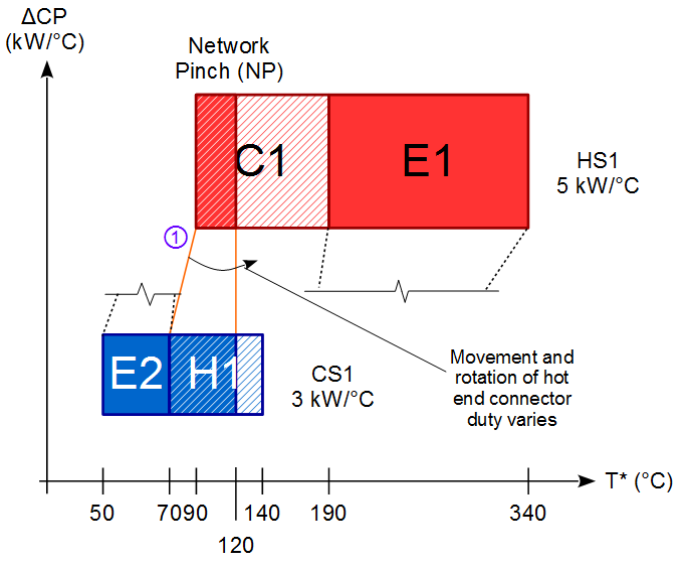

Figure 4.23: SRTGD of the HEN when HOCI is chosen during heat path development

On the other hand, if the HICI way is used instead (Figure 4.24), for $CP_H > CP_C$, the smaller temperature difference of the new match will be at the hot end of the new match. The inlet temperature of hot stream HS1 to the segment is 200 °C. The highest temperature of the available segment of cold stream CS1 is 140 °C, resulting in a temperature difference of 60 °C. The limitation in this case is not the temperature, but rather the duties available by the selected process stream segments. Maximum 210 kW of heat can be recovered, as the heating demand of the cold stream segment of CS1 is limiting the heat recovery.

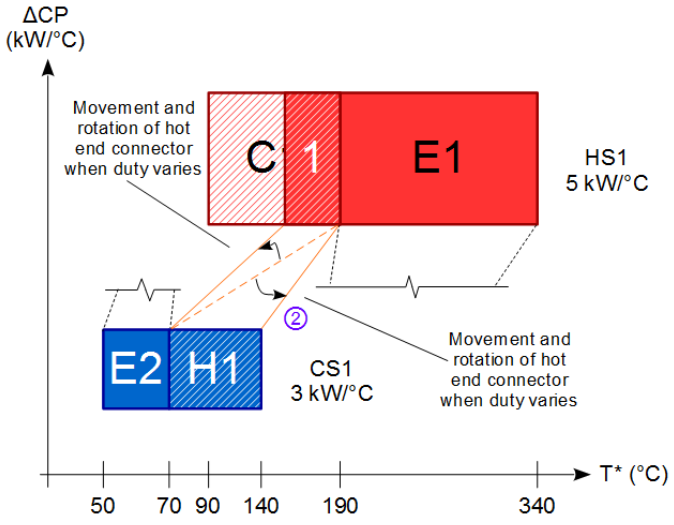

Figure 4.24: SRTGD of the HEN when HICI is chosen during heat path development

It may seem obvious that the HICI way should always be chosen during heat path development for maximum heat recovery. However, Figure 4.22 to Figure 4.24 only show part of the network. Stream CS1 might be the lowest temperature cold stream available. If HICI way is chosen, there may be no other cold stream to exchange heat with the remaining cold part of HS1. This would limit the scope for recovering more heat. Besides temperature and CP, the way of developing heat path and the whole network topology should be considered as well. More discussion and explanation are provided in the following sections.

4.2.1 Heat Path Development Considerations

This section discusses all four ways of developing a heat path, considering that new heat exchange match can be placed by fixing the temperatures of inlet or outlet of a hot stream and the inlet or outlet of a cold stream to be matched. The term “matching” in this context carries the meaning of connecting the chosen end of the hot stream to the chosen end of the cold stream. The hot and cold end links of a heat exchange match start from the same position – overlapping each other, as the newly added heat exchanger does not have any duty yet. The two ends are separated when the duty of the heat exchanger is increased, as shown in Figure 4.23 and Figure 4.24.

In every example, the heat path is developed from a heater to a cooler assuming that it does not pass through any heat exchanger existing before the path development. This simplifies the illustration and explanation.

The match placement examples, that follow, use a hot stream, at the top of the SRTGD. It is first cooled by a heat exchanger (E1 – shown partially) and then a cooler. The cold stream is shown at the bottom of the SRTGD. It is first heated by a heat exchanger (E2 – shown partially) and then a heater. Each figure contains two SRTGDs with the first one showing the developed heat path with zero heat duty of the new heat exchanger. The second one shows how the links move when heat duty is increased.

4.2.1.1 Hot inlet to cold inlet (HICI)

For this option the heat path is developed by matching the inlet of a hot stream segment with the inlet of a cold stream segment, initialising the match to a zero load. The chosen segments are currently served by a cooler and a heater – see Figure 4.25 and Figure 4.26. The hottest part of the hot stream is used to exchange heat with the coldest part of the cold stream. For determining the load, the hot end link has a fixed position at the hot side of the match on the hot stream and the cold end link has a fixed position at the cold side on the cold stream. The next step is to increase the duty of the new match to a desired magnitude. As a result, the hot end link changes position on the cold stream to the right, toward higher temperature. Symmetrically, the cold end link changes position on the hot stream to the left, toward lower temperature. Two cases are possible:

CPH > CPC: Figure 4.25 - as the duty is increased, the temperature on the cold stream increases at a faster rate than that of hot stream drops. Therefore, the hot end link would form a NP if the load is large enough.

CPH < CPC: Figure 4.26 - for unit load increase, the hot stream temperature of the cold end link drops faster than the temperature of the cold stream on the hot end increases. The cold end link would form a NP if the load is sufficiently large.

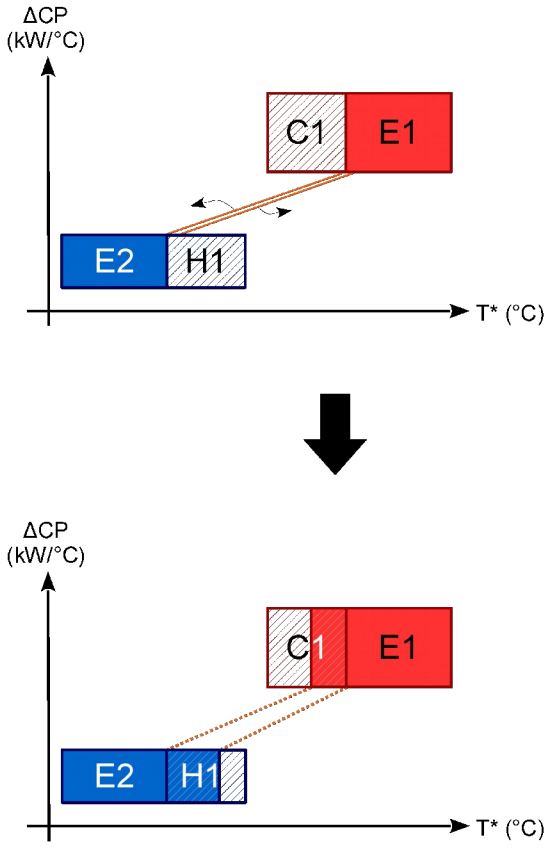

Figure 4.25: Heat path development showing HICI way when CPH > CPC

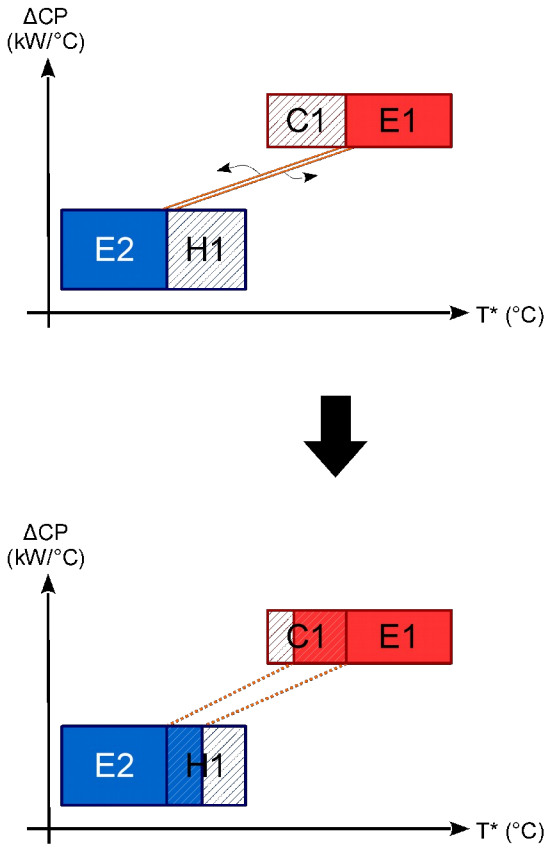

Figure 4.26: Heat path development showing HICI way when CPH < CPC

4.2.1.2 Hot inlet to cold outlet (HICO)

The heat path is developed by matching the inlet of a hot stream segment with the outlet of a cold stream segment, initialising the match to a zero load. The hottest part of the hot stream is used to exchange heat with the hottest part of the cold stream. For determining the load the hot end link has two fixed positions at the hot side of the match on the hot stream and hot side of the match on the cold stream. Cold end link does not have fixed position, therefore cold end link changes position on the hot and cold streams to the left, towards lower temperature. This option is shown in Figure 4.27 and Figure 4.28. The CP ratios again define two cases:

CPH > CPC: Figure 4.27 - the hot end link features the smaller temperature difference in the new match. As the load is increased, the cold end link moves away to the left (toward lower temperatures), while its temperature difference increases. In this case no NP would be formed.

CPH < CPC: Figure 4.28 - the cold end link features the smaller temperature difference. This link is also the movable for the current placement option. The load increase would reduce the temperature difference on the cold end of the match and this end would form a NP at sufficiently large duty.

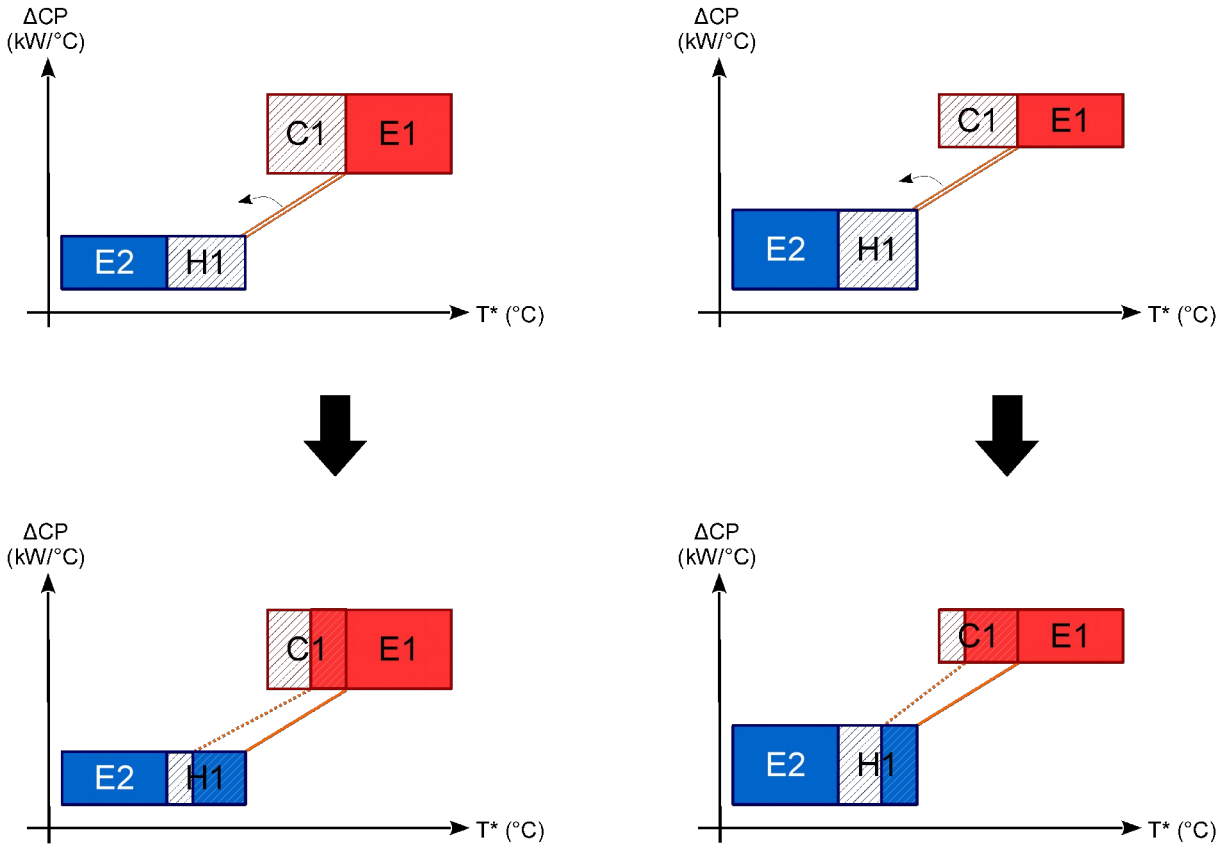

Figure 4.27: Heat path development showing HICO way when CPH > CPC

Figure 4.28: Heat path development showing HICO way when CPH < CPC

4.2.1.3 Hot outlet to cold inlet (HOCI)

The heat path is developed by matching the outlet of a hot stream segment with the inlet of a cold stream segment, initialising the match to a zero load. The coldest part of the hot stream is used to exchange heat with the coldest part of the cold stream. This considers the potential usage of low temperature heating, especially in the case of low grade heat. It is suitable when low grade heat is first considered to be utilised during retrofit, as it considers low grade heat exchange first. For determining the load the cold end link has two fixed positions at the cold side of the match on the hot stream and cold side of the match on the cold stream. Hot end link does not have fixed position, therefore hot end link changes position on the hot and cold streams to the right, towards higher temperature. It is shown in Figure 4.29 and Figure 4.30. The CP ratios define two cases:

CPH > CPC: Figure 4.29 - the hot end link features the smaller temperature difference. As this link is also the movable for the current placement option, the load increase would reduce the temperature difference on the hot end of the match and this end would form a NP at sufficiently large duty.

CPH < CPC: Figure 4.30 - the cold end link features the smaller temperature difference in the new match. As the load is increased, the hot end link moves away to the right (toward higher temperatures) while its temperature difference increases in the case no NP would be formed.

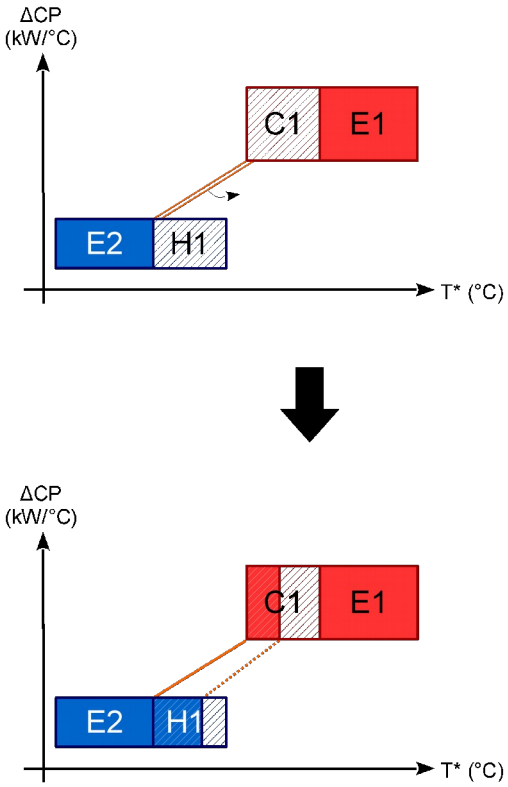

Figure 4.29: Heat path development showing HOCI way when CPH > CPC

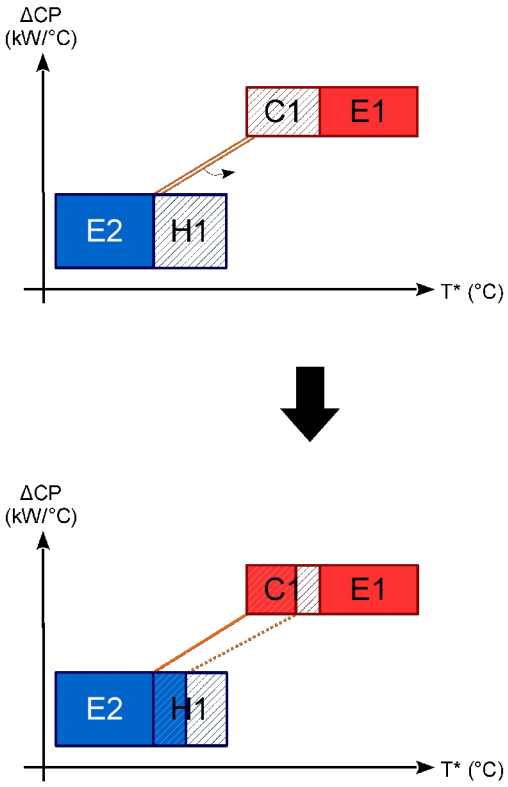

Figure 4.30: Heat path development showing HOCI way when CPH < CPC

4.2.1.4 Hot outlet to cold outlet (HOCO)

The heat path is developed by matching the outlet of a hot stream segment with the outlet of a cold stream segment. For this kind of heat path to be thermodynamically feasible, the outlet temperature of the cold stream segment has to be lower than the outlet temperature of the hot stream segment. The coldest part of the hot stream segment is used to exchange heat with the hottest part of the cold stream segment. This option is shown in Figure 4.31 and Figure 4.32. For determining the load, the hot end link has a fixed position at the cold side of the match on the cold stream and the cold end link has a fixed position at the cold side on the hot stream. The next step is to increase the duty of the new match to a desired magnitude. As a result, the hot end link changes position on the cold stream to the right, toward higher temperature, while cold end link changes position on the cold stream to the left, towards lower temperature. The CP ratios define two cases:

CPH > CPC: Figure 4.31 - for unit load increase, the cold stream temperature of the cold end link drops faster than the temperature of the hot stream on the hot end increases. However, both hot and cold end links will never become NPes as the outlet temperature of the cold stream segment is lower than the outlet temperature of the hot stream segment.

CPH < CPC: Figure 4.32 - for unit load increase, the cold stream temperature of the cold end link drops slower than the temperature of the hot stream on the hot end increases. However, both hot and cold end links will never become NPes as the outlet temperature of the cold stream segment is lower than the outlet temperature of the hot stream segment.

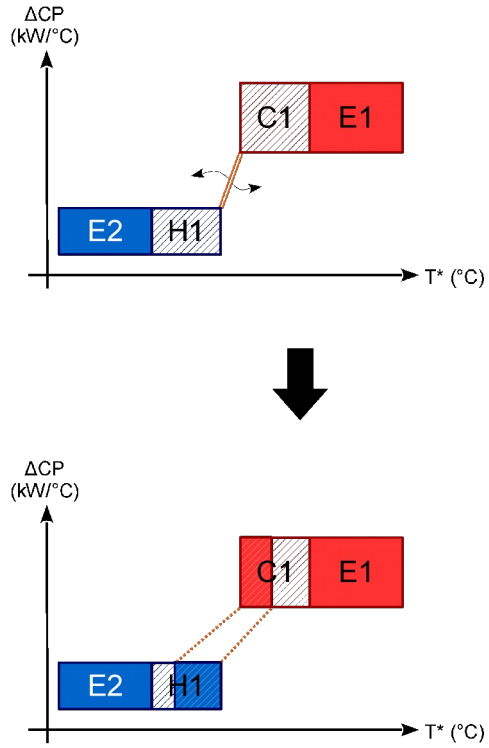

Figure 4.31: Heat path development showing HOCO way when CPH > CPC

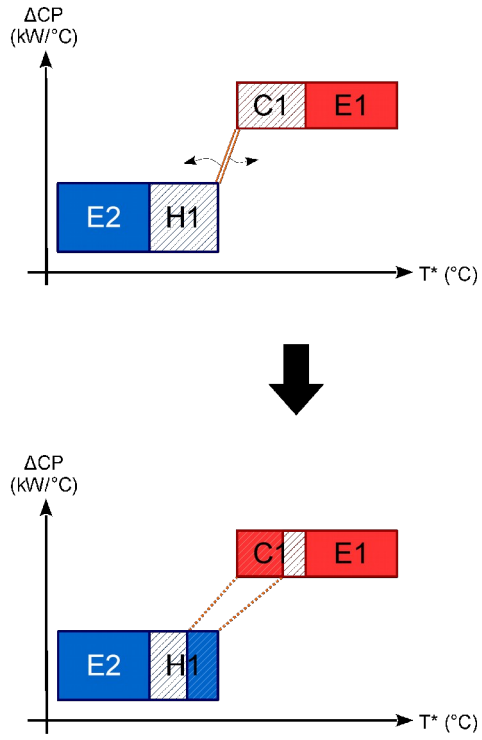

Figure 4.32: Heat path development showing HOCO way when CPH < CPC

4.2.2 Using SRTGD in Heat Path Development Steps for Identifying HEN Retrofit Options

In this section the use of the SRTGD is demonstrated – as a proper visualisation tool for HEN retrofit options identification and combination. The characteristics of SRTGD which help the user during heat paths development stage is discussed using examples.

All the heat paths are illustrated using SRTGD in this section are developed, but not limited to, using HOCI way as examples. The other development ways discussed are also applicable as well. For better illustration, segments of streams that use existing heat exchangers are coloured with solid filling, while utility-served segments are shaded with a light pattern, and dark shaded are the segments representing the heat recovered by path development.

4.2.2.1 Identification of feasible options and feasible heat path development

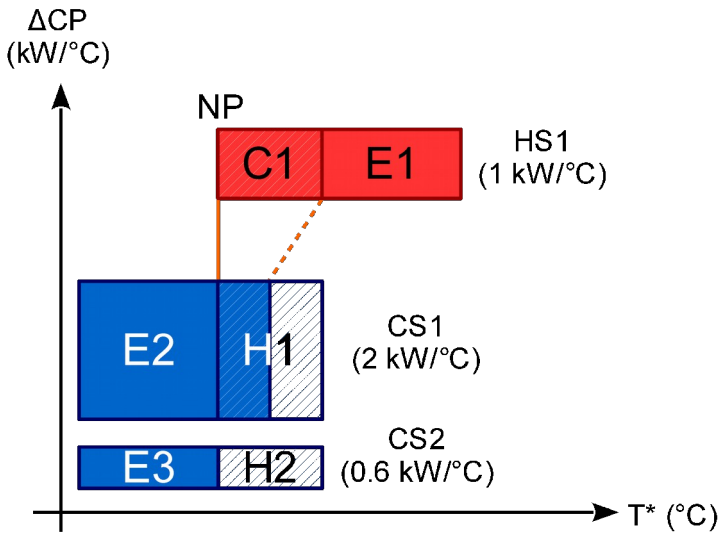

Figure 4.33: Two cold streams for consideration during heat path development.

Let us consider Figure 4.33 where SRTGD shows that heaters H1 and H2 have the same supply and target temperatures. Assume that the heat path is to be developed using HOCI way, matching cooler C1 with either heater H1 or H2 will form a NP (a vertical line) at cold end. However, as shown in Figure 4.33, heat path can only be developed between cooler C1 and heater H1. This is because cold stream CS1 has higher CP than hot stream HS1, such that when the duty of the new heat exchanger increases, the temperature span of hot stream HS1 increases at a faster rate than that of cold stream CS1. The hot end link will become more positively sloped which indicates heat transfer is not only thermodynamically feasible, but quite favourable in terms of temperature differences. Exchanging heat between cooler C1 and heater H2 is thermodynamically infeasible in HOCI way. It is because the CP of cold stream CS2 is lower than of hot stream H1. The temperature span of cooler C1 increases at a slower rate than of heater H2. The hot end of this new heat exchanger will be having temperature difference lower than ΔT_{min}. Showing the temperatures, temperature difference and CPs of the streams in a single view (the SRTGD) helps the user screening feasible from infeasible heat paths.

4.2.2.2 *Number of heat exchangers involved in a heat path*

It is desirable to develop a heat path that involves the smallest number of heat exchangers. This would tend to affect less heat exchangers and push less of their temperature differences close to each other when utilities are reduced. To cope with the duties, investment is needed to increase heat transfer areas or improve the heat transfer.

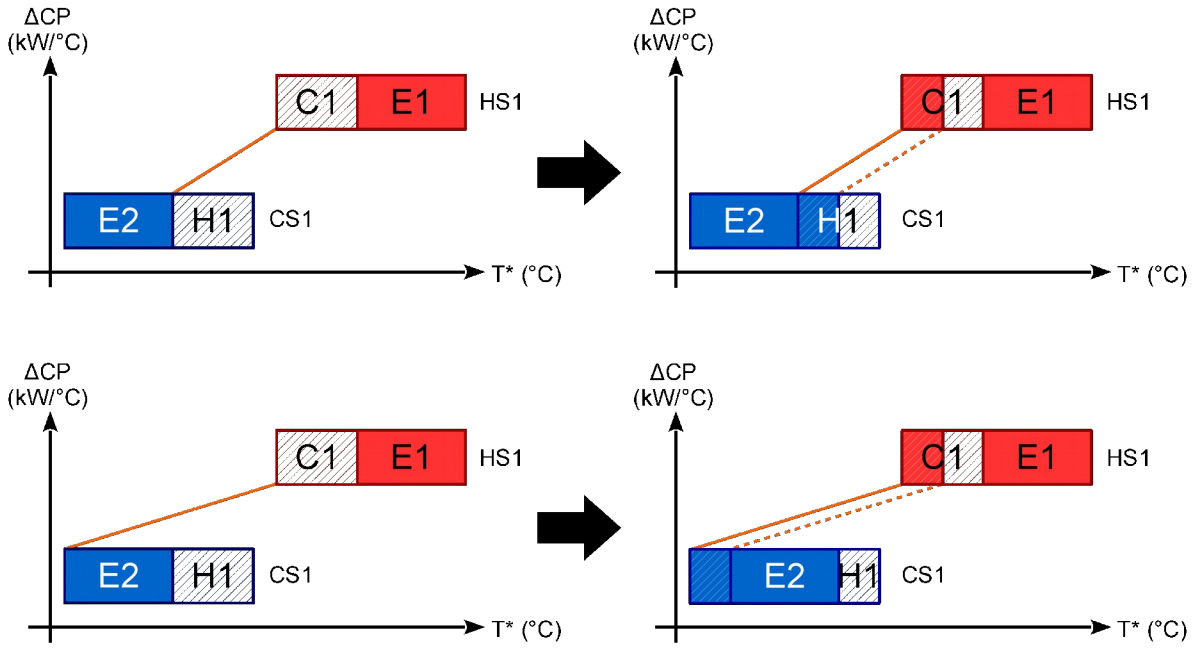

Figure 4.34: Heat path developed using HOCI way, with (a) heat path involving no other heat exchanger and (b) heat path involving one heat exchanger

Figure 4.34 shows two different heat path developments for the same HEN with a hot stream (HS1) and a cold stream (CS1). Figure 4.34(a) shows heat path development directly matching cooler C1 and heater H1. This heat path involves the least number of heat exchangers as it only requires installing one. Figure 4.34(b) shows heat path development involving heat exchanger E2 as well. When the same amount of utilities are reduced using this heat path, the inlet and outlet temperatures of heat exchanger E2 increase. Investment on heat exchanger E2 has to be made as well. Another concern with involving other heat exchangers is that the latter might limit the amount of heat recovered.

There are scenarios where heat paths inevitably involve other heat exchangers. Figure 4.35 has the same topology as Figure 4.34, but now the inlet temperature of heater H1 is higher than the inlet temperature of cooler C1. Heat path cannot be developed direct matching cooler C1 and heater H1 due to temperature infeasibility. The heat path developed has to involve one more heat exchanger, as shown in Figure 4.36.

SRTGD is particularly useful in providing visual information on the placement of new heat exchanger, so that the heat path is involving as few heat exchangers as possible.

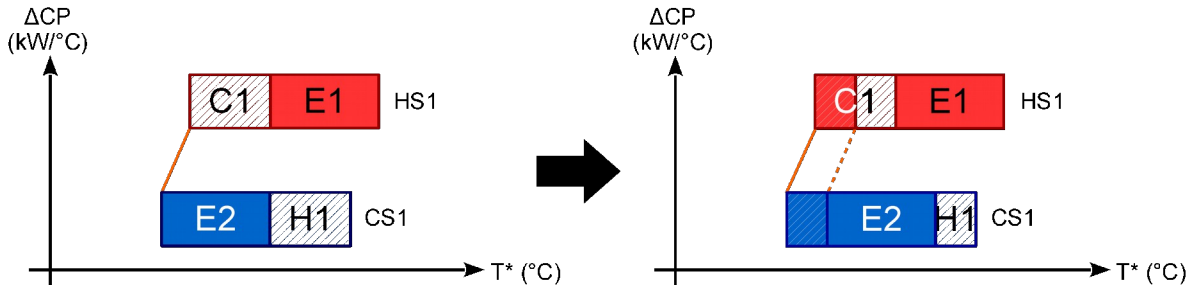

Figure 4.35: Heat path have to include a heat exchanger for heat recovery for this scenario

4.2.2.3 *Selection of favourable heat paths from several feasible options*

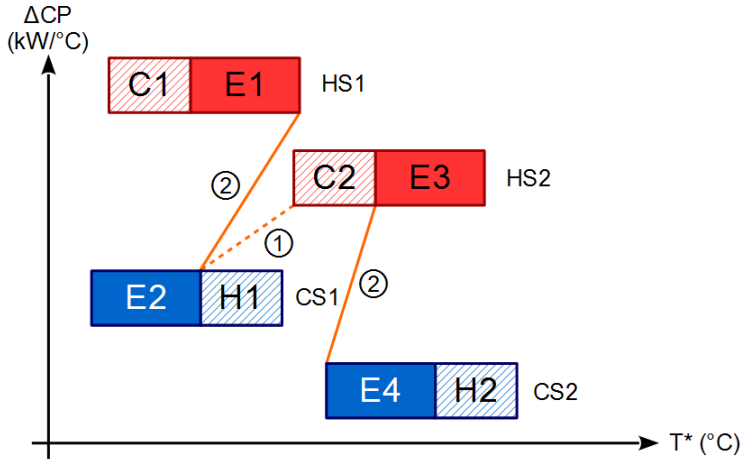

Figure 4.36: Two ways of developing heat paths with different amount of heat recovery

Figure 4.36 shows the inlet temperature of cold stream CS2 is higher than the inlet temperature of hot stream HS1. Heat path cannot be developed between these two streams. Two thermodynamically feasible ways of developing heat paths between heaters and coolers in this scenario. The ① way is indicated by a dashed line while the ② way is indicated by two solid lines. Hot stream HS2 can exchange heat with either cold stream CS1 or CS2. The ① way shows that heat path is developed directly between hot stream HS2 and cold stream CS1. It only requires one new heat exchanger. However the heat recovery potential of hot stream HS1 is not considered. The ② way has two heat paths where hot stream HS1 is considered first. It is matched with cold stream CS1 while hot stream HS2 have to be matched with cold stream CS2. Two new heat exchangers are required and heat transfer areas for heat exchangers E1 and E4 has to be increased for this way. Although the ② way is involving more heat exchangers, it is more favourable as it recovers more heat. Using SRTGD provides visual information to the user to select favourable heat paths from several feasible options.

4.2.2.4 *Shows the location of potential NP in a heat path*

Because SRTGD shows the heat exchangers involved in a heat path and temperature differences for all heat exchangers in the diagram, the potential NP which limits the maximum

heat can be recovered of the heat path can be determined. After finding the potential NP, it is possible to overcome it by either re-sequencing heat exchanger, repiping and splitting the stream. The example is taken from Yong et al. (2014), which discusses fully about finding potential NP and calculation of maximum heat recoverable of a heat path. Figure 4.37 shows SRTGD of a HEN which dashed green line showing the heat path. Thicken line shows the location of the potential NP, which is the cold end link of HEX-03. The temperature span of this line determines the maximum recoverable heat for this heat path.

4.2.3 SRTGD assessment

SRTGD has advantages over conventional HEN Grid Diagram. It shows the interactions of stream temperatures and CPs – quite useful in developing heat paths. It also shows the location of existing and potential Pinches. A problem of SRTGD is that it is difficult for showing streams with small temperature span or high CP. For example, a stream releasing latent heat would feature temperature span close to 0 °C for single-component stream, leading to undefined heat capacity flowrate. If it is drawn with streams that usually have 100 °C temperature range and around 40 kW/°C heat capacity flowrate, the resulting SRTGD would have a very tall and thin box representing the latent heat releasing stream.

An initial attempt to tackle this problem is to replace the CP with the load on the y-axis. This option is shown in Figure 4.37. A simple HEN (Klemeš et al., 2014) is represented with condensing stream shown for comparison. This type of SRTGD can provide a similar guidance.

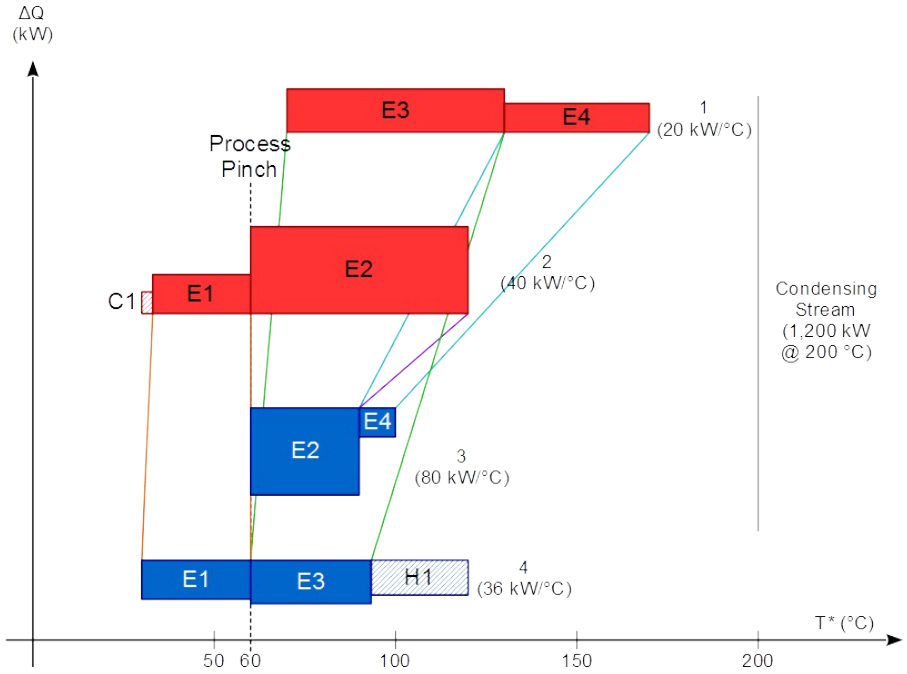

Figure 4.37: Another way of constructing SRTGD with ΔQ as y-axis.

4.2.4 Case Study Implementing SRTD

The case study is from Varbanov and Klemeš (2000). In that paper, there are seven heuristic rules defined and used for path development. The final result obtained is able to reach the minimum utilities usage.

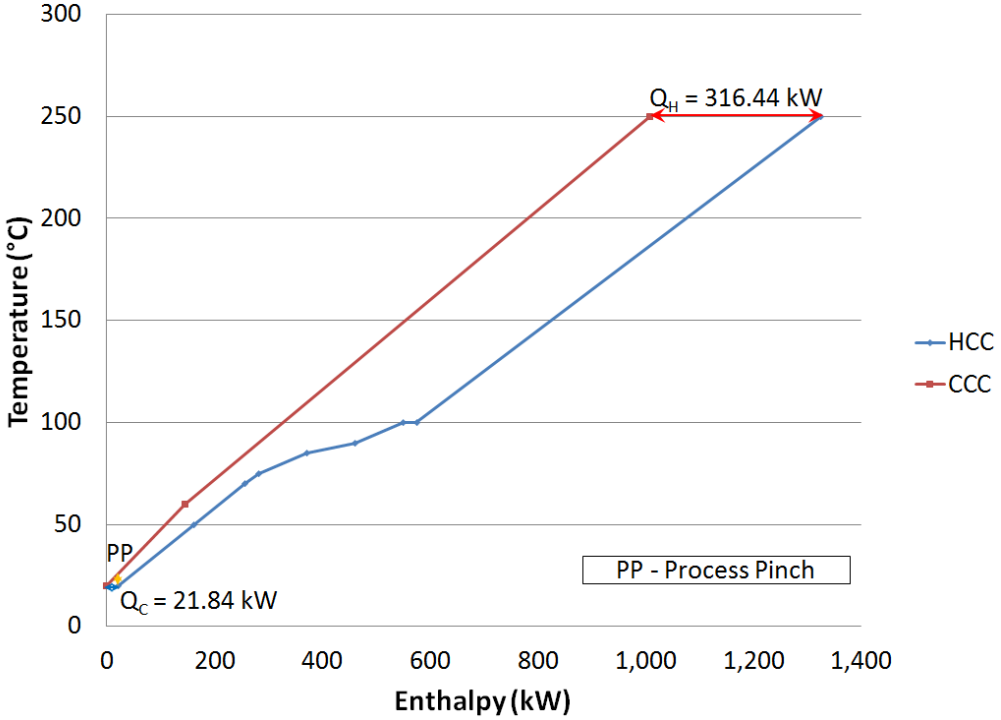

Figure 4.38: Composite Curves for the case study

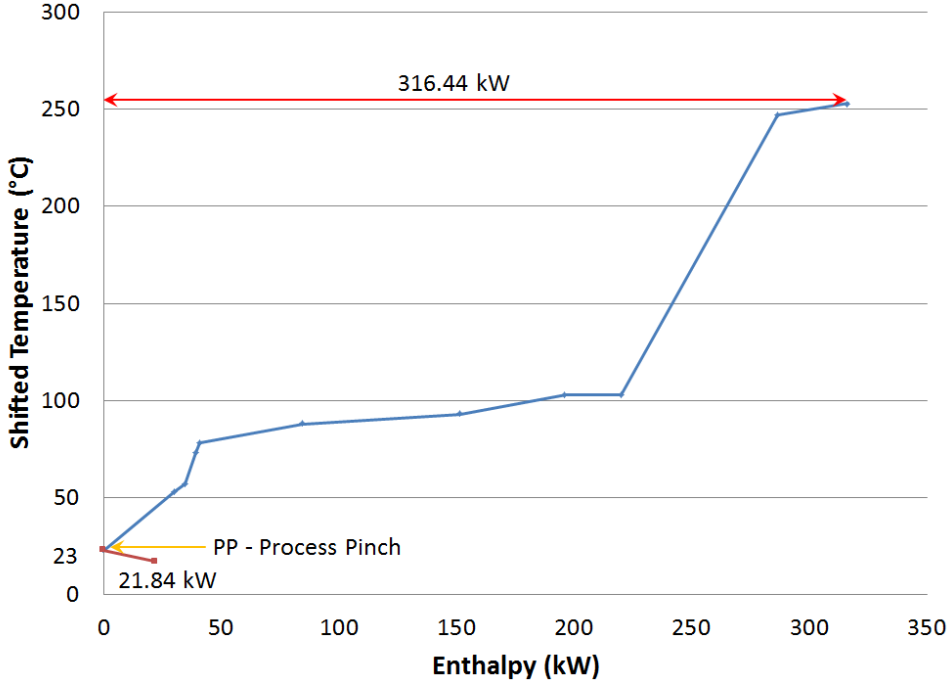

Figure 4.39: Grand Composite Curve for the case study

The case study considers a sunflower oil plant, first analysed by Nenov and Kimenov (1997). The ΔT_{min} used there was equal to 6 °C. For Figure 4.38 and Figure 4.39, the Pinch is at 26/20 °C with total hot and cold utility of 316.44 kW and 21.84 kW. The targets indicate 650.36 kW potential for additional heat recovery.

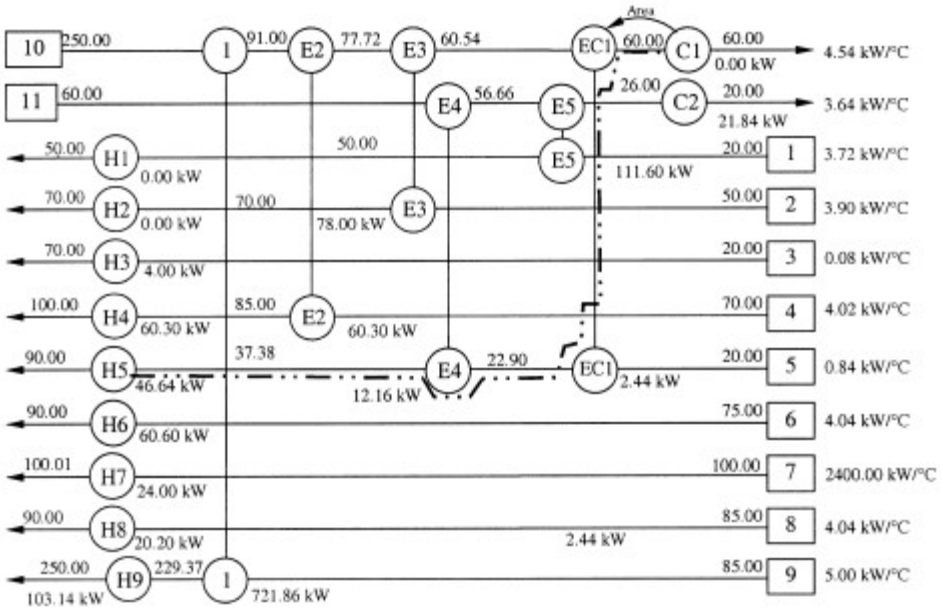

Figure 4.40: Final result of HEN from Varbanov and Klemeš (2000)

Figure 4.40 shows the final results obtained by Varbanov and Klemeš (2000). It can be seen that it uses 6 heat exchangers, 7 heaters and 1 cooler. This process has 11 process streams, the minimum number of required heat exchangers is 10. Although it achieves the minimum utility usage target, the total number of heat exchangers including heaters and coolers in the final result is 14. It is desired to reduce the amount of heat exchangers with different topology in this case study using mentioned steps. The algorithm applied is based on the system of heuristic by Varbanov and Klemeš (2000).

Figure 4.41 shows SRTGD of the existing HEN. A vertical dotted line denotes the lowest cold stream temperature at 20 °C. Any hot stream segments spanning to the left of this vertical line can only be cooled by using utility. In Figure 4.41 only a segment of hot stream 11 is of this type. The outlet temperature for hot stream 11 is 20 °C, and the shifted outlet temperature is 14 °C. The temperature difference between the shifted outlet temperature of hot stream 11 and the vertical line is 6 °C, and the cooling duty required for this hot segment is 21.84 kW. There is substantial violation of “Don’t transfer heat across the Pinch” rule.

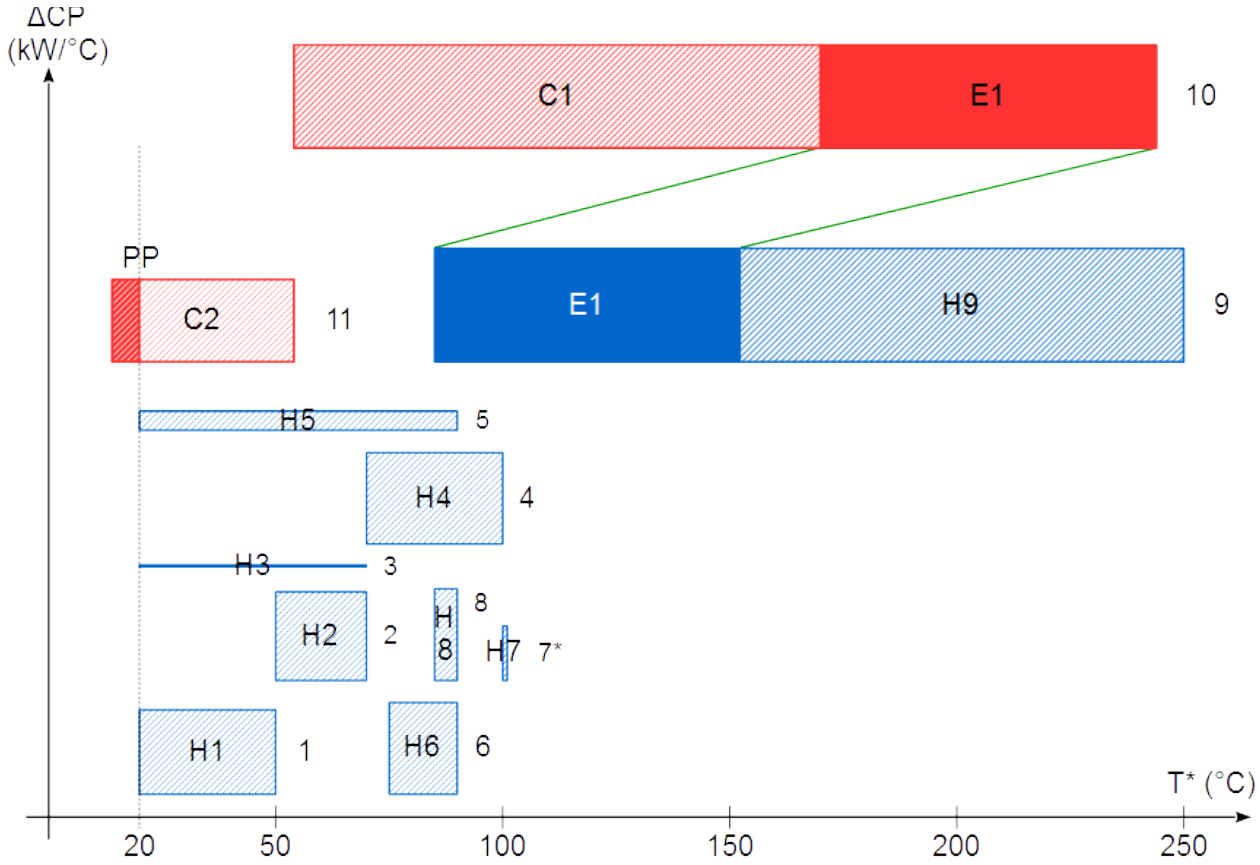

Figure 4.41: SRTGD representation of the case study, the CP is quoted in bracket. CP for cold stream 7 is scaled to fit the graph

From Figure 4.41, the first step is to identify the hot stream with cooler that has the lowest outlet temperature. It has been found that it is hot stream 11. The new heat exchanger in hot stream 11 is a NP at its cold end. From Figure 4.41, the potential matches according to temperature are cold streams 1, 3, and 5. According the value of CP, only cold stream 1 has higher CP value than hot stream 11. Hot stream 11 can only match with cold stream 1. Since the heat exchanger is built in HOCI way and the $CP_H < CP_C$, hot end link will never be the NP. Cold stream 1 limiting the maximum heat recovered for this heat path, recovering 145.60 kW of heat - see Figure 4.42.

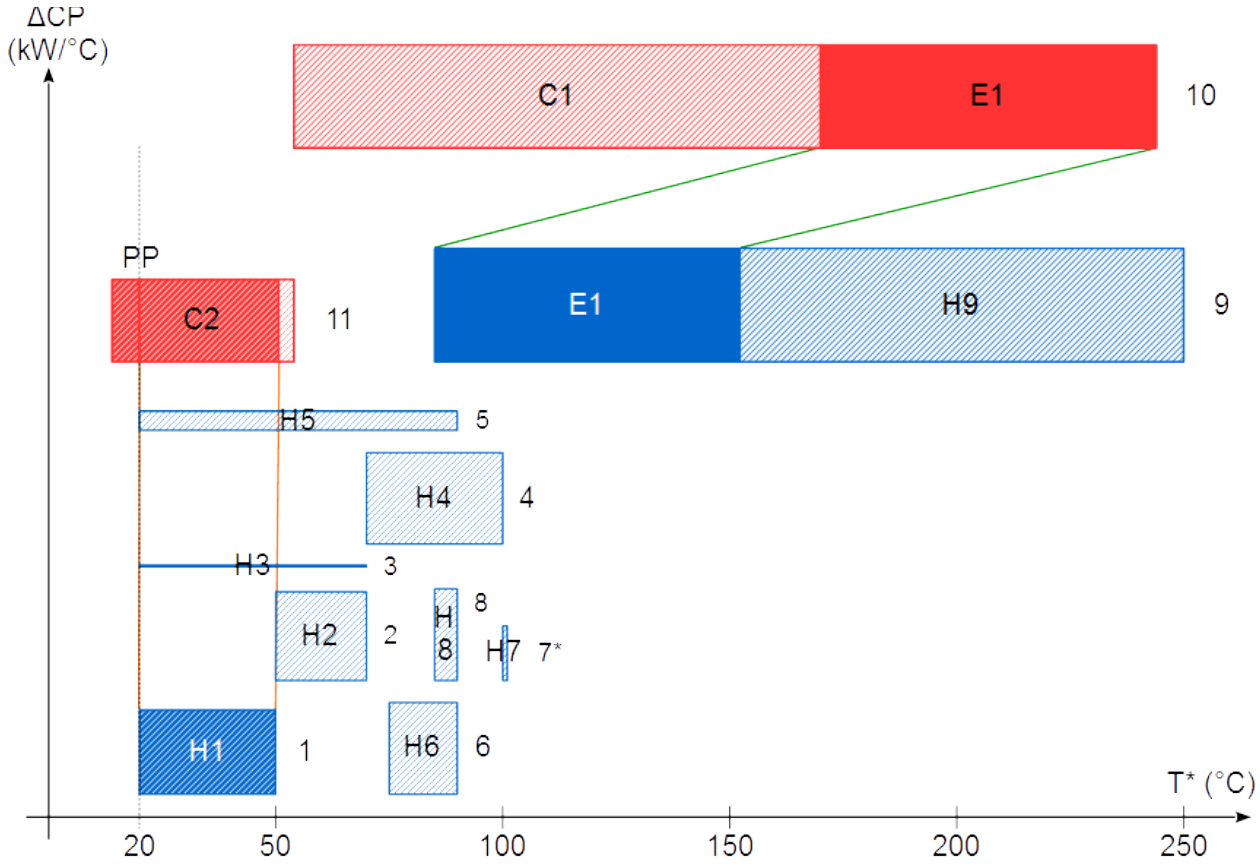

Figure 4.42: Modified HEN after the first heat path development

Figure 4.42 shows that cold stream 1 can be completely heated by hot stream 11. Remaining heat of cooler C2 is still having the lowest target temperature. The lowest supply temperature cold streams are still heaters H3 and H5. Heater H5 is chosen over heater H3 has it has higher CP. Heater H3 has too low heat duty to satisfy the remaining cooling requirement by cooler C2. The result is shown in Figure 4.43.

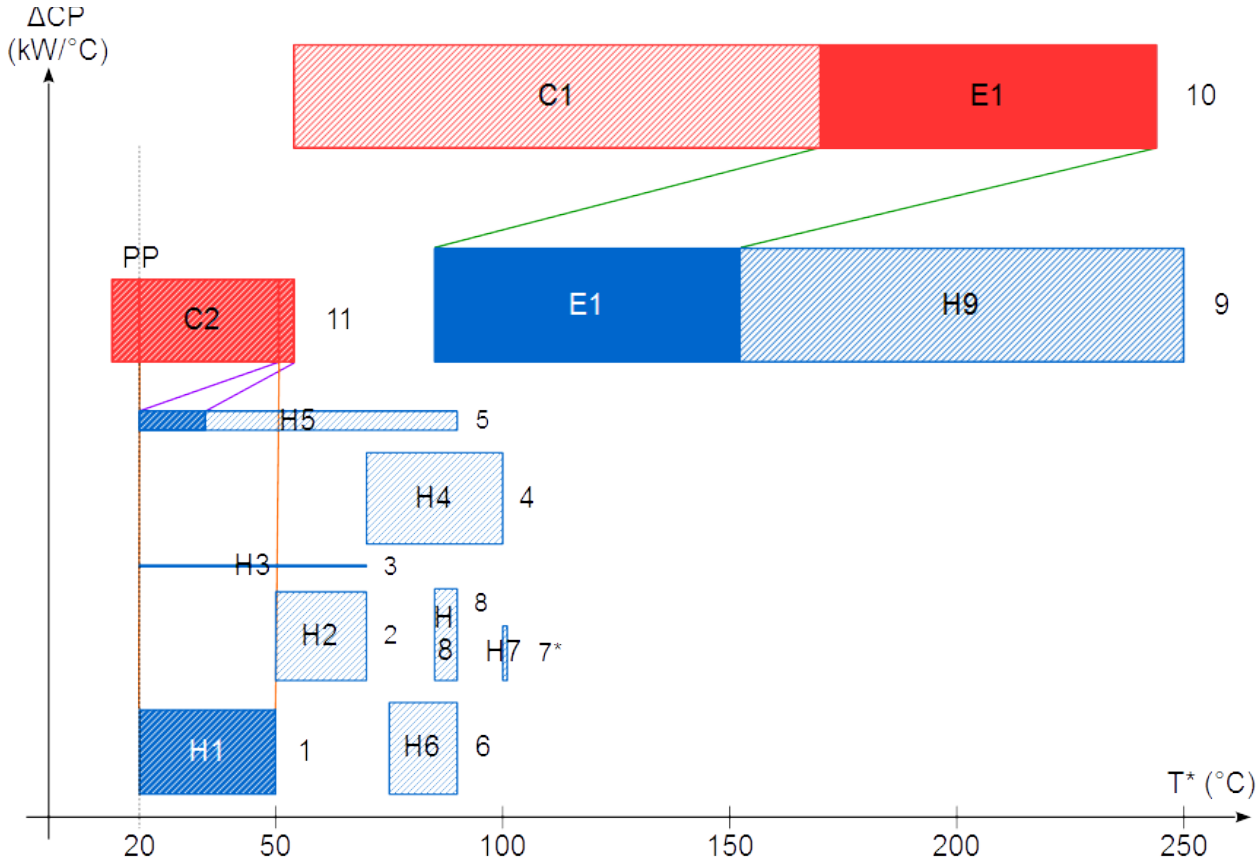

Figure 4.43: Modified HEN after the second heat path development

Cooler C2 has been fully cooled by utility, cold stream 1 and partial of cold stream 5 - Figure 4.43. The only hot stream left is hot stream 10 with its cooler C1. The next heat path should be matching cold stream 3 with heater H3. However if the new heat exchanger is built using HOCI way, and the $CP_H > CP_C$, the cold end link eventually becomes a Pinch. The maximum heat can be recovered for this heat path is too small (4 kW) for the investment. Cold stream 3 is ignored in involving heat recovery.

The next lowest feasible temperature is then the remaining of cold stream 5. Again, if the new heat exchanger is built using HOCI way, and since the $CP_H > CP_C$, the hot end link for this match will become NP as well, as shown in Figure 4.44. The Pinch occurs at 58.4/64.4 °C and only recovers 20.12 kW of heat. The remaining heat demand of cold stream 5, if the heat path is chosen, needs to be satisfied by using hot utility. It requires more than one heat exchanger to fulfill the demand.

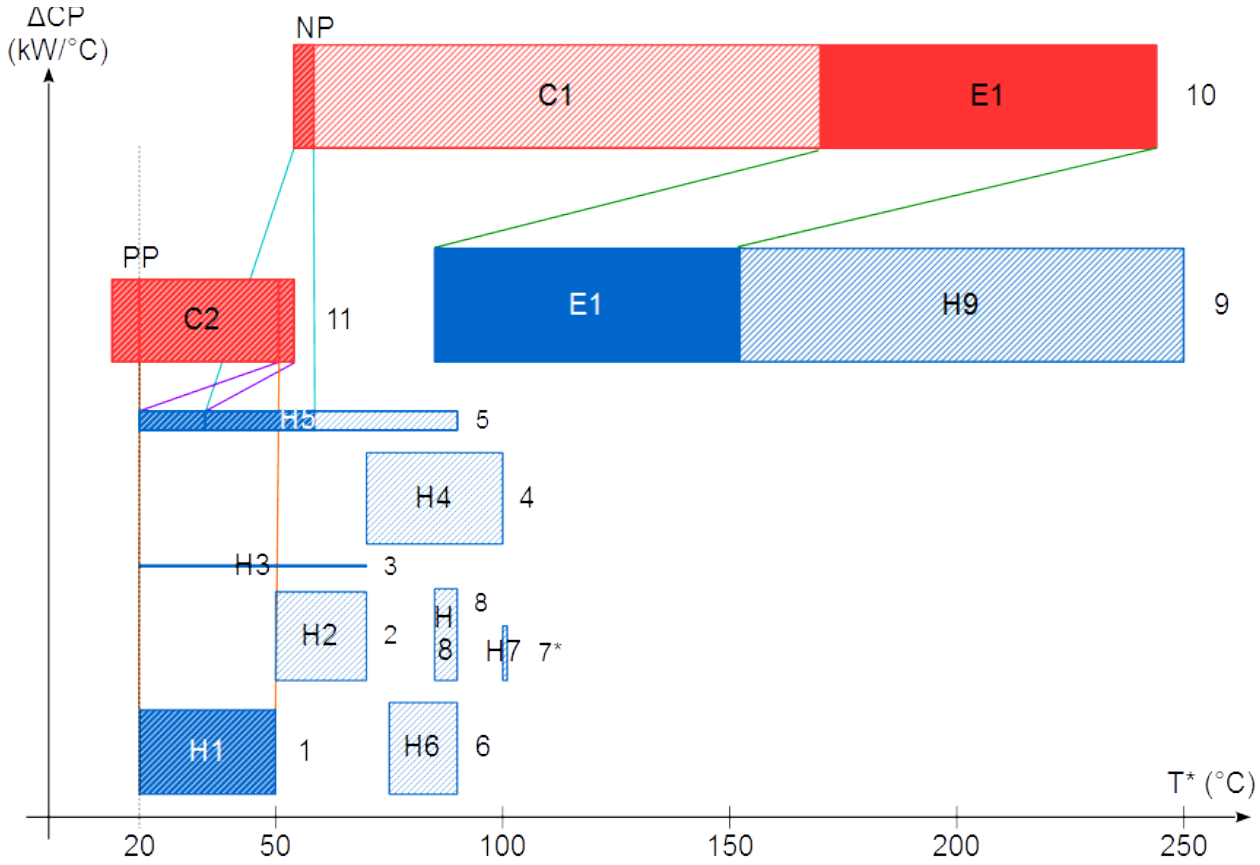

Figure 4.44: HEN showing if stream 5 is chosen instead at this stage

The remaining heat demand of stream 5 can be still satisfied by hot stream 10, but it requires more than one heat exchanger. Among the remaining cold streams, cold stream 2 has the lowest temperature and the only cold stream to exchange heat with low temperature part of hot stream 10. Although it is $CP_H > CP_C$ for heat path matching hot stream 10 and cold stream 2 and the new heat exchanger built in HOCI way, the hot end link has not become the Pinch as the maximum heat recoverable for this heat path is limited by heat content of cold stream 2. Heat demand of cold stream 2 can be fully satisfied by hot stream 10 at its lowest temperature end. The result is shown in Figure 4.45.

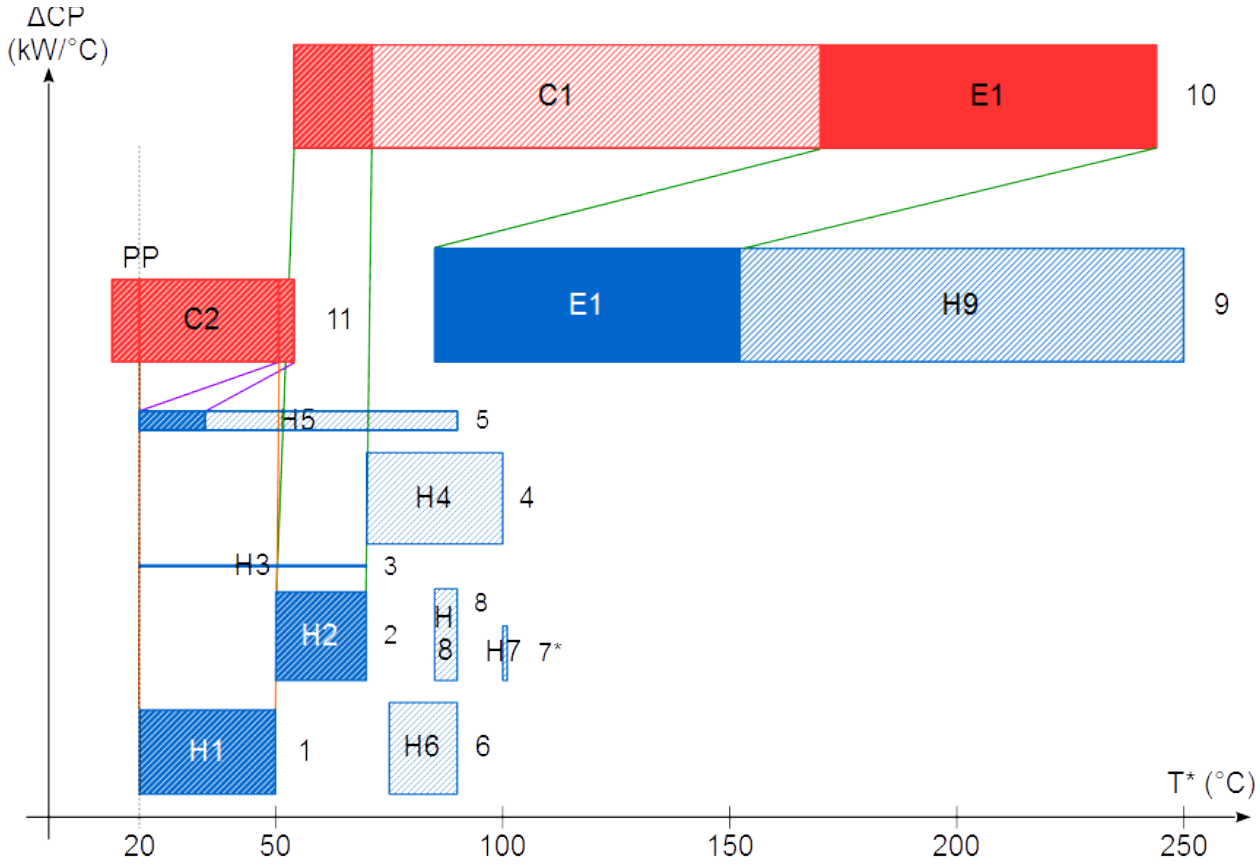

Figure 4.45: HEN showing after the third heat path development

Among the remaining cold streams 4, 6, 7 and 8, only cold stream 4 has the lowest temperature to exchange heat with hot stream 10, which just exchanged heat with cold stream 2. It is a HOCI heat exchanger and $CP_H > CP_C$ case again. This heat path match is unable to satisfy all the heat demand of stream 4, recovering 41.44 kW of heat only before reaching the Pinch at 86.3/80.3 °C.

There are no other cold streams to be fully satisfied by hot stream 10 in HOCI way, then these cold streams are exchanging heat with the available hot end of hot stream 10 using HICO way. Although it is $CP_H > CP_C$ for all the matches, the cold end link for all these new heat exchangers will be NPes due to the heat capacities of these cold streams limiting the amount of heat recovered. There are various ways of arranging which cold streams to be heated first. The heuristic from the work of Varbanov and Klemeš (2000) is followed to find the sequence, which is starting from cold streams 7, 4, 8, 6 and 5. This sequence is determined starting from highest outlet temperature of cold streams. The result is shown in Figure 4.46.

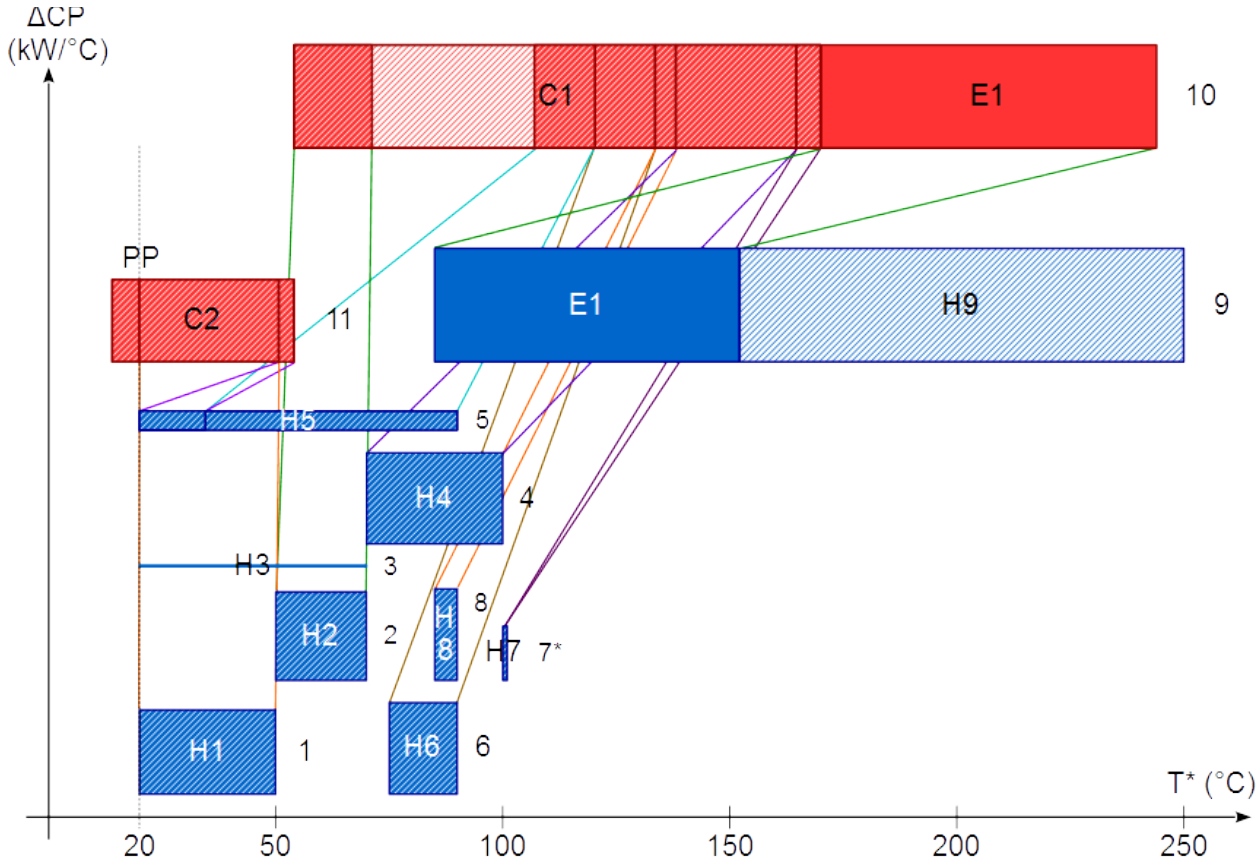

Figure 4.46: Using hot stream 10 to heat up cold streams 4, 6, 7 and 8.

There is remaining heat can be recovered from hot stream 10 at higher temperature, cold stream 2 can be heated using higher temperature end of hot stream 10 - Figure 4.47.

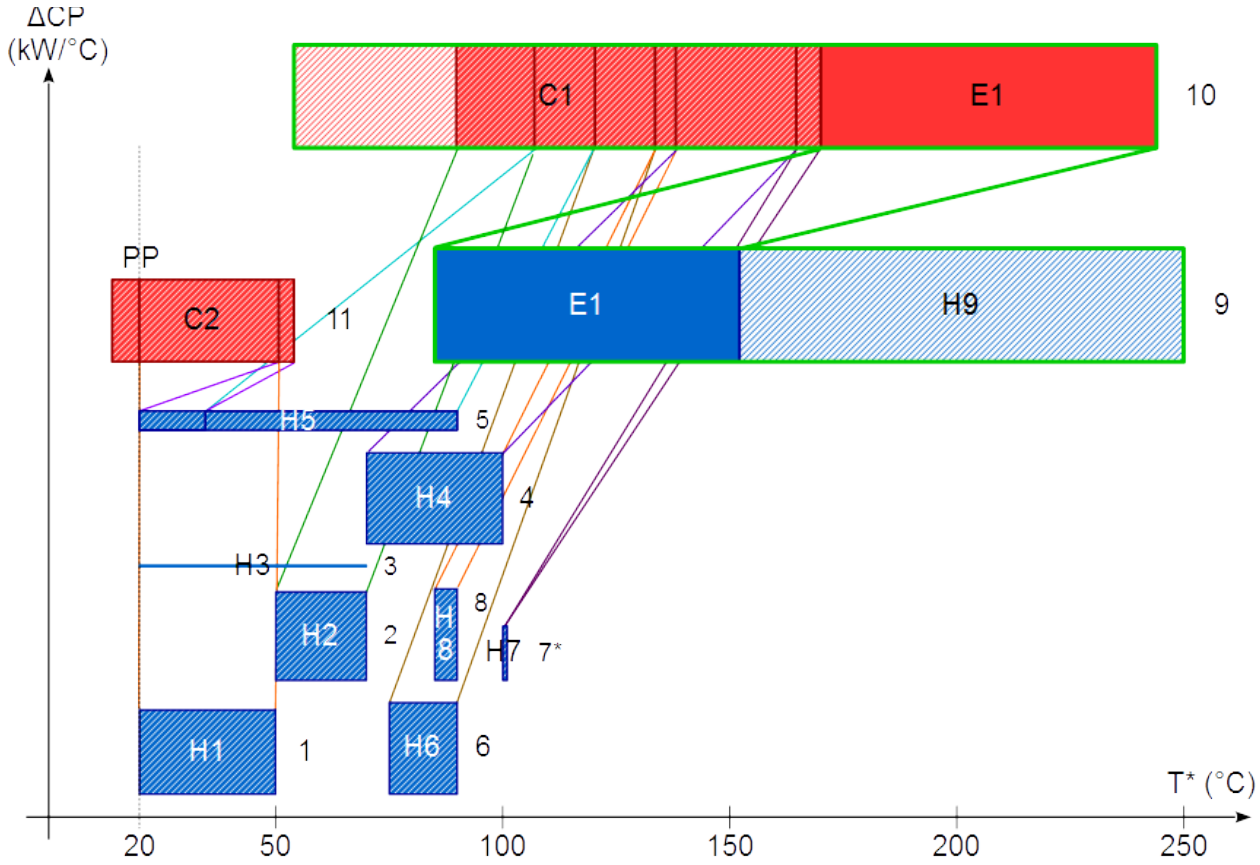

Figure 4.47: Cold stream 2 is heated with hotter pat of hot stream 10

The heat can be further recovered by increasing the duty of heat exchanger E1. The heat path is connecting the remaining heat of cooler C1 in hot stream 10 to heater H9 in cold stream 9 passing through heat exchanger E1 (indicated by thick green line). It can be seen that the heat path is Pinched at hot end of heat exchanger E6. The final result is shown in Figure 4.48. Comparisons are made between the result obtained from Varbanov and Klemeš (2000) and this study with the existing HEN. Table 4.1 shows the comparisons of utilities used.

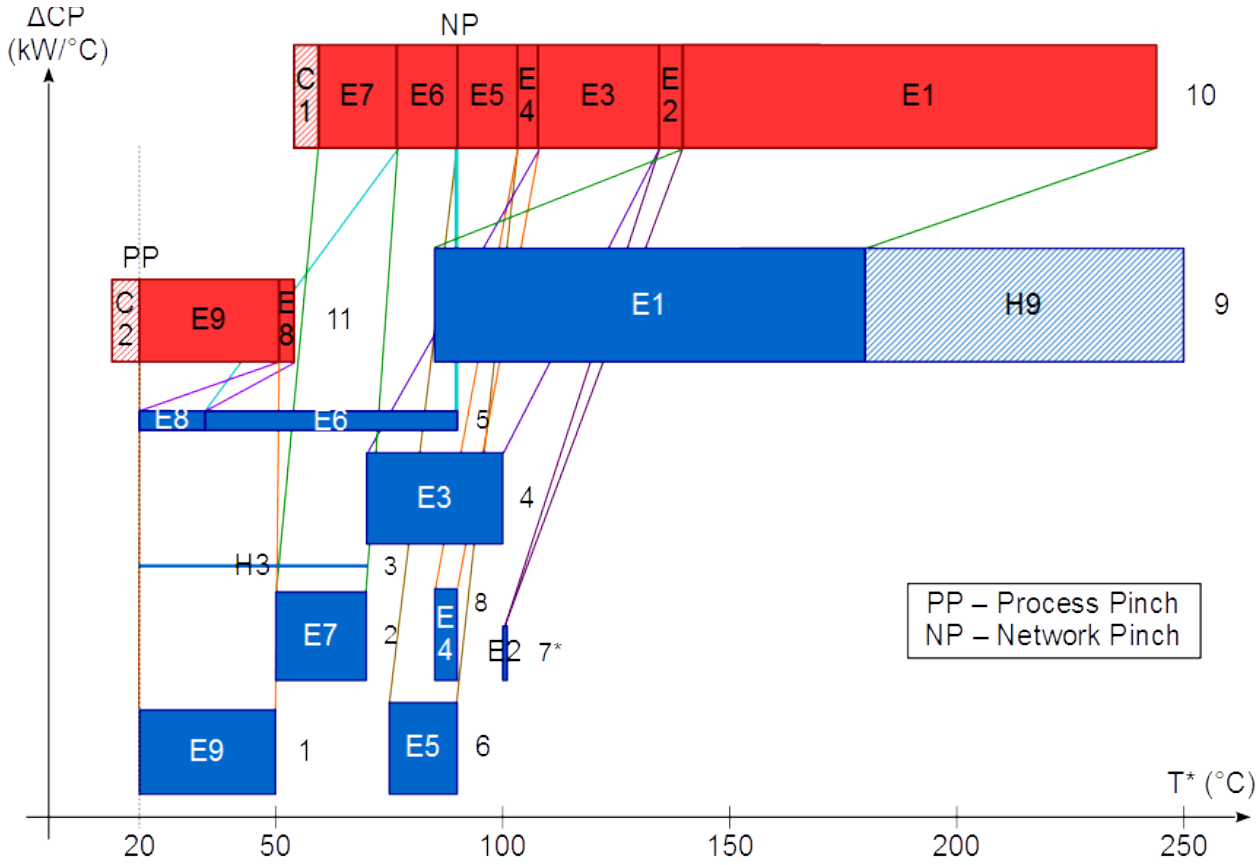

Figure 4.48: Final result of HEN for this study

The result obtained in this study uses one heat exchanger less than the one by Varbanov and Klemeš (2000). As a result (Table 4.1) it achieves 38.8 kW less utility savings. However, the topology obtained in this study is favourable compared to the results of Varbanov and Klemeš (2000). A preliminary economic analysis is shown in Table 4.2.

Table 4.1: Comparison of post-retrofit utility usage between Varbanov and Klemeš (2000) and this study against existing HEN

	Existing HEN	Varbanov and Klemeš (2000)		This study	
		Utility usage (kW)	Utility saving (kW)	Utility usage (kW)	Utility saving (kW)
Hot utility required (kW)	966.8	316.44	650.36	355.24	611.56
Cold utility required (kW)	672.2	21.84	650.36	60.64	611.56

Table 4.2: Economic analysis between Varbanov and Klemeš (2000) and this study against existing HEN with hot and cold utilities prices are taken as $ 123.83 /kW and $ 10.32 /kW

	Existing HEN	Varbanov and Klemeš (2000)	This study
Total Area Required (m²)	37.88	180.62	81.23
Utility saving* ($/y)	-	87,246	82,041
Retrofit Capital Cost ($)	-	248,227	214,013
Specific investment ($/(kW·y))	-	381.7	349.9
Payback Time (y)	-	2.85	2.61

Overall heat transfer coefficients are required to find the heat transfer areas for all heat exchangers are estimated from Smith (2005). The values of heat transfer areas are then used to calculate the cost of each heat exchanger.

The capital cost function for new heat exchangers (Eq(4.1)) is from (Soltani and Shafiel, 2011).

$$\text{New heat exchanger capital cost (\$)} = 29{,}073 + 727\, A^{0.81} \tag{4.1}$$

Where A is the heat transfer area of new heat exchanger in m².

The cost function for adding area not exceeding 10 % on existing heat exchanger in the case of using heat transfer intensification (Eq(4.2)) is obtained from the work of Pan et al. (2013):

$$\text{Cost for adding new effective area on existing heat exchanger (\$)} = 3{,}460 + 200\, \Delta A \tag{4.2}$$

where ΔA is the effective area added (m²). This cost type has much lower values than that installing a heat exchanger because it means reuse of an existing one and adding more heat effective area by heat transfer enhancement.

The prices for hot and cold utilities are obtained from Soltani and Shafiel (2011) as well, at $ 123.83 /kW and $ 10.32 /kW. The cost is updated to the latest year of 2013 using CE Index (Chemical Engineering, 2014).

The results (Table 4.2) show that the utility cost saving in the current study is less than the results by Varbanov and Klemeš (2000) due to higher utility usage. However, the savings are achieved at lower investment costs and lower specific investment. The payback time from this study is shorter. It should be noted that the price of utility have significant influence on choosing the better HEN modification. During the analysis the utility price is lower, the high utility usage is compensated by low investment cost. If the utility price is high, HEN modification from Varbanov and Klemeš (2000) is more favourable. Nemet et al. (2015) provides design of Total Site where fluctuating utility prices. This tool helps user in choosing better HEN modification base on this fluctuating utility prices, which has been recently the case.

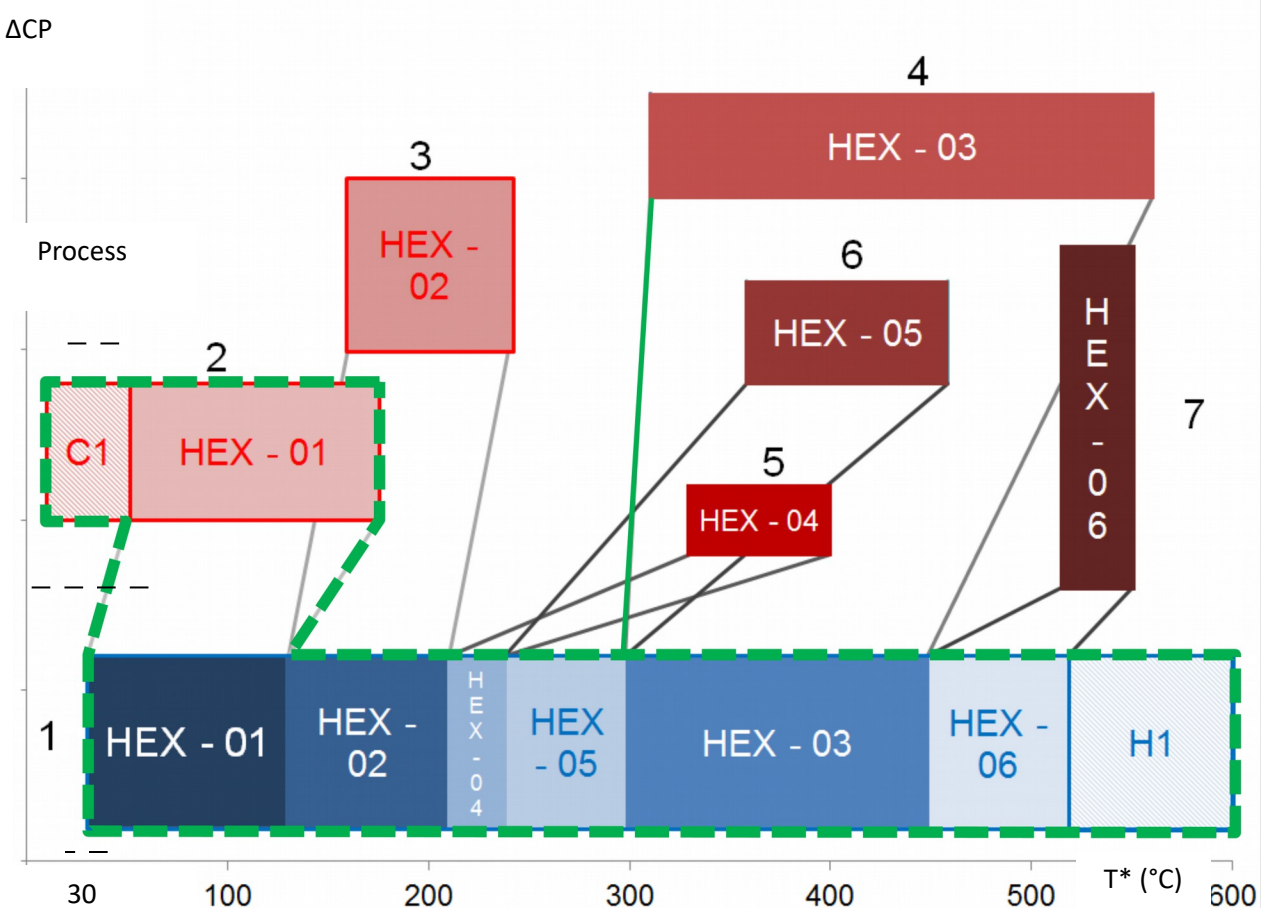

RTGD used for locating potential NP for a heat path.

4.2.5 Summary

This section introduces an extended Grid Diagram – the Shifted Retrofit Thermodynamic Grid Diagram (SRTGD). Its uses are demonstrated using the provided examples and the case study. From the case study, a different, more beneficial set of retrofit options featuring more economically attractive design, where around 8 % improvement has been achieved in the payback time. However the main importance comes with the possibility to assess the retrofit options for fluctuating energy prices and forecastles. With SRTGD showing thermodynamic feasibility, stream capacity and topology of a HEN, different topologies can be obtained. The retrofit should be done based on the assumption of the future price of fuel in the analysis, and SRTGD is help user in choosing better HEN modification base on this fluctuating utility prices.

4.2.6 Nomenclature

A	Heat transfer area of heat exchanger [m²]	NP	Network Pinch
CP	Heat capacity flowrates [kW/°C]	PP	Process Pinch
HICI	Hot-inlet-to-cold-inlet	Q	Heat capacity [kW]
HICO	Hot-inlet-to-cold-outlet	T	Temperature [°C]
HOCI	Hot-outlet-to-cold-inlet	T*	Shifted temperature [°C]
HOCO	Hot-outlet-to-cold-outlet	ΔTmin	Minimum allowed temperature difference [°C]

4.3 Heat Exchanger Matrix

Graphical HEN representations have some limitations. (i) The data accuracy is reduced using graphical representation. Exact values cannot be retrieved directly. (ii) The graphical representation becomes complicated when there are too many heat exchangers in the HEN. (iii) Important data such as temperature differences at the ends of heat exchangers are not able to be directly shown on the graph.

In this section the suggestion to represent HEN numerically in a matrix form is proposed. HEN Stream Matrix (HENSM) is able to improve the discussed limitations faced by graphical representations. Both SRTGD and HENSM contain equal information but HENSM is more flexible. However, HENSM doesn't provide the same insight as the graph and should be used in the combination. The data for each heat exchanger are recorded numerically and can be retrieved directly and accurate. This matrix is also able to record a HEN with high number of heat exchangers, as it does not use lines or connectors. This is a well-organised representation and is able to help to process the analysis. Temperature differences can be traced and evaluated directly, which helps in locating Pinches. During heat path tracing in retrofit analysis, the bottleneck heat exchanger limiting the heat recovery can be determined directly. Using the proposed matrix format to represent a HEN helps to increase the clarity.

This suggested HEN representation can be used as an alternative tool for synthesis and retrofit. It can also be used to generate graphical HEN visualisation such as GD and SRTD. In Pinch Analysis it is stated that there should be no heat transfer across the Pinch. The streams can be split into above and below Process Pinch in HENSM during HEN synthesis. To avoid heat transfer from hot stream above Pinch to cold stream below Pinch, HENSM can remind user from these forbidden matches. Any incorrect and thermodynamically infeasible matches can be seen using the temperature differences column. HENSM provides better notification of Network Pinch. How the heat exchangers behave along a heat path can be observed, using the temperature differences, which is important for the retrofit. The bottleneck heat exchanger limiting the heat recovery can be determined. The matrix implementation is demonstrated by retrofit analysis. It can also be used as an input and output interface for software tools, avoiding double input procedure.

4.3.1 Matrix Construction and Structure Description

Streams are divided into smaller unit called segments, where one hot segment exchanges heat with exactly one cold segment. Each segment may also additionally exchange heat with a utility. HENSM consists of hot and cold stream segments intersecting with each other, where the intersections are placeholders for duties of recovery or utility heat exchangers. Referring to HENSM sketch in Figure 4.50, the data of hot stream segments such as heat capacity flowrate (CP), supply and target temperatures are at the top. The segment placeholders run vertically from top to bottom as shown using vertical arrow in Figure 4.50. The arrangement of these hot stream segments is first according to hot stream. If more than one segment is found for a hot

stream, then the segments are arranged according to descending order of supply temperature. If a hot stream segment is served by a cooler, the duty of the latter is placed at the end of the vertical arrow. The cold stream segments start from the left and run horizontally to the right, shown using a horizontal arrow. The cold stream segments are arranged first according to the cold streams. For each cold stream the segments are arranged in ascending order of supply temperature. Similarly for a cold segment with heater, its duty is shown at the end of the horizontal arrow.

The temperature difference between hot and cold stream segments are calculated at hot ends (HETD) and cold ends (CETD) of all heat exchangers. When Pinch is considered in the analysis, ΔTmin is deducted from HETD and CETD, resulting in shifted parameters called HETD* and CETD*. These two parameters should have non-negative values at all time, for ensuring feasible heat exchange. A zero value at one of the ends of the heat exchanger indicates that that is a Pinch Point (Process or Network Pinch).

The hot and cold stream segments intersect each other in the recovery heat exchanger area in the middle of HENSM. The recovery heat exchanger duties are recorded in the intersection cells. To ensure that each hot stream segment exchanges heat with exactly one cold stream segment, there should be no other values in the other cells in the concerned row and column.

HENSM keeps precise values of temperatures and duties of each heat exchanger. Besides that, temperature differences at the ends of heat exchangers which cannot or are difficult to represent graphically can be traced and evaluated using the matrix. This helps locating the Process and Network Pinches. The HETD* and CETD* values also indicate how close are heat exchanger ends to Pinching condition. HENSM can also accommodate specifying different ΔTmin values in different parts of the network.

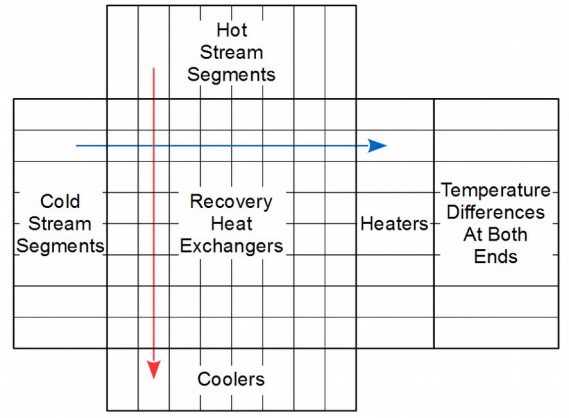

Figure 4.50: Sketch of HENSM as HEN representation

4.3.2 Heat exchangers considered along a heat path

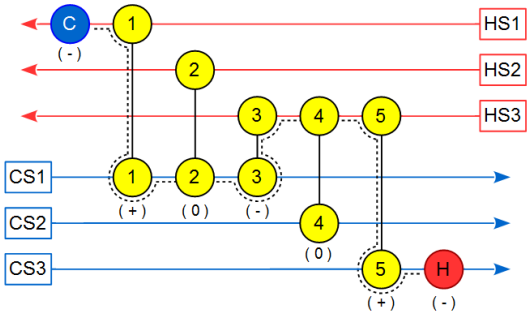

Figure 4.51: Heat path showing different kinds of heat exchangers

Consider Figure 4.51 where an example of a heat path on a HEN grid diagram is shown (Varbanov and Klemeš, 2000). Along the heat path there are all four kinds of heat exchangers. In this context, they are grouped into positive pass-through heat exchangers (i.e. 1 and 5), negative pass-through heat exchangers (i.e. 3), hot-fixed pass-by heat exchanger (i.e. 2) and cold-fixed pass-by heat exchanger (i.e. 4).

With the heat recovery increased over this heat path, the duties of cooler and heater decrease. To cope with energy changes, the positive pass-through heat exchanger increases its duty while negative pass-through heat exchanger decreases its duty. The supply temperatures for both hot and cold stream segments in positive pass-through heat exchangers do not change during the analysis. The target temperatures for both hot and cold stream segments in negative pass-through heat exchangers do not change during the retrofit analysis. For a hot fixed pass-by heat exchanger inlet and outlet temperatures of hot stream segment do not change during the analysis. For cold fixed pass-by heat exchanger inlet and outlet temperatures of the cold stream segment do not change during the analysis.

A Network Pinch would align at a heat exchanger, at one end, after reaching the maximum heat recovered. Depends on how the heat exchanger behaves in the heat path, the maximum heat recovered for this heat exchanger is the lower value between cold end to Pinch (CETP) and hot end to Pinch (HETP) calculated using Eq(4.3) to Eq(4.10) in Table 4.3. The lowest value among these heat exchangers is the Maximum Allowable Heat Transferred (MAHT) for this heat path.

The calculation of additional area for all heat exchangers starts from determining the new values of HETD and CETD. Using these two values the log mean temperature difference for each heat exchanger can be calculated directly. Some simple assumption can be such as the overall heat transfer coefficients are kept constant to find the new area for heat exchanger.

The cost of building the new heat exchanger used in the case study is calculated following the equation found in Jiang et al. (2014) where A is in m².

$$C\ (\$) = 44{,}186 + 388.8 \times A \qquad (4)$$

Table 4.3: Equations to determine the Network Pinch for all four discovered kind of heat exchanger

Heat Exchanger Kind		
Positive Pass-through	CETP = CETD* × CPC (4.3)	HETP = HETD* × CPH (4.4)
Negative Pass-through	CETP = CETD* × CPH (4.5)	HETP = HETD* × CPC (4.6)
Hot Fixed	CETP = CETD* × CPC (4.7)	HETP = HETD* × CPC (4.8)
Cold Fixed	CETP = CETD* × CPH (4.9)	HETP = HETD* × CPH (4.10)

4.3.3 Case Study Implementing HEM

A case study is used to demonstrate the use of HENSM. A simplified preheat train is adapted from Jiang et al. (2014). The stream data is given in Table 4.4. All hot streams exchange heat with the only cold stream. There are four coolers and a heater, while heat transfers between streams are done using seven heat exchangers. The HEN Grid Diagram is given in Figure 4.52.

Table 4.4: Stream properties for illustrative case study

Stream Name	Supply Temperature (°C)	Target Temperature (°C)	Heat Capacity Flowrate (kW/°C)	Duty(kW)
H1	310	95	86.0	18,490
H2	299	120	21.4	3,831
H3	273	250	184.7	4,248
H4	230	95	23.5	3,173
H5	206	178	129.4	3,623
C1	52	360	143.9	44,321

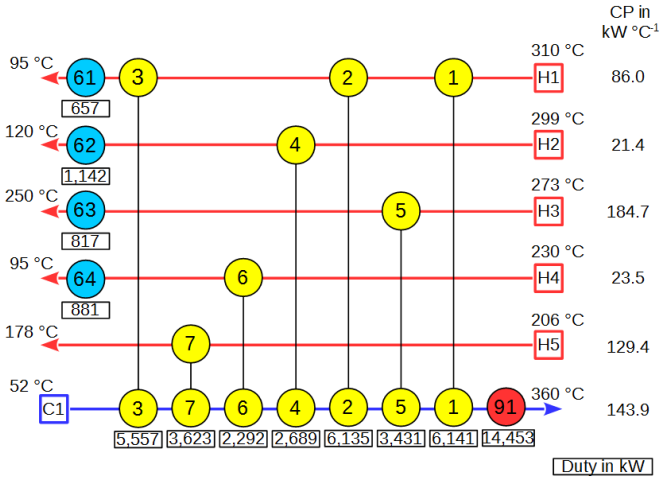

Figure 4.52: Current HEN represented by the Grid Diagram (after Jiang et al., 2014)

From HENSM shown in Table 4.5, it can be seen that there are several heat paths for recovery. Due to space constraint, the shifted temperature differences at the heat exchanger ends are shown separately in Table 4.6. All heat paths that can be formed from cooler 61 to heater 91 are listed in Table 4.7, along with the involved heat exchangers. In Table 4.8, the MAHT values for all heat paths are calculated using the equations from Table 4.3. The associated total capital costs are shown in Table 4.8.

In Table 4.8 heat path 2 has highest value of MAHT, followed by heat path 1. However, the actual amount of heat that can be recovered is actually limited by the duty of cooler 61. Heat paths 1 and 2 recover the same final amount of heat (in competition). Table 4.6 also shows that heat path 2, 3 and 4 have the same potential heat exchanger but heat path 2 has different MAHT. It is due to heat exchanger 2 having different roles in these heat paths. Heat path 2 is limited by low CETD* of heat exchanger 2 and CP of cold stream C1 as heat exchanger 2 is a positive pass-through heat exchanger. Heat path 3 and 4 are limited by low CETD* of heat exchanger 2 and CP of hot stream H1.

Table 4.5: HENSM representation of the case study

					Hot Stream	H1			H2	H3	H4	H5	
					CP (kW/°C)	86	86	86	21	185	24	129	
					TS (°C)	310	239	167	299	273	230	206	
					TT (°C)	239	167	103	173	254	133	178	
HEX Name	Cold Stream	CP (kW/°C)	TS (°C)	TT (°C)									Heater Duty (kW)
3	C1	144	52	91				5,557					
7	C1	144	91	116								3,623	
6	C1	144	116	132							2,292		
4	C1	144	132	150					2,689				
2	C1	144	150	193			6,135						
5	C1	144	193	217						3,431			
1	C1	144	217	260		6,141							14,453
					Cooler Duty (kW)			657	1,142	817	881		

Table 4.6: HETD* and CETD* for all heat exchangers

HEX Name	HETD*	CETD*
3	66.6	40.6
7	80.2	77.4
6	88.3	6.7
4	138.6	31.6
2	35.6	6.8
5	46.1	51.4
1	40.4	11.7

Table 4.7: Details for all heat paths

Heat Path		Pass-through HEX		Pass-by HEX		All Involving HEX
No.	Path	Positive	Negative	Hot Fixed	Cold Fixed	
1	61 > 3 > 91	3	-	7, 6, 4, 2, 5, 1	-	3, 7, 6, 4, 2, 5, 1
2	61 > 2 > 91	2	-	5, 1	3	3, 2, 5, 1
3	61 > 1 > 91	1	-	-	3, 2	3, 2, 1
4	61 > 3 > 2 > 1 > 91	3, 1	2	7, 6, 4	-	3, 7, 6, 4, 2, 1

Table 4.8: MAHTs and capital costs for all the heat paths found

Heat Path No.	Potential Pinch HEX	MAHT (kW)	Final Heat Recovered (kW)	Energy Saving ($/y)	Total Capital Cost ($)	Payback Period (y)
1	6	946.1	657.0	266,413	368,364	1.38
2	2	978.5	657.0	266,413	256,674	0.96
3	2	584.8	584.8	237,136	209,929	0.89
4	2	584.8	584.8	237,136	369,690	1.56

The energy price is taken at the same source as the capital cost for heat exchanger Eq(4). Price for hot utility is taken at 400 \$ kW^{-1} y^{-1} and cold utility at 5.5 \$ kW^{-1} y^{-1}. (Jiang et al., 2014)

Heat path 1 has higher capital cost but same final heat recovered as heat path 2. This is due to heat path 1 involving more heat exchangers than heat path 2. Although heat path 3 has the fastest payback period, it recovers smaller amount of heat compared to heat path 2. Heat path 2 maybe chosen if the investor decides to focus on saving more energy. This example has illustrated how to perform HEN path analysis on the developed matrix. The analysis considered all possible paths from cooler 61 to heater 91. As it is shown in Table 4.6, from the same cooler to heater, there are at least four heat paths can be obtained. Each heat paths has different potential Pinched heat exchanger and MAHT. Using HENSM, comparisons between energy saved and cost involved can be made among the heat paths.

4.3.4 Summary

A matrix representation of HENs is proposed in this section to support synthesis or retrofit tasks. Heat Exchanger Network Stream Matrix (HENSM) is demonstrated on a case study. During the retrofit analysis more than one heat path starting from the same cooler to the same heater was found. Further energy and economy analysis shows that different heat paths have different Potential Network Pinch heat exchanger. It is due that heat exchangers act differently on different heat paths. The result from the analysis provides a retrofit solution that has the fastest payback period. The second solution also recovers higher amount of energy at a slightly longer payback period. The matrix so far can't deal stream splitting.

4.4 Conclusion

In this chapter new representations for HEN are introduced. The first representation derived from conventional HEN - the Shifted Retrofit Thermodynamic Grid Diagram (SRTGD). It has unique feature set, helping to identify favourable retrofit options. Since it shows in the same view CP (or load), temperatures and the network, it allows the users to simultaneously account for the thermodynamics, stream capacities and the topology as factors. As a result, SRTGD can be efficiently used to incorporate Pinch Technology, identify Process Pinches and Network Pinches. The provided examples and the case study clearly illustrate the advantages offered by the new tool. It has been demonstrated that SRTGD is capable of screening feasible from infeasible solutions, providing visual information in choosing more favourable heat paths. When a heat path is chosen, SRTGD points to the location of potential Network Pinches as well as the maximum heat recovery achievable. This has been demonstrated in the case study where the SRTGD has enabled seeing. A different, more beneficial set of retrofit options featuring more economically attractive design. Another potential usage of SRTGD, compared to conventional HEN Grid Diagram, is that its ability to show varying heat load. With this feature it is believed that more factors can be in cooperated when HEN analysis and retrofit are performed.

Another HEN representation is introduced in a form of matrix, called Heat Exchanger Network Stream Matrix. The novelty of this representation is it does not require graphical illustration to contain the stream information and connection. The potential benefit of using HENSM is the convenience of not drawing the HEN out and still able to perform analysis. HENSM has the potential to be the input form of HEN analysing software. With just inputting HEN information in the matrix, the software is potentially able to translate the matrix into graphical representation, if required. It can be well-organised and can help engineers in analysing the system with preserved accuracy. HENSM records all the temperatures, temperature differences and duties of all heat exchangers in a HEN. Using the temperature differences at heat exchanger ends, the matrix is able to support the location of Process Pinches and Network Pinches. During retrofit Path Analysis, the potential of a heat exchanger in becoming a Network Pinch is shown in the matrix.

4.5 References

Gadalla M.A., 2015, A new graphical method for Pinch Analysis applications: Heat exchanger network retrofit and energy integration, Energy, 81, 159 – 174.

Jiang N., Shelly J.D., Doyle S., Smith R., 2014, Heat exchanger network retrofit with a fixed network structure, Applied Energy, 127, 25 – 33.

Lakshmanan R., Bañares-Alcántara R., 1996, A Novel Visualisation Tool for Heat Exchanger Network Retrofit, Industrial & Engineering Chemistry Research, 35, 4507-4522.

Lakshmanan R., Bañares-Alcántara R., 1998, Retrofit by inspection using thermodynamic process visualisation, Computer & Chemical Engineering, 22(1), S809-S812.

Linnhoff B., Townsend D.W., Boland D., Hewitt G.F., Thomas B.E.A., Guy A.R., Marsland R.H.,1994. A user guide on Process Integration for the efficient use of energy, IChemE, Rugby, UK.

Nemet A., Klemeš J.J., Kravanja Z., 2015. Designing a Total Site for an entire lifetime under fluctuating utility prices, Computers & Chemical Engineering, 72, 159 – 182.

Pan M., Bulatov I., Smith R., Kim J.-K., 2013, Optimisation for the retrofit of large scale heat exchanger networks with different intensified heat transfer techniques, Applied Thermal Engineering, 53(2), 373 – 386.

Piacentino A., 2011, Thermal Analysis and New Insights to Support Decision Making in Retrofit and Relaxation of Heat Exchanger Networks, Applied Thermal Engineering, 31(16), 3479 – 3499.

Smith R, 2005. Chemical process design and integration, Wiley, Chichester, UK.

Soltani H., Shafiel S., 2011. Heat exchanger network retrofit with considering pressure drop by coupling genetic algorithm with LP (linear programming) and ILP (integer linear programing) methods, Energy, 36(5), 2381 – 2391.

Varbanov P.S., Klemeš J.J., 2000, Rules for Path Construction for HENs Debottlenecking, Applied Thermal Engineering, 20 (15-16), 1409 – 1420.

Wan Alwi S.R., Manan Z.A., 2010, STEP – A new graphical tool for simultaneous targeting and design of a heat exchanger network, Chemical Engineering Journal, 162(1), 106 – 121.

Wan Alwi S.R., Manan Z.A., Misman M., Chuah W.S., 2013, SePTA – A new numerical tool for simultaneous targeting and design of heat exchanger networks, Computer & Chemical Engineering, 57, 30 – 47.

Yong J.Y., Varbanov P.S., Klemeš J.J., 2014, Shifted Retrofit Thermodynamic Diagram: a modified tool for retrofitting on heat exchanger network, Chemical Engineering Transactions, 39, 97 – 102.

Yong J.Y., Varbanov P.S., Klemeš J.J., 2015, Heat exchanger network retrofit supported by extended Grid Diagram and heat path development, Applied Thermal Engineering, 89, 1033-1045.

3. Heat Exchanger Network Modification for Waste Heat Utilisation

3.1 Introduction

Pinch Analysis has been used to set heat recovery targets and these can be used as indicators for the retrofit. Sophisticated heat exchanger network (HEN) designs based on Pinch Analysis are able to achieve thermodynamic targets of minimum utilities use (Klemeš, 2013). By appropriate HEN retrofit planning the utilities requirement can be reduced by increasing the heat exchange between hot and cold streams (Klemeš and Kravanja, 2013). For example, in the work of Li and Chang (2010), a simple pinch-based approach is proposed to retrofit existing HEN. Every cross-pinch match is removed to reduce the utility consumption. The work is able to keep the additional capital investment to a reasonable level. The work is further discussed by the authors (Li and Chang, 2017). New visualisation identification method is developed in the work to detect cross-pinch matches and further removing them.

Yong et al. (2014) provide an efficient visualisation tool for driving the modifications. In this analysis type, cold streams can be defined for representing preheating or drying operations. These streams have low temperature ranging from 50 °C to 150 °C. The retrofit can be done by re-sequencing or re-piping existing heat exchangers (Bakhtiari and Bedard, 2013), splitting streams (Pan et al., 2012), and by introducing new heat exchangers. It has also been found that the amount of heat exchanged can be increased by performing appropriate heat transfer enhancements guided by Pinch Analysis and Network Pinch identification (Pan et al., 2013).

The advantage of the latter is that the topology of the HEN remains the same implying minimal investments. The Network Pinch retrofit approach depends on the availability of a heat path. When no heat path is available, it can be constructed by introducing a new heat exchanger between a hot and a cold stream that would connect coolers and heaters (Varbanov and Klemeš, 2000).

Retrofitting an existing HEN to reduce utilities use is not always economically viable. This is especially true for HENs where such retrofits need many major topology modifications. When an existing HEN contains a number of non-optimally placed heat exchangers, major topology modifications may be needed. Having major topology modification does not only incur high capital investment, the time to perform such modification may take a long period. Without production during this period adds in extra cost for this modification. As a result, it may be more economical to achieve heat recovery smaller than the targets found using Pinch Analysis. In some cases, exploiting or constructing utility-exchanger heat paths may be too costly.

The HEN retrofit problem is further made uneconomical when the retrofit region is located at the low temperature region. High temperature utility is costly to produced and maintained, when compared to low temperature utility. Reduce the usage of high temperature utility is therefore saving the higher operating cost in producing and maintaining the utility, when compared with low temperature utility. Waste heat streams are often neglected due to their comparatively low temperatures, although they can still be utilised by retrofitting existing HEN. This is due to

capital investment cost per kWh low temperature utility is often lower then of high temperature utility.

They are also retrofit limitations for threshold problem. Heat path is the first step to be identified for potential HEN retrofit. There are few conditions when the heat path cannot be found. One of the conditions is the existing HEN does not have utilise either hot utility or cold utility. Heat path cannot be formed since it requires connecting from a cooler to a heater. Although a heat path can be connected from a heater to a heater, the reduction in the utility usage in a heater is increased in another heater. This is usually done when it is desired to reduce the usage of high temperature hot utility by increasing the usage of low temperature hot utility. A heat path cannot be formed as well when there is no linking heat exchanger between heater and cooler. The problem can be solved by introducing a new heat exchanger between the path, but it will incur extra investment cost that needed to be justified.

When retrofit for utilities usage reduction is deemed economically unfavourable for a network, the next level in hierarchy is to analyse heat utilisation options to produce value-added product. Instead of low temperature utility reduction, waste heat utilisation for added value side-product should be considered. Waste heat utilisation can provide additional degrees of freedom, when plant retrofit is performed. Waste heat loss is frequent in industry and especially in crude oil refineries. The low-grade heat utilisation can increase the plant profitability by reducing the cold utility requirement or generating extra income from selling excess utility streams – e.g. steam or hot water. Waste heat can be e.g. used to dry biomass, when the plant is surrounded with supplies of wet biomass for energy production.

In this chapter, the problems in retrofitting a HEN for utilities usage reduction are discussed. The benefits of not going for reducing the amount of utilities used but waste heat utilisation instead are shown. HEN modification analysis is performed aiming at generating hot water as the value-added product. As the operating conditions vary, the modified network should also be flexible. This work contributes by addressing these issues with a procedure development presented. The novel procedure allows different arrangements of HEN for modification to be evaluated to explore the best economic opportunity. The developed methodology is applied to an industrial case of a small crude oil refinery plant. Waste heat from a small crude oil refinery plant is utilised to produce hot water for district heating purpose. The utilities use of the plant could be further reduced only by enrolling significant changes in the topology, therefore a modification of smaller scope has been evaluated. The refinery plant is also located in a climatic zone, where it is significant differences in ambient conditions during summer and winter. The crude oil feed to the refinery also varies. With different ambient temperatures across the seasons and different feed qualities, the HEN is modified in a way that waste heat can be used to produce hot water accounting for the parameter variations.

3.2 Methodology

In this section, different options for HEN retrofit for waste heat utilisation under the described conditions are discussed. The usual step of retrofitting HEN is performing Pinch Analysis to determine the minimum amount of utilities required. After thorough economic analysis of the HEN retrofitting process, as shown in previous chapter, it is to determine if the retrofit is economical or otherwise. If it is not, then the option of using waste heat for utility generation can be considered. The main principle is to use valorisation when internal heat recovery is cost prohibitive. The further details depends on the case to solve.

Waste heat stream can be used for various purposes as mentioned. Hot water generation is one of the utilisations of waste heat stream. Hot water stream be considered as a cold utility. It is because its mass flowrate is not fixed by explicit specification. It provides an additional degree of freedom to the HEN under retrofit. Small waste heat loads may be sometimes not utilised if it is not economical. Other factors may also affect the decisions for splitting the process stream or the new utility stream. These include the cost for the piping, pipe and heat exchangers foundations and also some other important issues as e.g. the level of hazard of the process stream providing the waste heat (Chew et al., 2013). The water supply temperature can be lower if it is directly taken from a fresh source (e.g. river) or higher if water is returning from a hot water circuit. There are different ways of modifying the network for hot water generation from waste heat.

For hot water generation, the first step is to determine the supply and required target temperature. The minimum temperature difference between the stream and hot water should be determined as well. Using more advanced graphical HEN representations, such as SRTGD, it is able to locate the temperature region that is capable of producing hot water. The amount of hot water produced can be calculated from the heat load in the temperature region. Preliminary economic analysis can be done by just calculating the capital cost and revenue by selling the hot water generated. Further economic analysis can be done by including the arrangement of the hot water generation circuit and heat exchangers need.

3.2.1 Parallel water heating with splitting the utility generation stream

The hot water generation stream can be split into branches matching the number of waste heat process streams. The distribution of the water CP for splitting depends on the amount of heat available and the final temperature of the water to be achieved after mixing. The advantage of a parallel arrangement is that the temperature differences in the new heat exchangers would be maximal as the hot water generation branches would always enter the heat exchangers at the water supply (starting) temperature. It would tend to require less heat transfer area than a series arrangement. Another advantage is that higher flexibility can be achieved accommodating the scenario variations.

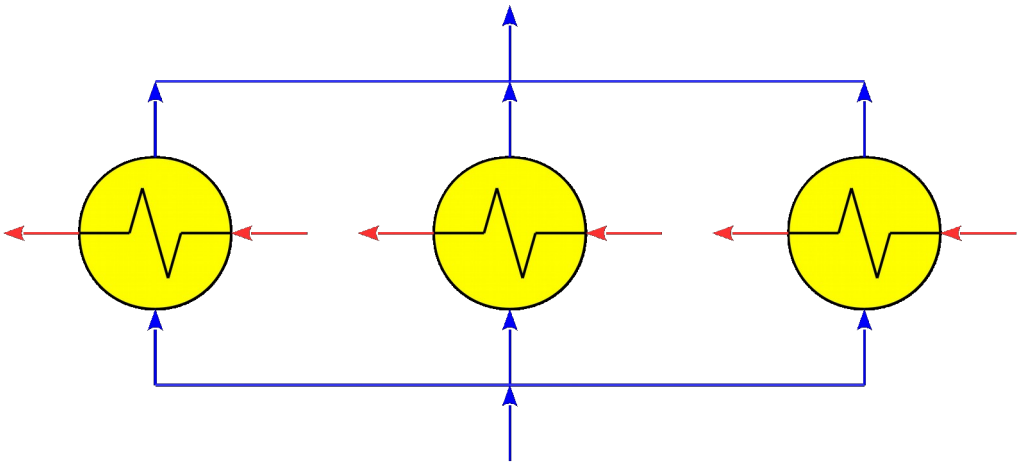

Figure 5.53: Parallel arrangement showing three heat exchangers capable of generating hot utility

The potential disadvantages of splitting include more complex piping, and more complex control. For instance, an added complexity in the simulation and optimisation for this arrangement is to ensure that the hot water target temperature specification is achieved without too much overshoot. There should be at least one branch that has a temperature higher than the target temperature for water specification. Potential other issues to prevent include evaporation and the danger of some branches not reaching the specified target temperature. As a result, it is important to specify the supply and target temperatures of the hot water to be produced, as this determines the waste heat streams suitable and the number of the hot water generation branches. Simulations and optimisations are necessary to identify the duties of the heat exchangers and the splitting ratios of the water stream. The final HEN should ensure that all the waste heat streams are considered, so that that each stream is utilised at least once in a scenario.

3.2.2 Series heating of the utility generation stream

In the second option the heat exchangers are arranged in series on the hot water generation stream. Choosing the right sequence of the heat exchangers is very important as the outlet temperature of one heat exchanger is the inlet temperature of another. This arrangement is easier to simulate and optimise as only the mass flowrate of the water stream and heating duties of heat exchangers are the variables. The disadvantage of this arrangement is that the modified network can be too specific for each scenario. Due to the single stream on the hot water generation side, the flexibility of this topology would be lower. The supply and target temperatures of the hot water stream are important for this arrangement as well. The waste heat streams utilised should have temperatures high enough to be matched with the water stream. There are different ways to determine the order of waste heat streams to be heated, one of it is by ascending outlet temperature. This arrangement also needs simulation and optimisation to find the heat capacity flowrate and duties of the heat exchangers. To ensure that the final HEN is flexible, modifications should be done in a way permitting the feasible hot water generation in all scenarios. Different network modifications may be prompted by the various scenarios. One

way to find the final network is to attempt adapting every modified network on every scenario. Any network topology found infeasible even in one scenario should be discarded. Should there be more than one feasible network, some criteria such as highest amount of hot water generation can be used to select final network.

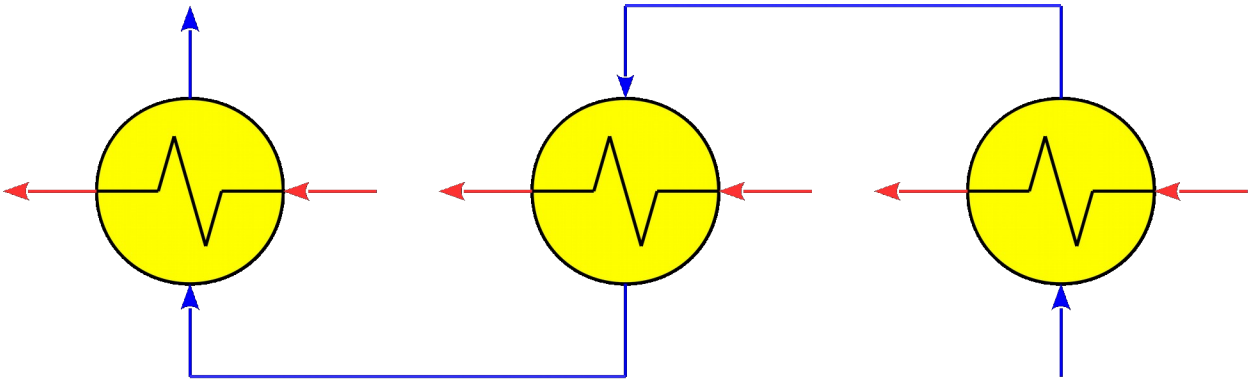

Figure 5.54: Series arrangement showing three heat exchangers capable of generating hot utility

3.2.3 Combination of parallel and series heating

The HEN retrofit can also combine both parallel and series arrangements. Waste heat streams that have lower supply temperature are preferably cooled using in parallel arrangement. After the branches are heated up by the waste heat streams, they should then be mixed. Normally the temperature will be lower than the target hot water temperature specification. The merged stream can then be heated up with the higher temperature hot streams. The idea of having such an arrangement is to recover maximum amount of heat by having lowest possible temperature on the water side to receive heat from the lower temperature waste heat streams and highest possible heat capacity flowrate for high temperature waste heat stream. However, in this case the HEN would be more complicated to modify to this arrangement as it needs more simulation and optimisation. Besides, the flexibility of this modification in different scenarios can also be questionable.

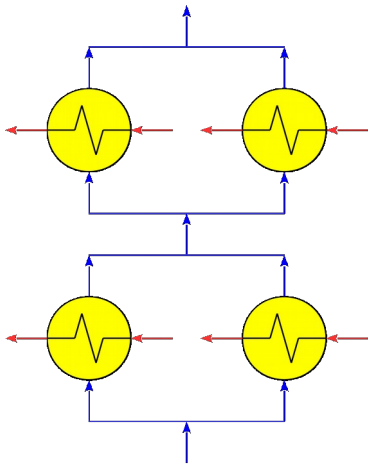

Figure 5.55: Series and parallel arrangement showing four heat exchangers capable of generating hot utility

3.3 Case Study

3.3.1 Illustrative Case Study

The case study from section 4.3.3 is revisited. A simplified preheat train is adapted from Jiang et al. (2014). The stream data is given in Table 4.4. All hot streams exchange heat with the only cold stream. There are four coolers and a heater, while heat transfers between streams are done using seven heat exchangers. The HEN Grid Diagram is given in Figure 4.52. Table 5.2 shows the specifications of coolers and heaters in the illustrative case study.

Table 5.1: Stream properties for illustrative case study

Stream Name	Supply Temperature (°C)	Target Temperature (°C)	Heat Capacity Flowrate (kW/°C)	Duty(kW)
H1	310	95	86.0	18,490
H2	299	120	21.4	3,831
H3	273	250	184.7	4,248
H4	230	95	23.5	3,173
H5	206	178	129.4	3,623
C1	52	360	143.9	44,321

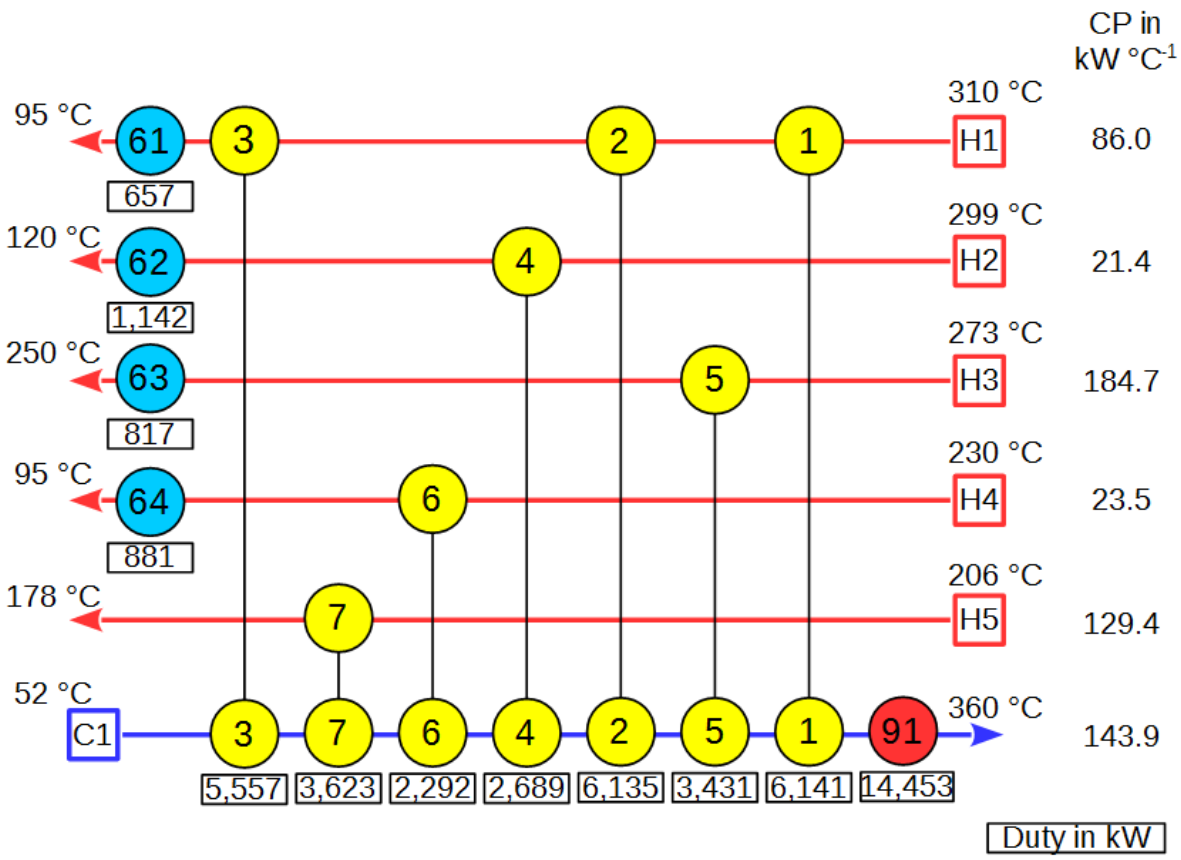

Figure 5.56: Current HEN represented by the Grid Diagram (after Jiang et al., 2014)

Table 5.2: Specification of heaters and coolers in the illustrative case study

Heater / Cooler Name	Supply Temperature (°C)	Target Temperature (°C)	Heat Capacity Flowrate (kW/°C)	Duty(kW)
61	103	95	86.0	657
62	173	120	21.4	1,142
63	254	250	184.7	817
64	132	95	23.5	881
91	260	360	143.9	14,453

It is determined that the hot water will be supplied at 90 °C and returned at 50 °C. The minimum temperature difference between the hot water and stream is 5 °C, as hot water and streams are in liquid state. From Table 5.3, it can be observed that streams H1, H2, H3 and H4 can be fully utilised for hot water generation after exchanging heat with the only cold stream. It is due to the target temperature of the stream is higher than the return temperature of the hot water. If Table 5.3 is compared with Table 5.2, it can be observed that all the heat loads of coolers 61, 62, 63 and 64 is completely used to generate hot water. It generates 3,497 kW of hot water, equivalent to 20.8 kg/s or 75 t/h of hot water.

Table 5.3: Waste heat streams qualified to produce hot water for illustrative case study

Stream	Supply Temperature (°C)	Target Temperature (°C)	Useful Target Temperature (°C)	Heat Capacity Flowrate (kW/°C)	Useful Duty (kW)
H1	103	95	95	86.0	657
H2	173	120	120	21.4	1,142
H3	254	250	250	184.7	817
H4	132	95	95	23.5	881

3.3.2 Industrial Case Study

The case study is a small crude oil refinery applying atmospheric distillation in the Central Europe. The data obtained are modified to protect the identity of the refinery. The refinery experiences summer and winter seasons and different feed condition of the crude oil results from the variation of the suppliers. There are total four scenarios labelled as A, B, C and D, with scenarios A and C occurring in the winter. Figure 5.57 shows the existing HEN in the plant with scenario A data.

The Pinch Analysis (Figure 5.58) on this unit shows that this is a threshold problem with no cold utility demand and hot water generation is not needed for maximum heat recovery. Further analysis has been performed and it shows that the minimum temperature difference in the current HEN is around 8 °C, which is a Network Pinch problem as the Pinch is not on the Pinch Temperatures (Asante and Zhu, 1997). The previous Pinch Analysis Targeting has been based on minimum temperature difference approach at 5 °C, identifying the Process Pinch. As the current HEN is not designed according to the Pinch Design Method (Klemeš, 2013), there is a larger use of hot utilities and high temperature hot streams exchange heat with low temperature cold streams, i.e. in the case of C1 exchanging heat with H14 and H15. This also results in excessive usage of cold utility compared with the thermodynamic target. All hot streams in the current HEN, that use cold utility, have low supply temperature (around 150 °C and below). They are considered as waste heat streams.

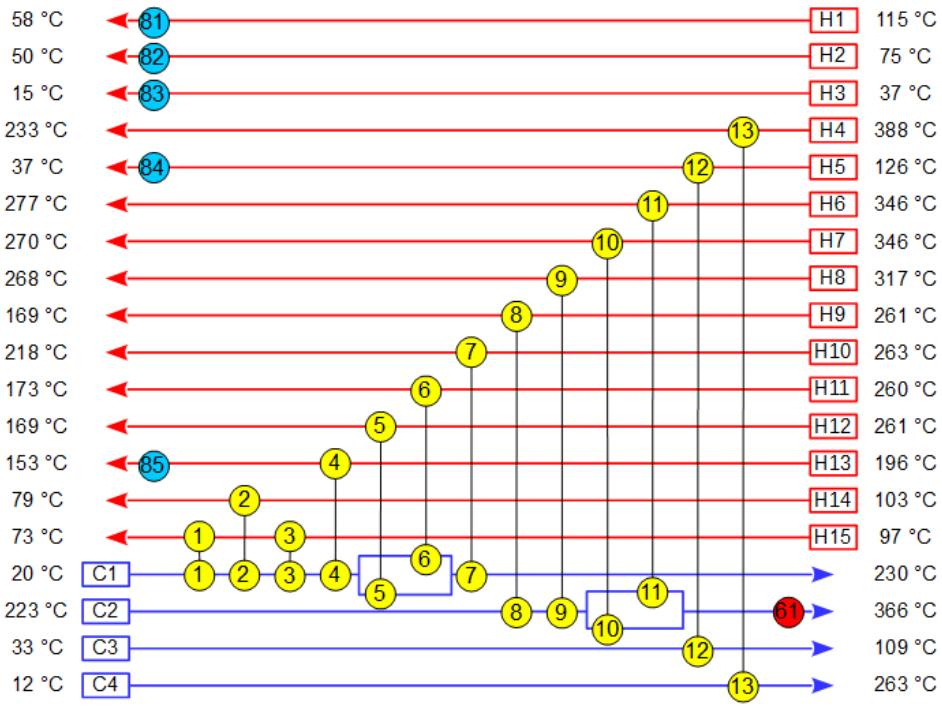

Figure 5.57: HEN of case study, data taken from Scenario A

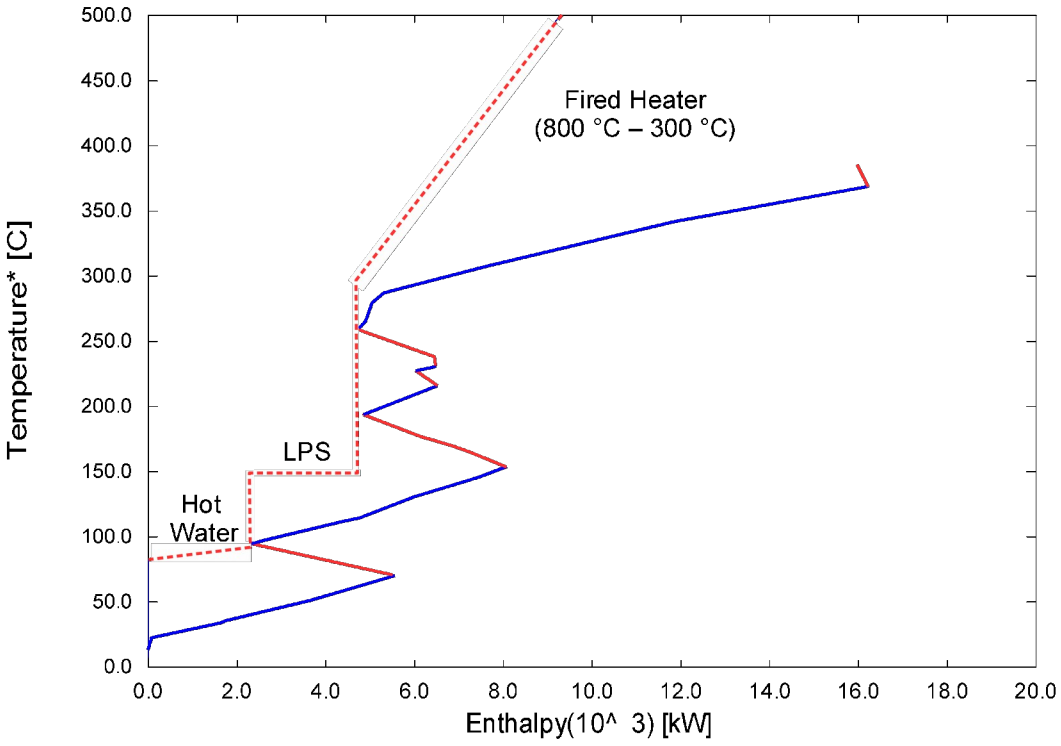

Figure 5.58: GCC for Scenario A

Table 5.4: Waste heat streams qualified to produce hot water

Stream	Supply Temperature (°C)	Target Temperature (°C)	Useful Target Temperature (°C)	Heat Capacity Flowrate (kW/°C)	Useful Duty (kW)
H1	115	58	58	4.35	248
H2	75	50	55	34.2	684
H13	159	153	153	71.9	431

The two-level hierarchy has been applied in the analysis, with the first level of attempting to utilise waste heat for reduction of utility demands of the unit, while the second level attempts to utilise the waste heat for generating hot water as a side-product. The utility use reduction can be effected in an existing HEN by increasing the heat exchange between hot and cold streams. Finding paths that connect heaters to coolers or cooler-cooler / heater-heater via recovery heat exchangers was attempted for this purpose. It is noticed that no existing heat paths could be found. It is because that there are only four cold streams in the network. From the streams, three cold streams (C1, C3, C4 – Figure 5.57) are completely served by exchanging heat with hot streams, leaving only one cold stream that uses hot utility. Stream C2 that is heated using furnace. No heat path exists that connects the furnace to a cooler. Constructing a heat path on this stream is impossible as its supply temperature for this stream is too high for the waste heat (hot) streams. To utilise the waste heat streams for utilities reduction, they can only be matched with the stream C1. This retrofit would require too many retrofit actions – such as re-sequencing, re-piping heat exchangers and splitting the cold stream. Attempting to construct new paths by adding new or moving the existing heat exchangers indicated that there would be needed more than two such modifications before a path would be established. Reducing the use of utilities is possible but is likely to come at high investment cost.

The second level of the retrofit hierarchy is then attempted. In this industrial case study, parallel arrangement of the HEN is applied, i.e. the hot water generation stream is split and each waste heat stream is matched to a branch to exchange heat with the same low supply temperature of the water stream.

3.3.2.1 Modification steps on HEN for scenario A

The example HEN is modified according to steps described in section 3.2.1 for scenario A. According to the first step, the hot water generation stream is specified to have supply and target temperatures of 50 °C and 90 °C and minimum temperature difference approach between process and hot water is set at 5 °C. The waste heat streams to be used should be able to supply heat starting from 55 °C. Performing step 2 produces all the qualified waste heat streams from the network (Table 5.4).

The third step is to split the water stream according to the number of the identified waste heat streams in Table 5.4. The water stream is then to be split into three with three heat exchangers connecting them. Table 5.4 also shows that there is one having target temperatures less than 95 °C. At least one stream has to heat the water stream above 90 °C, so that when the branches are merged, the water stream should be able to reach the desired target temperature. Care is taken so that the evaporation does not occur for the water stream, as doing so would induce higher equipment cost. Should there be no stream having target temperature higher than 95 °C,

then there is no hot water generated and the modification process fails. Alternatively, the insufficiently hot water would need to be passed via heaters spending fuel. The target temperature of the water stream should then be revised to have lower value. Step 4 connects each split stream and waste heat stream with heat exchangers.

Commercial software called Heat-INT (Process Integration Limited, 2014) is used to simulate and optimise the network for maximum hot water production. The heat exchanger duties and split ratio for the water system are obtained. Figure 5.59 shows the final optimised HEN modified for hot water production for scenario A. Table 5.5 shows the duties and split ratio for all three heat exchangers in scenario A.

Table 5.5: Specification for heat exchangers producing hot water for scenario A

Heat exchanger	Duty (kW)	Split ratio
14	413.7	0.628
15	5.5	0.008
16	240.0	0.364

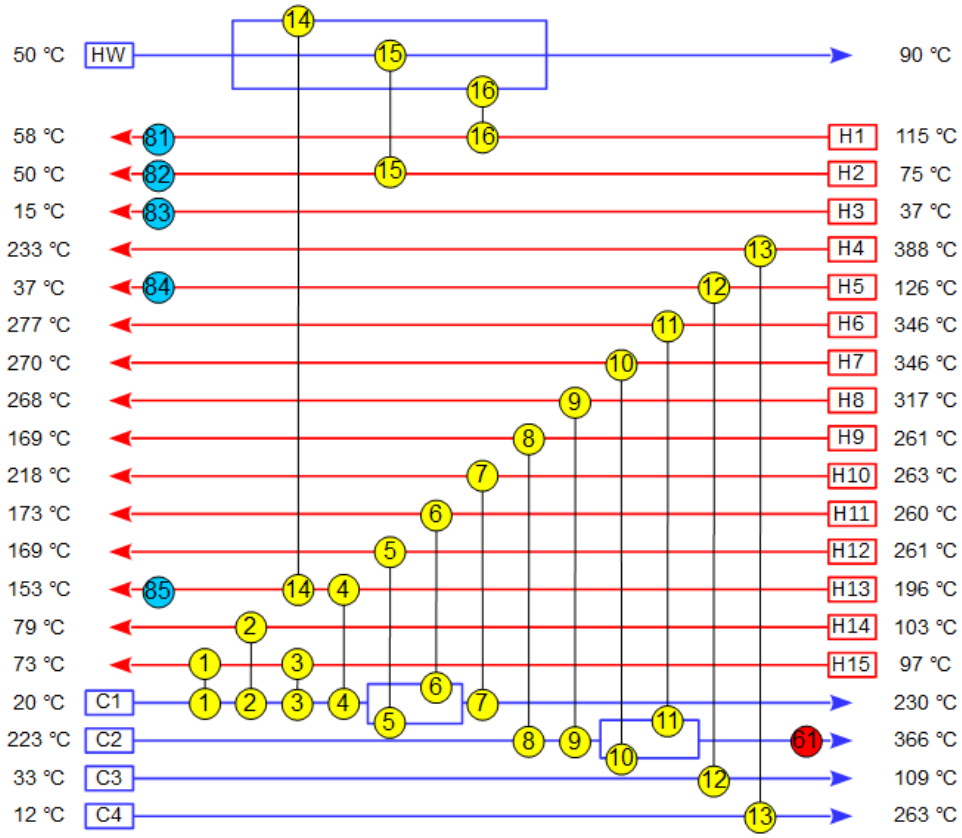

Figure 5.59: Modified HEN of the case study for scenario A

3.3.2.2 HEN for other scenarios

The steps are repeated, as mention in section 3.3.2.1, to produce the modified network for the other scenarios. All scenarios have the same topology as scenario A. Table 5.6 shows the simulated and optimised result.

3.3.2.3 Result and Discussion

In the analysis and modification, the modified topology of HENs in all four scenarios is the same. Only maximum three same waste heat streams are chosen to produce hot water in all four scenarios.

Table 5.6: Specifications for heat exchangers producing hot water for scenario B, C and D

Scenario	Heat exchanger	Duty (kW)	Split ratio
B	14	705.50	0.988
	15	6.55	0.009
	16	0.23	0.003
C	14	349.50	0.766
	15	15.33	0.034
	16	91.6	0.200
D	14	350.50	0.704
	15	2.34	0.020
	16	150.70	0.276

Table 5.7: Heat transfer area for all heat exchanger area in all the scenarios

Heat Exchanger	Scenario				Final Size
	A	B	C	D	
14	14.11	**19.27**	11.88	8.81	19.27
15	0.80	1.22	**2.70**	0.27	2.70
16	**62.02**	0.04	16.60	12.55	62.02

*All values are in m².

The final topology has three split streams and is compatible with each scenario. Table 5.7shows the heat transfer areas for all heat exchangers in all the scenarios.

The bolded values in Table 5.7 are the highest values for each heat exchanger. The heat exchangers should be then designed according to these values. However, specific request can be accommodated when designing the network. Although the network modifications are the same for all scenarios, the heat transfer area requirement is different for the same heat exchanger in different scenarios. It is desired to design the heat exchangers as small as possible to save the investment cost by considering different request. For example, if there is no hot water demand during the summer season and economic analysis shows that it is not profitable to produce it, the production of hot water can be stopped until is needed in winter. Then the heat exchangers can be designed according to the maximum values in scenarios A and C. During summer, the waste heat streams can be cooled by current existing coolers. Also an opportunity for the absorption cooling can be explored.

3.4 Summary

This section has successfully utilised waste heat under different feed conditions. Through a case study, it is determined that waste heat streams have too low temperature to reduce utilities consumption. Attempt to construct heat path for this purpose in this case study will lead to high investment cost. The HEN is then modified to generate hot water from the waste heat streams instead. The section discussed different arrangements of heat exchanger and the effects of its

flexibility and complexity under different conditions. The HEN in the case study is successfully modified using parallel arrangement. It uses three more heat exchangers with minimum production of 456 kW of hot water. All the heat transfer areas of heat exchangers are determined, which the highest values are used as the basis for design.

3.5 References

Asante, N.D.K., Zhu X.X., 1997, An automated and interactive approach for heat exchanger network retrofit, Chemical Engineering Research and Design, 75(part A), 349-360.

Bakhtiari B., Bedard S., 2013. Retrofitting heat exchanger network using a modified network pinch approach, Applied Thermal Engineering, 51, 973 – 979.

Chew K.H., Klemeš J.J., Wan Alwi S.R., Manan Z.A., 2013. Industrial implementation issue of Total Site Heat Integration, Applied Thermal Engineering, 61(1), 17 – 25.

Klemeš J.J. Kravanja Z., 2013. Forty years of Heat Integration: Pinch Analysis (PA) and Mathematical Programming (MP), Current Opinion in Chemical Engineering, 2(4), 461 – 474.

Klemeš J.J., 2013. Handbook of Process Integration (PI): minimisation of energy and water use, waste and emissions, Woodhead Publishing Limited/Elsevier, Cambridge, UK.

Klemeš J.J., Varbanov P.S., Wan Alwi S.R., Manan Z.A., 2011. Process Integration and Intensification: saving energy, water and resources. De Gruyter: Berlin, Germany .

Pan M., Bulatov I., Smith R., 2012. Novel MILP-based optimisation method for heat exchanger network retrofit considering stream splitting, Computer Aided Chemical Engineering, 31, 395 – 399.

Pan M., Bulatov I., Smith R., 2013, Heat transfer intensified techniques for retrofitting heat exchanger networks in practical implementation, Chemical Engineering Transactions, 35, 1189-1194.

Process Integration Limited, 2014. i-HEAT: innovative software for the design and optimisation of heat recovery system <www.processint.com/chemical-industrial-software/i-heat> accessed 05.12.2014

Varbanov P.S., Klemeš J.J., 2000. Rules for paths construction for HENs debottlenecking, Applied Thermal Engineering, 20, 1409 – 1420.

Yong J.Y., Varbanov P.S., Klemeš J.J., 2014. Shifted Retrofit Thermodynamic Diagram: a modified tool for retrofitting on heat exchanger network, Chemical Engineering Transactions, 39, 97 – 102.

4. Novel Scientific Developments in the Current Thesis

The first discovery is Data Reconciliation on existing Heat Exchanger Network (HEN) for the purpose of Heat Integration and Pinch Analysis. This is a crucial step before any retrofit process can be commerce. There are only two types of parameters to be reconciled, which is mass flowrate and temperature. As each network having numerous heat exchangers, each heat exchanger is given a set of temperature and flowrate data. The complexity arises when the constraint equations used in the model is highly non-linear. Conventional method that used in the data reconciliation process is too computational effort demanding. Iterative method is introduced in this work to solve the non-linearity occurred during the data reconciliation process. Iterative method provides accurate result with less computational effort. Although Iterative Method has limitations, strategies are also developed in this work to solve these limitations. The scope is then extended to energy and steam system at Total Site level. Without complicating the model, as Total Site has numerous heat exchangers, only equipment involved in the energy and steam system are reconciled first.

The second discovery derived from HEN Grid Diagram. A new representative diagram is introduced called Shifted Retrofit Thermodynamic Grid Diagram (SRTGD) that is used during retrofit process. Compared to conventional Grid Diagram, SRTGD displays heat capacity of each stream on y-axis, while maintaining temperature differences on x-axis. SRTGD does not only shows heat duty of each heat exchanger according to the area enclosed, but the locations of pinches as well. SRTGD is also shown in the work for retrofitting existing HEN. Early concept of a matrix representation is discussed as well, called HEN Matrix. Such representation reduces the hassle of drawing any graphical representation and can be used to serve as an input for simulation software.

The third discovery is the waste heat utilisation for utility generation. The general purpose of retrofitting HEN is to reduce the amount of utility consumption. By using various tools such as Pinch Analysis, minimum utility consumption can be targeted and improvement can be made from towards the target. It is noted that there are some cases that although the suggested HEN retrofit options are thermodynamically feasible, it is infeasible in other aspects. Economic feasibility is one of the factors hindering the progress of the HEN retrofit. After Heat Integration Analysis being performed, it may be concluded that although the retrofit is feasible but economic infeasible. Particularly in the low temperature region of the HEN, such low temperature streams are often considered waste heat and generally discarded. In this work discussion is made on how to utilise such waste heat to generate utility for additional revenue. Simple steps in identifying the potential of waste heat in the streams to be utilised are presented. The configuration of hot water generation circuit is discussed and gave a general idea on how to maximise the usage of waste heat that otherwise ignored.

5. Conclusions

Heat exchanger network (HEN) retrofit is currently the focus of chemical industry after the introduction of heat integration four decades ago. With current energy prices, existing HEN has to be retrofit to keep the chemical industry competitive in the market. Without redesigning and rebuilding a whole new HEN, and with fraction of capital cost, retrofitting existing HEN can reduce the amount of utility consumption. The importance of retrofitting HEN can also be seen when extra revenue can be generated by producing side products.

The first step of starting a retrofit process in HEN is data extraction on existing HEN. Design value data maybe obsolete and not accurate after years of adjustment and unit additions. Data reconciliation is an important step in the process of extracting data for retrofitting heat exchanger. Only two types of parameters needed to be reconciled in the process. Of all the constraints used, energy balance constraint causes the non-linearity in the model as it contains two types of parameters. A new method is introduced to solve this non-linearity in section 3.2 that iterates between two linear sub-models. Through case studies iterative method is shown to be able to provide satisfying result with less computational time. In section 3.3, limitation encountered when using iterative method is discussed. To overcome this limitation, three different strategies are developed. Section 3.4 presents a new way to solve data reconciliation problem on Total Site. Model to solve data reconciliation on utility system is presented with demonstration from both illustrative case study and industrial case study. Overall, the iterative method is shown to have less computational effort in the expense of lower accuracy, when compared to simultaneous method. It is suitable to be used in Heat Integration study particularly retrofitting heat exchange network, which does not need high level of accurate data.

After having the reconciled data, the next step is to construct HEN grid diagram for analysis. Using conventional grid diagram is insufficient and inconvenience during the heat integration analysis. An advance visualising tool for HEN is needed to ease the heat integration analysis. Section 4 introduced an extended Grid Diagram – the Shifted Retrofit Thermodynamic Grid Diagram (SRTGD). SRTGD has unique feature set, helping to identify favourable retrofit options. Since it shows in the same view CP (or load), temperatures and the network, it allows the users to simultaneously account for the thermodynamics, stream capacities and the topology as factors. As a result, SRTGD can be efficiently used to incorporate Pinch Technology, identify PPes and NPes. The provided examples and the case study clearly illustrate the advantages offered by the new tool. It has been demonstrated that SRTGD is capable of screening feasible from infeasible solutions, providing visual information in choosing more favourable heat paths. When a heat path is chosen, SRTGD points to the location of potential NPes as well as the maximum heat recovery achievable. However, the main importance comes with the possibility to assess the retrofit options for fluctuating energy prices and forecastles.

A matrix representation of HENs is proposed in section 4 to support synthesis or retrofit tasks. It can be well-organised and can help engineers in analysing the system with preserved accuracy. HENSM records all the temperatures, temperature differences and duties of all heat exchangers

in a HEN. Using the temperature differences at heat exchanger ends, the matrix is able to support the location of Process and Network Pinches. During retrofit Path Analysis, the potential of a heat exchanger in becoming a Network Pinch is shown in the matrix. HENSM is demonstrated on a case study. The matrix so far can't deal stream splitting.

During the process of heat integration analysis, there are some cases where retrofitting HEN for utility consumption reduction is infeasible in other aspect. The proposed HEN retrofit is thermodynamically feasible but might not be economically feasible. Particularly in the low temperature region in HEN where it is generally regarded as waste heat, most of the heat in this region is not recovered. If that is the case, waste heat can be utilised during the HEN retrofication. Section 5 has successfully showed that when utility cannot be reduced due to economic reason, waste heat utilisation can be another option for this. Using an illustrative case study and an industrial case study, it is noted that it is determined that waste heat streams have too low temperature to reduce utilities consumption. Attempt to construct heat path for this purpose in this case study will lead to high investment cost. Therefore, the HEN is then modified to generate hot water from the waste heat streams instead. The section discussed different arrangements of heat exchanger and the effects of its flexibility and complexity under different conditions.

In future work, the focus will be given on varying heat capacity. In all these works, it is assumed that heat capacity is constant and independent of temperature. It is particularly not so true for petrochemical process spanning huge temperature differences. Research should be done on the effect of varying heat capacity on the HEN retrofit. The differences in results using constant heat capacity and using varying heat capacity should be investigated and compared. The degree of significance of the differences In current work of data reconciliation, linear least square method is used to find the reconciled parameters. The term "linear" indicates that cp = m where m is the constant to be found by the model. To incorporate varying heat capacity into the model, it can be assumed that cp = aT + b where T is the temperature, a and b is the constant to be found by the model. Detailed model and to solve the model using Iterative Method requires more research in the future. As for HEN visualisation tool, current SRTGD can be modified to include the feature of showing varying heat capacity. As mention in the work, an area of a stream on SRTGD is proportional to the duty of heat exchanger. By modifying the lines enclosing the area is able to show that the stream has varying heat capacity. The effect of varying heat capacity on HEN retrofit process can be visualised. The idea of involving into HENSM however requires further researches. Waste heat utilisation can also incorporate varying heat capacity in the analysis. In this work, initial attempt is done on the industrial case study where it has different heat capacity according to quality of the feed stream. Further analysis is required to see varying heat capacity on HEN structure, economic performance and feasibility when varying heat capacity is accounted.

Appendix

Appendix 1

A diagram called Heat Interval Pairing Diagram (HIPD) is found in the work of Nagy et al. (2001). It has a similar feature when compared to Shifted Retrofit Thermodynamic Grid Diagram (SRTGD). An example of the diagram is directly taken in the work and shown in Figure 8.60.

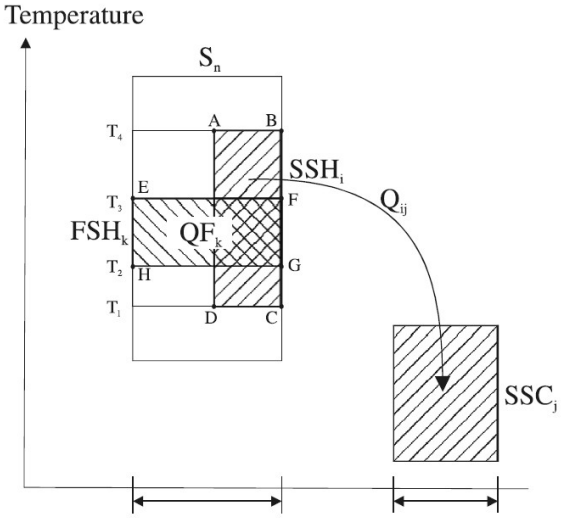

Figure 8.60: Heat Interval Pairing Diagram

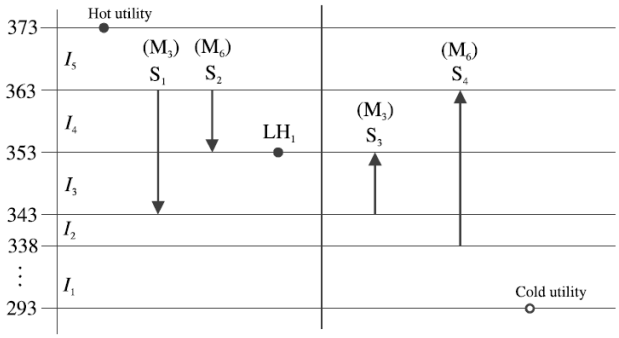

Figure 8.61: Motivating example from Nagy et al. (2001)

In Figure 8.60, the y-axis of HIPD represents the temperature scale and x-axis, while it is not stated, represents the heat capacity flowrates. The temperature scale is also believed to be shifted according to minimum temperature difference. This is the only similarity to SRTGD, although for SRTGD is the opposite.

The purposes of using these two diagrams are different. In HIPD, each stream are divided into sections according to the temperatures of other streams. For example, in motivating example taken directly from the work shown in Figure 8.61, Stream S1 has shifted temperature of from 363 °C to 343 °C. It has two sections as the middle temperature (353 °C) is determined by the shifted outlet temperature of S3. As its name suggest, HIPD is used for potential pairing of a section of a hot stream and a section of a cold stream. It is therefore HIPD can only be used during the initial design of heat exchanger network (HEN). It has also the limitation of showing only one hot stream and one cold stream. Multiple streams are not shown in HIPD.

For SRTGD, it can be used during the initial designing stage as well as retrofit stage of a HEN. All the streams involved in heat integration are shown in SRTGD together with all the possible pairing and heat path options. Only Pinch Temperature divide the streams into two sections (above pinch and below pinch) if a HEN is designed according to the heuristics of Pinch Technology.

Appendix 2

In this section, the procedures of processing raw data is shown. The general procedure is given in the diagram shown in Figure 8.62. All these steps can be categorised into three main steps; data acquisition, data extraction and data processing,

Figure 8.62: General procedure of data processing before data reconciliation

As the steps of data acquisition and data extraction is very dependent with individual and chemical plant, only the step of data processing will be discussed in this section. The example used is the illustrative case study in Section 3.2.3. In the case study it is assumed that all stream which data are to be extracted are involved in the HEN as shown in Figure 8.63. It can be seen that there are six heat exchangers (numbered from 1 to 6), a heater (H1) and two coolers (C1 and C2).

Figure 8.63: HEN of the illustrative case study used in Section 3.2.3

It should be noted that it is not the stream data but rather the stream data in every inlets and outlets of all heat exchangers are required. Assuming that for a single heat exchanger there are only one hot stream and one cold stream involved, therefore it has two inlets and two outlets for respective streams. There are two type of parameters to be reconciled; temperature (T) and heat capacity flowrate (CP). It is therefore eight parameters to be measured for a single heat exchanger. In the illustrative case study, there are total of nine heat exchangers, this is equivalent to 72 parameters to be measured. In some real cases, not all parameters are readily available. It may due to various reasons such as absence of online measuring apparatus or unreachable places for portable measuring apparatus. The detail process of dealing with missing parameters is not discussed here as it is out of the scope of this study. One of the ways is to use design value of the missing parameters a constant in the model. This will reduce the number of parameters to be reconciled in the model. Initially, all the parameters are measured and recorded for 12 times. The raw measurements are given according to the tables below.

All the measurements are then plotted in a graph to remove any outlier, if any. For example, according the Table 8.1, the following graph is plotted and shown in Figure 8.64. It can be seen that there is an outliers at the sixth measurement of heat exchanger no. 5. In this thesis, the sixth measurement of all the parameters are removed. Further analysis also showed that there is an outlier at the 11^{th} measurement of $CP_{i,HO}$ of heat exchanger no. 3. After removing these two outliers, ten sets of measurements of all parameters is only then used as input for data reconciliation.

Table 8.1: Raw measurement for inlet temperature for hot streams (Ti,HI)

i	1	2	3	4	5	6	H1	C1	C2
1	185	250	572	410	469	560	799	61	372
2	187	251	570	407	465	561	802	58	373
3	183	248	573	411	465	562	799	59	372
4	185	253	567	407	465	561	798	58	369
5	186	250	568	413	470	561	803	63	370
6	182	247	571	410	500	562	798	62	368
7	188	252	567	413	469	560	798	57	371
8	185	249	567	408	470	557	803	60	369
9	183	248	573	410	465	561	801	62	372
10	185	247	568	411	471	562	797	63	369
11	184	252	572	408	466	559	800	58	369
12	182	248	568	413	470	557	802	62	372
Mean	184.6	249.6	569.7	410.1	470.4	560.3	800.0	60.3	370.5

Table 8.2: Raw measurement for outlet temperature for hot streams ($T_{i,HO}$)

i	1	2	3	4	5	6	H1	C1	C2
1	62	173	369	339	371	525	699	17	321
2	63	170	369	341	370	525	700	23	319
3	63	172	369	337	369	522	702	17	319
4	60	167	370	338	365	524	698	18	322
5	62	173	368	339	367	528	702	21	322
6	60	173	371	339	371	528	699	21	317
7	63	172	368	340	365	523	701	18	317
8	62	167	369	338	369	524	699	17	318
9	62	171	371	339	365	522	700	19	317
10	62	173	371	342	366	528	700	18	317
11	63	167	369	337	369	527	701	18	317
12	61	167	372	340	370	525	700	22	323
Mean	61.9	170.4	369.7	339.1	368.1	525.1	700.1	19.1	319.1

Table 8.3: Raw measurement for inlet temperature for cold streams (Ti,CI)

i	1	2	3	4	5	6	H1	C1	C2
1	27	127	211	332	357	419	489	5	4
2	27	130	208	333	355	418	491	4	5
3	27	131	209	333	361	419	491	6	5
4	27	133	207	329	358	415	488	5	4
5	32	128	210	331	359	419	488	5	4
6	30	131	213	328	358	418	491	6	4
7	27	132	209	329	360	418	489	4	6
8	30	129	213	329	359	416	485	4	6
9	32	130	208	332	359	419	486	4	5
10	30	127	213	333	358	420	491	5	5
11	33	128	207	331	358	417	489	6	5
12	27	130	212	328	360	415	491	4	6
Mean	29.1	129.7	210.0	330.7	358.5	417.8	489.1	4.8	4.9

Table 8.4: Raw measurement for outlet temperature for cold streams (Ti,CO)

i	1	2	3	4	5	6	H1	C1	C2
1	132	207	327	361	416	485	551	9	11
2	128	213	331	358	416	487	549	11	10
3	128	210	332	358	417	485	549	9	11
4	127	211	330	356	421	486	547	11	10
5	130	208	329	357	420	486	548	9	9
6	128	208	330	357	420	487	547	11	11
7	131	212	333	357	421	491	547	9	10
8	131	212	331	361	420	490	547	10	10
9	129	209	328	360	419	485	551	11	10
10	133	213	333	357	417	486	548	9	9
11	131	207	332	358	419	488	551	11	11
12	127	211	327	359	416	491	546	11	9
Mean	129.6	210.1	330.3	358.3	418.5	487.3	548.4	10.1	10.1

Table 8.5: Raw measurement for inlet heat capacity flowrate for hot streams (CPi,HI)

i	1	2	3	4	5	6	H1	C1	C2
1	400	505	304	197	297	1,000	302	397	305
2	400	502	296	205	295	1,002	297	397	301
3	403	504	302	205	299	1,004	301	397	305
4	401	502	299	198	302	997	305	403	303
5	404	500	304	200	304	1,004	300	400	299
6	403	500	302	195	299	1,001	296	405	304
7	404	502	297	205	298	996	295	404	302
8	398	498	303	197	303	1,000	299	395	300
9	398	503	301	197	300	1,003	295	400	303
10	397	500	305	200	297	1,001	298	404	305
11	404	498	301	203	297	1,005	301	401	305
12	404	499	300	197	298	1,001	303	396	305
Mean	401.3	501.1	301.2	199.9	299.1	1,001.2	299.3	399.9	303.1

Table 8.6: Raw measurement for outlet heat capacity flowrate for hot streams (CPi,HO)

i	1	2	3	4	5	6	H1	C1	C2
1	402	500	303	205	303	1,004	299	403	298
2	395	495	300	199	298	997	302	395	298
3	395	495	303	195	296	999	302	400	296
4	398	503	295	195	305	995	302	403	298
5	399	497	305	199	301	1,004	299	401	305
6	396	497	301	195	304	1,004	302	395	297
7	404	502	301	201	304	1,005	305	404	298
8	400	499	303	203	301	998	301	398	300
9	396	504	297	203	299	997	299	399	303
10	395	502	304	202	298	1,000	296	403	302
11	398	505	290	198	296	1,003	303	403	299
12	404	505	302	201	303	1,004	298	403	298
Mean	398.5	500.3	300.3	199.7	300.7	1,000.8	300.7	400.6	299.3

Table 8.7: Raw measurement for inlet heat capacity flowrate for cold streams (CPi,CI)

i	1	2	3	4	5	6	H1	C1	C2
1	500	500	495	497	504	500	504	3,195	3,002
2	500	495	504	504	499	497	498	3,195	3,004
3	499	503	499	501	501	499	495	3,199	3,001
4	495	502	499	501	500	499	496	3,201	2,995
5	502	499	501	504	499	502	501	3,197	2,996
6	498	499	505	503	496	496	498	3,198	2,999
7	497	502	501	504	500	498	501	3,198	2,995
8	499	496	501	496	499	500	498	3,197	3,002
9	497	496	500	500	500	504	501	3,198	3,003
10	496	504	497	505	496	501	499	3,200	3,003
11	498	498	499	496	498	502	502	3,198	2,996
12	495	504	500	502	497	500	502	3,196	3,005
Mean	498.0	499.8	500.1	501.1	499.1	499.8	499.6	3,197.7	3,000.1

Table 8.8: Raw measurement for outlet heat capacity flowrate for cold streams (CPi,CO)

i	1	2	3	4	5	6	H1	C1	C2
1	496	502	502	501	502	499	496	3,202	3,002
2	496	495	505	500	501	500	496	3,197	3,004
3	503	497	501	496	499	504	497	3,203	3,003
4	504	500	498	498	504	502	501	3,202	2,996
5	496	501	499	500	501	498	496	3,199	3,002
6	502	498	503	503	505	495	498	3,205	2,995
7	495	500	500	497	500	505	498	3,204	2,996
8	498	499	500	497	499	505	505	3,195	3,000
9	501	498	503	498	502	502	505	3,195	3,004
10	498	504	499	505	504	503	503	3,205	3,000
11	500	505	504	505	496	501	497	3,201	3,005
12	499	505	501	503	505	503	501	3,202	2,998
Mean	460.6	461.8	462.7	461.8	462.9	462.8	461.0	2,954.6	2,769.6

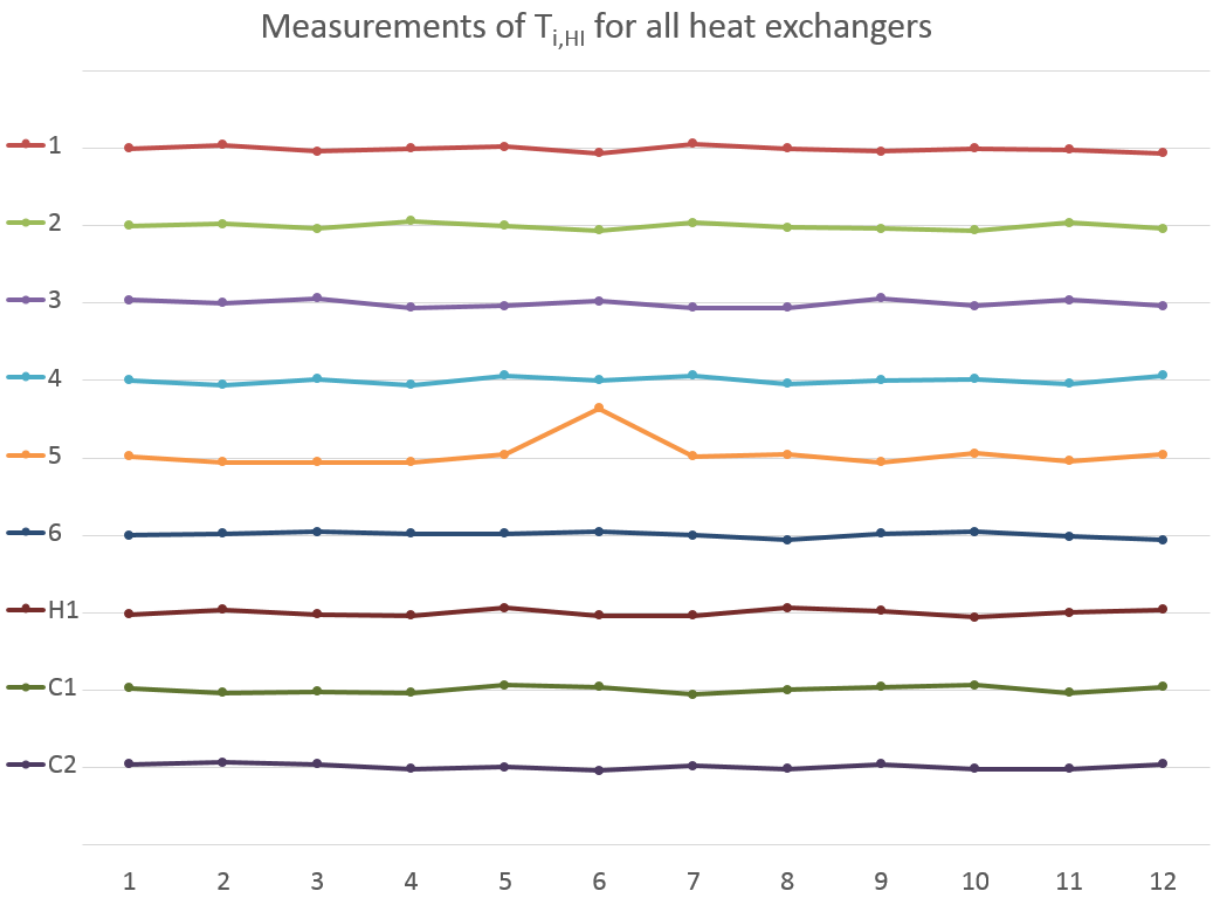

Figure 8.64: Comparison between measurements of $T_{i,HI}$ for all heat exchangers